MODELLING OF TUNNEL BEHAVIOUR UNDER STATIC LOAD

Submitted to

DELHI TECHNOLOGICAL UNIVERSITY

in partial fulfilment of the requirements for the award of the degree of

DOCTOR OF PHILOSOPHY

In

CIVIL ENGINEERING

By

PARVESH KUMAR
(Reg. No. 2K16/PhD/CE/06)

Under the supervision of

Prof. (Dr.) Amit Kumar Srivastava

DEPARTMENT OF CIVIL ENGINEERING

DELHI TECHNOLOGICAL UNIVERSITY

SHAHBAD, DAULATPUR, BAWANA ROAD, DELHI - 110042 (INDIA)

August 2022

Dedicated

To

My Late Father

and

Family

DELHI TECHNOLOGICAL UNIVERSITY

Shahabad Daulatpur, Main Bawana Road

Delhi-110042 (India)

DECLARATION

I hereby declare that the thesis entitled **"MODELLING OF TUNNEL BEHAVIOUR UNDER STATIC LOAD"** submitted by me for the award of the degree of ***Doctor of Philosophy*** to **Delhi Technological University (Formerly Delhi College of Engineering)** is a record of bonafide work carried out by me under the guidance of Prof. (Dr.) Amit Kumar Srivastava, Department of Civil Engineering, Delhi Technological University.

I further declare that the work reported in this thesis has not been submitted and will not be submitted, either in part or in full, for the award of any other degree or diploma in this Institute or any other Institute or University.

Parvesh Kumar

Reg No: 2K16/Ph.D/CE/06

Department of Civil Engineering

Place: New Delhi

Date:

DELHI TECHNOLOGICAL UNIVERSITY
Shahabad Daulatpur, Main Bawana Road
Delhi-110042 (India)

CERTIFICATE

This is to certify that the thesis entitled **"Modelling of Tunnel Behaviour under Static Load"** submitted by **Mr. Parvesh Kumar** to **Delhi Technological University (Formerly Delhi College of Engineering)**, for the award of the degree of "*Doctor of Philosophy*" in Civil Engineering is a record of bonafide work carried out by him. Parvesh Kumar has worked under my guidance and supervision and has fulfilled the requirements for the submission of this thesis, which to our knowledge has reached requisite standards.

The results contained in this thesis are original and have not been submitted to any other university or institute for an award of any degree or diploma.

Dr. Amit Kumar Srivastava
Professor
Department of Civil Engineering
Delhi Technological University (DTU)
Bawana, Delhi-110042

ACKNOWLEDGEMENTS

First of all, I am thankful to almighty god who made this work possible from beginning to the end and gives me the strength and patience during my PhD journey.

I would like to express my wholehearted gratitude and sincere appreciation and thanks to my Ph.D. supervisor, Dr. Amit Kumar Srivastava, Professor, Department of Civil engineering, Delhi Technological University for his inspiring guidance and continuous support through my PhD journey. Without his active involvement and constant guidance, this research would not exist in its current form. The lines are dedicated to my guide:

"सब धरती कागज करूँ, लेखनी सब बनराय/

सात समुंदर की मसि करूँ, गुरु गुण लिखा न जाय//"

His exceptional guidance and advice helped me during every stage of this research work. He will always remain a source of inspiration for me throughout my life.

Besides my supervisor, I would like to thank all the staff members of Delhi Technological University for their support and cooperation.

I would like to thank Mr. Amit Malik and Mr. Vinod for extending help during the development of the compression testing machine.

There are no words sufficient to express my thanks to my parents and for all of their sorrow and suffering in bringing me to this stage. Throughout this journey they are the source of motivation and encouragement for me. My special thanks to my younger brother Mr. Munish Kumar for his constant support and helping me at every stage in this journey.

I would like to express my sincere thanks to my fellow researcher and friends Mr. Sandeep Panchal, Abhishek Paswan, Rajat Gautam, Archita Goyal for their cooperation during my

research work. I am thankful to the lab staff member of Rock Mechanics lab specially Mr. Rakesh and Mr. Shashikant who helped me during my lab work.

I would like to appreciate the efforts of the anonymous reviewers for reviewing our research papers and giving constructive feedback which ultimately improved the quality of our research publications over the course of time.

At last I would like to express my gratitude to everyone who has helped me achieving this goal, whether directly or indirectly.

Parvesh Kumar

(2K16/Ph.D./CE/06)

ABSTRACT

The continuous development of cities caused a deficiency of land in metro regions which arises various transportation problems. The construction of underground structures is extremely effective in solving these problems, as they have solved various traffic issues in significant urban areas. In the transportation system, underground structures play a vital part. Various civil structures essentially depend on underground frameworks in metro areas, where there is an absence of ground space for moving vehicles. Underground structures are utilized for different purposes in civil engineering. The most remarkable of these structural design uses is the utilization of the underground framework of the metro tunnels. Therefore in the improvement of traffic problems, the development of underground constructions plays a vital role. Tunnel deformation mainly depends upon various types of loading, like static loading, dynamic loading or impact loading. It is hence very important to keep these underground structures safe from the burdens of following up on them in field conditions. When a tunnel is constructed in weak rock, the primary motive should be to keep it protected from the stresses that act on it.

The main objective of the present study is to evaluate the extent of deformation experienced in single and Twin tunnels under the effect of static loading. Numerous investigations have been done in the past to determine the deformation of tunnels under static loading conditions using numerical and analytical solutions. Whereas limited experimental study has been done to determine the deformation of single and twin tunnels. Due to a variety of adverse conditions, performing the in-situ tests in the field is extremely difficult. As a result, an advanced laboratory compressing testing facility is essential for determining the degree of deformation that occurs in tunnels. For the safe and cost-effective construction of underground openings in rocks, accurate estimation of deformation behaviour is very essential.

Hence there is a need to design and fabricate an equipment where these difficulties and limitations can easily be overcome. As a result, there is a need to build a compression testing device that can easily control such difficulties and limitations. A digital compression testing machine is designed and fabricated in the present study that can perform experimental tests on physical rock tunnel models. This automated compression testing unit calculates the deformation behaviour of single and twin tunnels under static loading conditions.

In the present study, the extent of deformation is measured with the help of experimental investigation and numerical analysis. For the experimental investigation, the selection of the model material is done according to the feasibility and easy accessibility of the material. For single tunnel models, Plaster of Paris, Sand and Kaolinite clay are mixed in different proportions. Three types of model materials are selected according to their strength characteristics. The basic engineering properties of all three model materials are determined in the laboratory. In the single tunnel samples, the cover depth of the tunnel is varied as 3cm and 5cm. Lined and unlined samples of single tunnels are prepared in the laboratory. For lined tunnels, PVC pipe is used as the liner material. After the preparation of the samples, the tunnel models are subjected to static loading conditions in a compression testing machine. Then the deformation is measured with the help of LVDTs which are fixed in the tunnel sample from the bottom side. The reading obtained from the LVDTs is recorded in the CPU data.

After the testing of single tunnel samples, Twin tunnel samples are also casted in the laboratory. For the Twin tunnel sample, the model material is kept the same for all the models. All the samples of Twin tunnels are prepared with the help of Plaster of Paris by adding the prescribed amount of water into it. In Twin Tunnel samples, the spacing between the tunnels is varied as 1.5D, 2D and 2.5D where “D” is denoted as the diameter of the tunnel. The diameter of the

tunnel is kept the same in both single and Twin Tunnels sample i.e. 5cm. The cover depth of the tunnel in the Twin Tunnel sample is varied as 3cm and 5cm similar to the case of a single tunnel model. After the preparation of Twin Tunnel samples, these samples are subjected to static loading conditions in a compression testing machine after fixing LVDTs in the sample. Then the load is applied with the help of a compression testing machine on the Twin Tunnel sample and the reading is recorded. The present study is basically conducted in two steps. Firstly, the deformation behaviour of small scale tunnels model is determined in the laboratory with the help of experimental investigation and then the results obtained from experimental modelling are validated with numerical modelling with the help of ANSYS software. For single tunnel numerical models, the cover depth of the models is varied as 3cm and 5cm. Similarly, for the Twin tunnel sample, the spacing between the tunnels is varied as 1.5D, 2D and 2.5D same as in the case of experimental investigation. Then the meshing and boundary conditions are provided to the tunnel model and subjected to static loading. The results obtained from numerical modelling are recorded.

After the experimental and numerical analysis of single and Twin tunnels, the results are then compared with each other for validation. From the results it can be concluded that both experimental and numerical modelling results are in close agreement with each other. From the study, it can also be concluded that there are various factors such as cover depth of tunnels, strength properties of rock, spacing between the tunnels and presence of liner material which affect the deformation of single and Twin tunnels under the effect of static loading conditions. Hence, it can be concluded from the present study, the tunnel structure can remain safe if the design parameters are well selected.

Keywords: Underground Structure; Geo-material; Liner; Deformation; Tunnel distance; Physical modelling; Numerical analysis; Static loading.

TABLE OF CONTENTS

Topics		*Page No.*
CANDIDATE DECLARATION		i
CERTIFICATE		ii
ACKNOWLEDGEMENTS		iii
ABSTRACT		v
TABLE OF CONTENTS		ix
LIST OF FIGURES		xv
LIST OF TABLES		xxii
LIST OF ABBREVIATIONS		xxv
LIST OF NOTATIONS		xxvi
Chapter 1	**INTRODUCTION**	1
1.1	General	
1.2	History of Development of Tunnels	3
1.3	Need for the Thesis	4
1.4	Objectives of the Thesis	7
1.5	Organization of the Thesis	7
Chapter 2	**LITERATURE REVIEW**	10
2.1	General	10
2.2	Terminology in tunneling	11

2.2.1	Crown	12
2.2.2	Lining	12
2.2.3	Bench	12
2.2.4	Invert	12
2.3	Types of Tunnel Sections	13
2.3.1	Circular Section	13
2.3.2	Horse Shoe Section	13
2.3.3	D-Shaped or Segmental Section	15
2.3.4	Egg Shape Section	15
2.3.5	Rectangular Shaped Section	15
2.4	Method of Tunneling	15
2.4.1	Full Face Method	16
2.4.2	Heading and Benching Method	17
2.4.3	Drift Method	17
2.4.4	Pilot Tunnel Method	18
2.4.5	Perimeter Method	19
2.5	Stresses around underground opening	19
2.6	Factors affecting the stability of Tunnels	21
2.6.1	Type of Tunnel Section	21
2.6.2	Effect of Overlying Strata	22
2.6.3	Type of Loading	23
2.6.4	Effect of joints in tunnel	24
2.6.5	Effect of Alignment of tunnels	26

2.7	Physical Modelling of tunnels	28
2.8	Numerical Modelling of tunnels	41
2.9	Gaps from Literature Review	56
Chapter 3	**EXPERIMENTAL SETUP**	59
3.1	General	59
3.2	Design and fabrication of Compression testing machine	60
3.2.1	Frame and the Loading Unit	62
3.2.1.1	Base Platen and Side platen	63
3.2.1.2	Upper Head	63
3.2.1.3	Jack and Jack Cover	63
3.2.1.4	Spacer	64
3.2.1.5	Lower Platen	64
3.2.1.6	Spherical Seating	64
3.2.1.7	Electronic Display Unit and ON/OFF Switch	65
3.2.1.8	Booster Lever and Limit Switch	65
3.2.1.9	Release Valve	65
3.2.1.10	Pressure Sensor	66
3.2.1.11	Motor	67
3.2.2	Pumping Unit	68
3.2.3	Data Acquisition and Controlling System	69
3.2.3.1	LVDT's	69
3.2.3.2	LVDT full connection, location and Placement arrangement	70

3.2.3.3	LVDT full connection	71
3.2.3.4	Calibration of LVDTs	72
3.2.3.5	Location of LVDTs	72
3.2.3.6	LVDT placement arrangement	74
3.3	Moulds for Preparation of Samples	76
3.3.1.	Dimension of the Moulds	77
3.4	Summary	79
Chapter 4	**EXPERIMENTAL INVESTIGATIONS**	**80**
4.1	General	80
4.2	Testing Program of Single Tunnels	81
4.2.1	Selection of Model Material	81
4.2.2	Characterization of Geo-materials	82
4.2.3	Engineering Properties	85
4.3	Rock Tunnel Model	91
4.3.1	Fixing dimension of tunnel models	91
4.4	Casting of models	92
4.5	Marking the dimensions and Drilling	95
4.6	Physical modelling of single and twin tunnel	98
4.6.1	Deformation of single tunnel of GM-1 material	101
4.6.2	Deformation of single tunnel of GM-2 material	105
4.6.3	Deformation of single tunnel of GM-3 material	119
4.6.4	Deformation of twin tunnel of having 1.5D spacing	113

4.6.5	Deformation of twin tunnel of having 2D spacing	117
4.6.6	Deformation of twin tunnel of having 2.5D spacing	120
4.7	Concluding Remarks	124
Chapter 5	**NUMERICAL MODELLING OF SINGLE AND TWIN TUNNEL**	**126**
5.1	Load and Boundary Conditions	126
5.2	Meshing	127
5.3	Numerical analysis of Single Tunnels	129
5.3.1	Deformation of a single tunnel of GM-1 material	129
5.3.2	Deformation of a single tunnel of GM-2 material	132
5.3.3	Deformation of a single tunnel of GM-3 material	136
5.4	Numerical analysis of Twin Tunnels	139
5.4.1	Deformation of twin tunnel of 1.5D spacing	139
5.4.2	Deformation of twin tunnel of 2D spacing	143
5.4.3	Deformation of twin tunnel of 2.5D spacing	146
5.5	Concluding Remarks	150
Chapter 6	**DISCUSSION AND VALIDATION OF RESULTS**	151
6.1	General	151
6.1.1	Comparison of deformation profiles of GM-1 material	152
6.1.2	Comparison of deformation profiles of GM-2 material	153
6.1.3	Comparison of deformation profiles of GM-3 material	154
6.1.4	Comparison of deformation profiles of 1.5D spacing Twin Tunnel	157

6.1.5 Comparison of deformation profiles of 2D spacing Twin Tunnel 159

6.1.6 Comparison of deformation profiles of 2.5D spacing Twin Tunnel 160

6.2 Concluding Remarks 162

Chapter 7 CONCLUSIONS AND FUTURE SCOPE 163

7.1 Conclusions 163

7.2 Future Scope 165

References 168

List of Publications 182

LIST OF FIGURES

S.No.		PageNo.
Fig. 1.1	Tunnel constructed in hilly area	2
Fig 1.2	Traffic problems during transportation	5
Fig 1.3	Construction in big Crowed Cities	5
Fig 1.4	Photograph of the collapse in the tunnel extending towards the face	6
Fig 2.1	Common structure of tunnels in rock engineering	11
Fig 2.2	Various parts of tunnel cross section	12
Fig 2.3	Various types of tunnel sections	14
Fig 2.4	Full Face Method	16
Fig 2.5	Heading and Benching Method	17
Fig 2.6	Drift Method	18
Fig 2.7	Pilot Tunnel Method	19
Fig 2.8	Tangential and radial stresses around circular openings	20
Fig 2.9	Shaped of different tunnel sections (Khan et al. 2015)	21
Fig 2.10	Layouts of different shapes of Twin Tunnel (Elshamy et al. 2013)	22
Fig 2.11	Finite element mesh in the study (Nunes and Meguid2009)	23
Fig 2.12	Displacement obtained in (a) static loading (b) Dynamic loading.	24
Fig 2.13	Test model of tunnel (Zhu et al. 2015).	25
Fig 2.14	A cement mortar tunnel model and its loading device (Zhu et al.	26

2015)

Fig 2.15 Geometric alignment used in the study (Oliaei and Manafi 2015) 27

Fig 2.16 Different alignments of Twin tunnels adopted for the study (Chehade and Shahrour, 2008) 28

Fig 2.17 Photograph of 3-dimensional geo-mechanical model test platform (Li et al. 2005) 29

Fig 2.18 Jointed rock tunnel model prepared in laboratory (Sagong et al. 2011) 30

Fig 2.19 Damage zone from the numerical and experimental results 31

Fig 2.20 Experimental results of gradual failure. 31

Fig 2.21 Joints given in tunnel mode at different inclinations (Yang et al. 2019) 32

Fig 2.22 The comparison of the deformation obtained from numerical modeling with the deformation obtained from physical modeling (Chen et al. 2016). 34

Fig 2.23 Rock Tunnel models having different coverdepths (Sharma et al. 2018) 36

Fig 2.24 Photograph of the experimental setup used in the study (Sharma et al. 2018) 36

Fig 2.25 Photograph of the experimental setup (Sohaei et al. 2020). 39

Fig 2.26 Components of experimental setup used in the study (Yang et al. 2019) 41

Fig 2.27 Plane strain model under consideration (Do et al. 2014) 44

Fig 2.28	Alignments of tunnels used in the study (Bayoumi et al. 2016)	45
Fig 2.29	Different alignments of twin tunnel (Channabasavaraj and Visvanath 2013)	46
Fig 2.30	Geometry used in twin tunnel simulation (Singh et al. 2018).	48
Fig 2.31	Plane-strain model used in the study for dual circular tunnels (Zhang et al. 2019).	49
Fig 2.32	Distribution of stresses around the tunnel (Lv et al. 2020)	50
Fig 2.33	Deformed Shape of Ground Surface after Excavation of Tunnel (Mahalakshmi et al. 2012)	52
Fig 2.34	Joint orientation provided in the circular opening (Yoo et al. 2017)	54
Fig. 3.1	Schematic diagram of the loading unit.	61
Fig. 3.2	Compression testing machine with electronic display unit and pumping unit	62
Fig. 3.3	Close Up of Rear View of Electronic Box	67
Fig. 3.4	Pumping Unit attached to the loading unit	68
Fig. 3.5	AC Slim Line LVDT	70
Fig. 3.6	Close Up View of Data Acquisition System	71
Fig. 3.7	Close Up of Rear View of LVDT Data Logger	71
Fig. 3.8	16-Channel Plate attached with LVDT Data acquisition system	72
Fig. 3.9	Placement of LVDT’s in the Single Tunnel Model	73
Fig. 3.10	Placement of LVDT’s in the Twin-Tunnel Model.	74

Fig. 3.11	Extension fixed to LVDT for fixing inside the tunnel sample	75
Fig. 3.12	Tri-nut system for fixing LVDT inside the tunnel sample	75
Fig. 3.13	Placement of LVDT inside the tunnel sample	76
Fig. 3.14	Geometrical view of Single Tunnel Model with varying Overburden along x-x axis; (b) Lining Thickness	78
Fig. 3.15	Geometrical view of Twin Tunnel Model with varying Overburden along x-x axis	78
Fig. 3.16	Single Tunnel and Twin Tunnel model Dimension	79
Fig. 4.1	Various constituents for preparing synthetic rock .	83
Fig. 4.2	Prepared specimens of different Geo materials	86
Fig. 4.3	Specimens of different Geo materials prepared for Brazilian test to determine the indirect tensile strength	86
Fig. 4.4	Stress-strain Curve for all three model materials	87
Fig. 4.5	Deformed UCS specimens after testing	88
Fig. 4.6	Specimen tested for indirect tensile strength	88
Fig. 4.7	The flowchart of the experimental program	90
Fig. 4.8	Final sample prepared	93
Fig. 4.9	Single lined and unlined tunnel samples with different cover depths	94
Fig. 4.10	Twin Tunnel Samples having different c/c spacing and cover depth	94
Fig. 4.11	Rock Tunnels Model prepared for experimental analysis.	95
Fig. 4.12	Marking the dimensions on the bottom of the tunnel sample	96

Fig. 4.13	Drilling holes inside the tunnel sample	97
Fig. 4.14	Holes drilled in the twin tunnel model for fixing LVDT's	97
Fig. 4.15	Schematic diagram of the static load acting on single tunnel model	99
Fig. 4.16	Schematic diagram of the static load acting on the twin tunnel model.	100
Fig. 4.17	Deformation profiles of GM-1 single tunnels models	104
Fig. 4.18	Load vs. Deformation graph of GM-1 single tunnels models	105
Fig. 4.19	Deformation profiles of GM-2 single tunnels models	108
Fig. 4.20	Load vs. Deformation graph of GM-2 single tunnels models.	109
Fig. 4.21	Deformation profiles of GM-3 single tunnels models	112
Fig. 4.22	Load vs. Deformation graph of GM-3 single tunnels models.	113
Fig. 4.23	Deformation profiles of 1.5D c/c spacing twin tunnels models obtained from experimental results	116
Fig. 4.24	Deformation profiles of 2D c/c spacing twin tunnels models obtained from experimental results	120
Fig. 4.25	Deformation profiles of 2.5D c/c spacing twin tunnels models obtained from experimental results.	124
Fig. 5.1	Loading arrangement of Single Tunnel	127
Fig. 5.2	Boundary Conditions	127
Fig. 5.3	Meshing of the Elements	128
Fig. 5.4	Deformation profiles of GM-1 single tunnels models obtained from numerical analysis.	132

Fig. 5.5	Deformation profiles of GM-2 single tunnels models obtained from numerical analysis	135
Fig. 5.6	Deformation profiles of GM-3 single tunnels models obtained from numerical analysis.	139
Fig. 5.7	Deformation profiles of 1.5D c/c spacing twin tunnels models obtained from numerical analysis	142
Fig. 5.8	Deformation profiles of 2D c/c spacing twin tunnels models obtained from numerical analysis	146
Fig. 5.9	Deformation profiles of 2.5D c/c spacing twin tunnels models obtained from numerical analysis.	149
Fig. 6.1	Comparison of deformation profile obtained from experimental and numerical modelling at 3cm and 5cm overburden for single tunnel of GM-1 material	153
Fig. 6.2	Comparison of deformation profile obtained from experimental and numerical modelling at 3cm and 5cm overburden for single tunnel of GM-2 material.	154
Fig. 6.3	Comparison of deformation profile obtained from experimental and numerical modelling at 3cm and 5cm overburden for a single tunnel of GM-3 material	156
Fig. 6.4	Comparison of deformation profiles of all three model materials at 3cm overburden obtained from experimental results	156
Fig. 6.5	Comparison of deformation profiles of all three model materials at	157

5cm overburden obtained from experimental results.

Fig. 6.6 Comparison of deformation profile obtained from experimental and numerical modelling of 1.5D centre to centre spacing tunnels 158

Fig. 6.7 Comparison of deformation profile obtained from experimental and numerical modelling of 2.0D centre to centre spacing tunnels 160

Fig. 6.8 Comparison of deformation profile obtained from experimental and numerical modelling of 2.5D centre to centre spacing tunnels. 161

LIST OF TABLES

S.No.		Page No.
Table 4.1	Composition of the Synthetic Material used for making single tunnel models.	83
Table 4.2	Properties of Kaolinite Clay	84
Table 4.3	Properties of Sand	85
Table 4.4	Parameters determined for different Geo-materials	89
Table 4.5	Deformation of Unlined Tunnel in GM-1 sample for C/D =0.6	102
Table 4.6	Deformation of Unlined Tunnel in GM-1 sample for C/D =1.0	102
Table 4.7	Deformation of lined Tunnel in GM-1 sample for C/D =0.6	103
Table 4.8	Deformation of lined Tunnel in GM-1 sample for C/D =1.0	104
Table 4.9	Deformation of Unlined Tunnel in GM-2 sample for C/D =0.6	106
Table 4.10	Deformation of Unlined Tunnel in GM-2sample for C/D =1.0	106
Table 4.11	Deformation of lined Tunnel in GM-2sample for C/D =0.6	107
Table 4.12	Deformation of lined Tunnel in GM-2 sample for C/D =1.0	108
Table 4.13	Deformation of Unlined Tunnel in GM-3 sample for C/D =0.6	110
Table 4.14	Deformation of Unlined Tunnel in GM-3sample for C/D =1.0	110
Table 4.15	Deformation of lined Tunnel in GM-3 sample for C/D =0.6	111
Table 4.16	Deformation of lined Tunnel in GM-3 sample for C/D =1.0	112
Table 4.17	Deformation of unlined Tunnel in 1.5D c/c spacing for C/D =0.6	114

Table 4.18	Deformation of unlined Tunnel in 1.5D c/c spacing for C/D =1.0.	114
Table 4.19	Deformation of lined Tunnel in 1.5D c/c spacing for C/D =0.6.	115
Table 4.20	Deformation of lined Tunnel in 1.5D c/c spacing for C/D =1.0.	116
Table 4.21	Deformation of unlined Tunnel in 2D c/c spacing for C/D =0.6.	117
Table 4.22	Deformation of unlined Tunnel in 2D c/c spacing for C/D =1.0.	118
Table 4.23	Deformation of lined Tunnel in 2D c/c spacing for C/D =0.6	119
Table 4.24	Deformation of lined Tunnel in 2D c/c spacing for C/D =1.0.	119
Table 4.25	Deformation of unlined Tunnel in 2.5D c/c spacing for C/D =0.6.	121
Table 4.26	Deformation of unlined Tunnel in 2.5D c/c spacing for C/D =1.0	122
Table 4.27	Deformation of lined Tunnel in 2.5D c/c spacing for C/D =0.6	123
Table 4.28	Deformation of lined Tunnel in 2.5D c/c spacing for C/D =1.0.	123
Table 5.1	Deformation of Unlined Tunnel in GM-1 for C/D =0.6	129
Table 5.2	Deformation of Unlined Tunnel in GM-1 for C/D =1.0	130
Table 5.3	Deformation of lined Tunnel in GM-1 for C/D =0.6	131
Table 5.4	Deformation of lined Tunnel in GM-1 sample for C/D =1.0	131
Table 5.5	Deformation of Unlined Tunnel in GM2 sample for C/D =0.6	133
Table 5.6	Deformation of Unlined Tunnel in GM2 for C/D =1.0	133
Table 5.7	Deformation of lined Tunnel in GM-2 for C/D =0.6	134
Table 5.8	Deformation of lined Tunnel in GM-2 for C/D =1.0	135
Table 5.9	Deformation of Unlined Tunnel in GM-3 sample for C/D =0.6	136

Table 5.10	Deformation of Unlined Tunnel in GM3 for C/D =1.0	137
Table 5.11	Deformation of lined Tunnel in GM-3 for C/D =0.6	138
Table 5.12	Deformation of lined Tunnel in GM-3 for C/D =1.0	138
Table 5.13	Deformation of unlined Tunnel in 1.5D c/c spacing for C/D =0.6	140
Table 5.14	Deformation of unlined Tunnel in 1.5D c/c spacing for C/D =1.0	141
Table 5.15	Deformation of lined Tunnel in 1.5D c/c spacing for C/D =0.6	141
Table 5.16	Deformation of lined Tunnel in 1.5D c/c spacing for C/D =1.0	142
Table 5.17	Deformation of unlined Tunnel in 2D c/c spacing for C/D =0.6.	144
Table 5.18	Deformation of unlined Tunnel in 2D c/c spacing for C/D =1.0.	144
Table 5.19	Deformation of lined Tunnel in 2D c/c spacing for C/D =0.6.	145
Table 5.20	Deformation of lined Tunnel in 2D c/c spacing for C/D =1.0.	145
Table 5.21	Deformation of unlined Tunnel in 2.5D c/c spacing for C/D =0.6	147
Table 5.22	Deformation of unlined Tunnel in 2.5D c/c spacing for C/D =1.0.	148
Table 5.23	Deformation of lined Tunnel in 2.5D c/c spacing for C/D =0.6.	148
Table 5.24	Deformation of lined Tunnel in 2.5D c/c spacing for C/D =1.0.	149

LIST OF ABBREVIATIONS

POP	Plaster of Paris
GM	Geo-material
PVC	Polyvinyl Chloride
FEM	Finite Element Method
LVDT	Linear Variable Deformation Transducer
Exp	Experimental
Num	Numerical
TT	Twin tunnel
UCS	Uniaxial Compressive Strength
t/r	Thickness/Radius
c/c	Centre to centre
C/D	Cover Depth/Diameter

LIST OF NOTATIONS

r	Radial Distance
a	Radius of the tunnel
σ_x	Horizontal Pressure
σ_z	Overburden Pressure
σ_θ	Tangential Normal Stress
$\tau_{r\theta}$	Shear Stress
σ_r	Radial Normal Stress
β	Angle of inclination

Chapter 1

INTRODUCTION

1.1 General

Tunnels are horizontal underground manmade passageways that are built without causing any surface disruption. Tunnels are generally used for transporting materials. Tunnels can be constructed through rock mass hills and rivers etc. In the present era, tunnels are used for various purposes. Tunnels have a wide variety of applications such as highways, railroads, water supply and sewage tunnels, underground power stations, storage converns etc. With that kind of wide variety of underground applications, it is essential to consider the different aspects of underground opening as well as their stress and deformation features. Rock is stressed at first, and any opening causes initial stress. In terms of the type of load acting on the system, the design of underground structures in rock is different from other types of design and construction. The outcome of the initial state of stress and stresses caused by the opening is the post-excavation state of stress in the structure. As a result, any design analysis of an underground structure requires an evaluation of the state of stress. The study of the state of stresses around the underground structure provides an insight into the basic phenomenon such as displacement and stress fields and aids in the provision of appropriate support for the underground structure. Road tunnels, rail tunnels, rapid transit tunnels, water tunnels, sewage tunnels, and service and utility tunnels are examples of tunnels and underground structures. Fig. 1.1 shows the construction of a tunnel in a hilly area.

In metropolitan locations, the building of a new transportation and utility infrastructure frequently necessitates the construction of tunnels beneath existing surface structures. As

population pressures drive the need for more infrastructures while also causing more surface space to be constructed for housing and other development, underground construction will continue to thrive as the preferred solution for infrastructure provision. The construction of tunnel structures is growing with an increase in economical factors. The tunnel construction is much cheaper compared to the surface development in metropolitan areas because of the high cost of acquiring property in big cities. The cost of construction in metropolitan areas is roughly 5 Crores per Kilometer, though the cost has been reducing at a rate of around 4% per year in recent years, making the construction of underground tunnels even more feasible. The construction of tunnels in soft ground conditions may cause damage to the existing superstructures therefore protective measures are required to prevent the damage to the already existing structures.

Fig. 1.1 Tunnel constructed in hilly area (Source: Google image)

Various methods available to assess the behaviour of underground structures subjected to static loading include large-scale in-situ tests, physical modelling and numerical simulations. For practical reasons, the in-situ experiments are difficult to conduct and hence physical model tests

and numerical methods have to be used. However, the accuracy of the numerical model has to be verified through calibration of either the in-situ tests or physical model results.

1.2 History of Development of Tunnels

The construction of the underground tunnel is very old. Basically, a tunnel structure is required when there is an obstacle met in the alignment of a railway or highway track. In ancient times, tunnels were constructed to convey clean water to main cities. Even today also such types of tunnels are used in Greece, Rome, Egypt and Jammu and Kashmir for the same purpose. Historically several tunnels were excavated in hard rock with the help of hand mining methods. Timber was used as the temporary support to provide safety to the workers working inside the tunnel. In the 19^{th} century, Brunel invented the tunnelling shield with the help of which many lives were saved from the timber collapses. Firstly, this tunnel shield was used as a supporting system for constructing a tunnel below the Thames River where the soil conditions were very poor. In the 20^{th} Century, the method of tunnelling was slightly modified and named as 'open-faced' method which is still in use. Later on, in the 20^{th} century, circular tunnel lining was used for carrying the load of soil and rock. Around 4000 years ago the first tunnel was constructed. The purpose of that tunnel was to connect two buildings in Babylon. It was constructed by Egyptians and Babylonians. The width, height and length of that tunnel were 3.6m, 4.5m and 910m respectively. Later in Europe, the first tunnel was built by Roman Emperor Claudius for carrying spring water through Appennine Mountains. The cross-section of that tunnel was 3.0x 1.8 m. Its length was about 5.8km. It was completed in 12 years by 30,000 labourers. Romans adopted the following improvement in the construction of the tunnel.

a) For cooling the rocks they used vinegar in place of water to attack the rock chemically as well as mechanically simultaneously.

b) They used fire as a disintegration agent to disintegrate the rock.

c) To work at the several points simultaneously they introduced shafts.

The necessity of tunnels cannot be underestimated as they are very helpful to manage the transportation problem in cities and hilly areas. The presence of tunnels can lead to improving the connectivity issue and it also shortens the lifelines. The construction of tunnels can be economical and safe if it designed parameters are accurate. Although it requires highly skilled effort for the construction of tunnels as the failure of these structures may lead to loss of lives.

1.3 Need for the Thesis

Modern and highly developed cities are continuously struggling to face increased traffic problems. Due to the constant growth in the construction of superstructures, there is a scarcity of land in the present era. In metro cities, many transportation problems have to face due to insufficient space as shown in Fig. 1.2. Moreover, the space required for expansion or upgrading the already existing infrastructure is very limited as a result of that various public disruptions are caused. Because of this over construction, the transportation system is getting affected. Even in hilly areas, due to the presence of hills and terrains, the transportation system is affected. Therefore, to solve this problem, the construction of an underground tunnel structure can be considered a good alternative. Tunnelling is now considered a preferable solution as it is safe and economical. Due to the advancement in tunnel boring methods, it is possible to deal with any type of geological complexity. Fig. 1.3 shows the construction of building in big crowded cities.

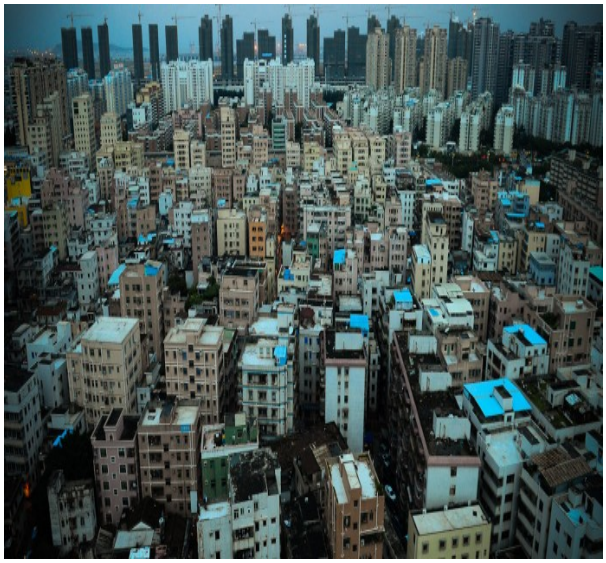

Fig 1.2 Traffic problems during transportation Fig 1.3 Construction in big Crowed Cities

(Source: Google image) (Source: Google image)

In big and crowded cities, the construction of underground tunnels can solve the traffic problem to some extent. When the tunnel is excavated beneath the soil or rock strata, it is subjected to various types of loading such as static loading, dynamic loading or impact loading etc. As a result of that, these tunnel structures experience stresses which may cause the deformation of the structure. These continuous acting stresses on the underground tunnel structures may lead to the deterioration of their engineering and mechanical properties as shown in Fig. 1.4. In the past various tunnel structure failures have been observed in the Himalayas such as the Katra tunnel, Quizikund Tunnel, Chennani-Nashri tunnel and Maneri project. The failure of these structures can cause loss of lives and increases the construction cost.The use of physical and numerical modelling methods is increased as they give more dependable results. In previous studies, physical modelling of the tunnel to access their stability behaviour was used by (Messerli et al. 2010 and Kirsch et al. 2009) various researchers.

Fig 1.4 Photograph of the collapse in the tunnel extending towards the face (Source: Google image)

Hence it is very essential to ensure the correct evaluation of the stresses acting on the tunnels to make it a safe and economical design. The stability of tunnels depends upon various factors. Some of the main factors which are responsible for the deformation of tunnels are the type of tunnel section, inaccurate calculation of loads acting on the tunnels, insufficient spacing between the tunnels in case of twin tunnels, the cover depth of the tunnel etc.

The motivation behind the thesis is to determine the deformation behavior of tunnels under the effect of static loading conditions. In the present study, an attempt is made to determine the effect of various factors on the stability analysis of tunnels under the effect of static loading. The stability behaviour of both single and twin tunnels is studied under static loading. Then the results obtained from experimental and numerical modeling are validated. The results obtained from the present study are helpful in deciding the design parameters of tunnels for the safe and economical design.

1.4 Objectives of the Thesis

The main objective of the thesis is to evaluate the deformation behaviour of tunnels under static loading conditions. The present study explains the effect of various parameters on the deformation behaviour of underground tunnels. Mainly the effect of strength characteristics of rock, cover depth of the tunnel, spacing between the tunnels and introduction of liner material is studied. The objectives for the present study are given below.

i. To design and fabricate an automatic compression testing facility in the laboratory, for conducting experimentation work on small-scale physical models of single and twin tunnels.

ii. To study the effect of strength of rock, cover depth, liner material and spacing between the tunnels on the stability behaviour of tunnels.

iii. To determine the deformation behaviour of single and twin tunnels under static loading at different conditions through experimental analysis.

iv. To develop a numerical model of single and twin tunnels and find deformation behaviour under different conditions.

v. To validate the results obtained from numerical analysis with experimental results and propose the suitability of numerical models.

1.5 Organization of the Thesis

The thesis is organized into seven different chapters followed by references.

In Chapter 1, the motivation and need behind the present study is presented. A general introduction to the tunnelling, its purpose and the importance of predicting the stability

behaviour of tunnels under various loading conditions are briefly explained in this chapter. The chapter also includes the main objectives of the present study. The various problems faced during the stability analysis of tunnels in actual site conditions are identified. The various factors affecting the stability behaviour of tunnels are highlighted.

Chapter 2 contains a detailed review of the research work done on the stability analysis of tunnels using experimental and numerical modelling by various researchers in past. A comprehensive review of the various factors affecting the deformation of tunnels, physical modelling methods used in past by various researchers, and numerical modelling techniques which are helpful in assessing the extent of damage in tunnels is done. The review on the numerical modelling for single and twin tunnels under various loading conditions using various software has been studied. Various theories proposed to determine the stress concentration in tunnels is studied. This chapter also explains the development of testing equipment for determining the deformation of tunnels under various loading conditions.

Chapter 3 explains the development and fabrication of the compression testing facility for the present study. The chapter includes a detailed discussion about the working and purpose of each component of the testing unit. The dimension of the moulds used for preparing the tunnel models is also discussed. Finally, the calibration of the loading unit and LVDTs are discussed.

Chapter 4 presents the detailed investigation of the experimental tests carried out in the present study for the selection and characterization of model materials which are used to simulate the actual rock conditions. The basic properties of different constituents used in making the geometrical is also explained in this chapter. Finally, the various steps for the preparation of single and twin tunnel samples prepared in the laboratory are discussed. This chapter also explains the physical modelling of single and twin tunnels under static loading conditions. The

study is carried out for both lined and unlined rock tunnel models. The deformations obtained along the tunnel axis at different locations is recorded. Variations in deformation along the length of the tunnel have been determined. The effect of cover depth on the extent of deformation is calculated. In the case of twin tunnel samples, the effect of change in the spacing between the tunnel is explained. The effect of the cover depth and the presence of the liner material is also studied.

Chapter 5 outlines the numerical analysis of predicting the deformation behaviour of tunnels under static loading conditions. Numerical analyses are carried out for both single and twin tunnel models having different parameters. Experimental results obtained for different cases at different cover depths have been compared and validated with the results obtained from numerical modelling.

Chapter 6 discusses the various results obtained from the experimental and numerical study and their validation.

Chapter 7 discusses the various conclusions and findings from the study. This chapter also discusses the future scope of the thesis.

Chapter 2

LITERATURE REVIEW

2.1General

Tunnels have a wide range of applications such as railway tracks, highways, sewage tunnels, water supply and underground power plants, storage caverns, and other subsurface apertures. In the modern era, the construction of underground structures has proven a very effective solution to overcome the transportation problem. Therefore, for the safe and economical construction of these underground structures, it becomes very essential to understand the deformation behaviour of the tunnels due to the stresses acting on them. The tunnel excavated in the rock is subjected to various types of stresses. The design parameters of underground structures vary with the type of loads acting on them. The original state of strains and stresses caused by excavation combine to create the post-excavation state of stress in the structure. As a result, any design analysis requires the evaluation of the state of stress. The study of stresses surrounding underground openings provides insight into basic phenomena such as displacements and stress fields, as well as assisting in the provision of adequate support for the underground entrance.

Rail tunnels, highway tunnels, water tunnels, service and utility tunnels, tunnels for underground parking, underground passages, transit tunnels, hydropower tunnels, station tunnels and so on are all examples of tunnel excavation (Ramamurthy, 2015). These tunnel structures are subjected to various types of stresses. So it becomes very essential to protect them from distortion when subjected to different loading conditions. The common structure of tunnels in rock engineering is shown in Fig. 2.1.

Tunnels can be found in hard rock, soft rock, stiff soil, or mixed earth. The cutting or excavatin g process is very important in the overall design.

Any of the following methods can be used to excavate rock.

- Drilling and blasting
- Using tunnel boring machines (TBM).
- Road headers 97
- Sequential excavation with small mechanical equipment

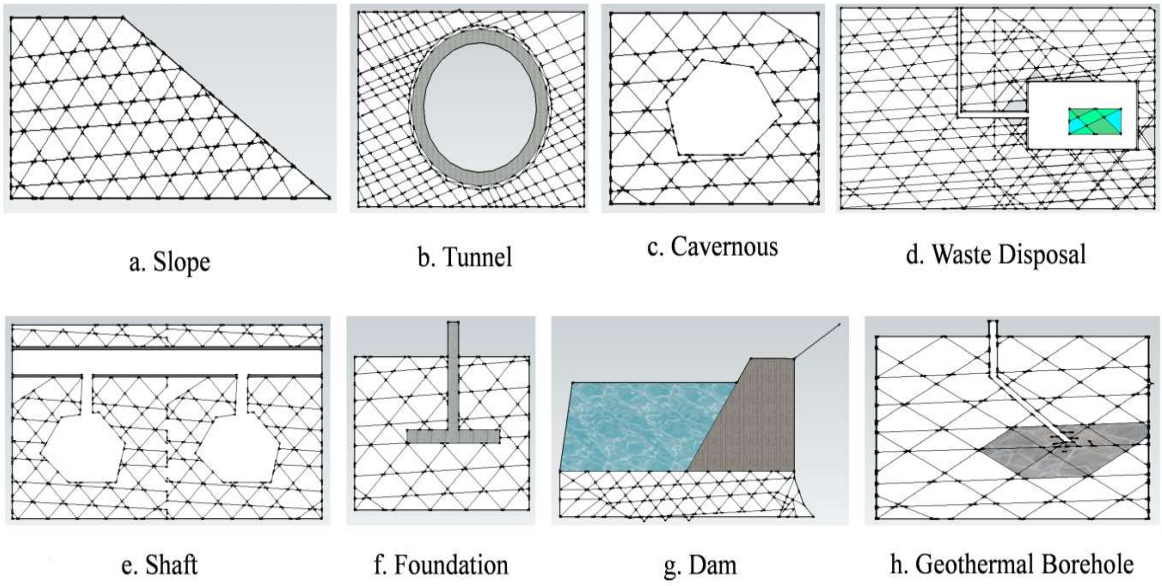

Fig. 2.1 Common structure of tunnels in rock engineering (Source: Google image)

2.2 Terminology in tunnelling

The various parts of the tunnel cross-section are donated by their name in Fig. 2.2 (Kolymbas, 2005) .

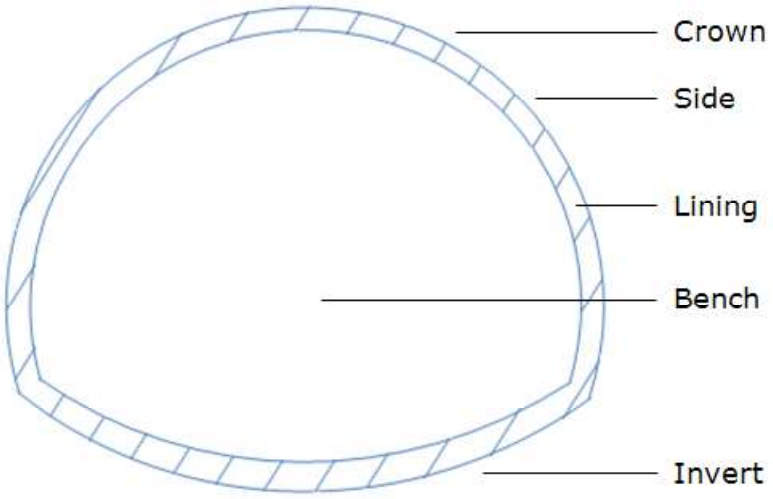

Fig. 2.2 Various parts of tunnel cross-section (Kolymbas, 2005)

2.2.1 Crown: The top surface of the tunnel is known as the crown of the tunnel also known as the roof of the tunnel. It is referred to as the highest point of the curved surface of the cross-section of the tunnel.

2.2.2 Lining: Lining act as a cover for rock and soil profile at the periphery of tunnel excavation. Lining can be of two types i.e. primary lining and secondary lining. Primary Lining is referred to as the structural lining which is placed against the ground surface whereas Secondary lining is the lining which is used for decoration, improving the flow of fluid and protection purposes.

2.2.3 Bench: The bench is referred to as the in-situ ground surface which is present at the lower face of the tunnel.

2.2.4 Invert: The bottom surface of the tunnel cross-section is referred to as invert.

2.3 Types of Tunnel Sections

The deformation caused along length of the tunnel section largely depends upon the shape of tunnel section. Hence the shape of tunnel section has an essential role in deformation behaviour of the tunnel. The various types of tunnel sections are shown in Fig. 2.3 (Ramamurthy, 2015).

2.3.1 Circular Section

The circular section is considered the most suitable section where there is heavy radial pressure is exerted on tunnels. This type of section is capable of taking heavy load exerted by overlying strata and water pressure. Various studies conducted by different researchers show that this is the best type of section. The circular section is generally used for sewers and water carrying pipelines purposes. This type of section is not recommended for railways and highways tunnel because in circular sections a lot of filling is required to obtain a flat surface. Lining can also be provided to the circular section so that it can withstand high external load conditions.

2.3.2 Horse Shoe Section

This type of section is considered the most popular and suitable type of section for highways and railway tunnels worldwide. It is a combination of a circular and segmental type of section. As the name implied, the shape of this type of section is similar to the horseshoe. This section is made of three components i.e. semicircular roof, arched sides and curved invert. The horseshoe type of section provides good resistance to the external ground pressure if it is lined with cement concrete. This type of section is most commonly found in the case of soft rock. Because of its flat floor surface, during the process of construction, it provides more space for keeping the material which is convenient for workers also.

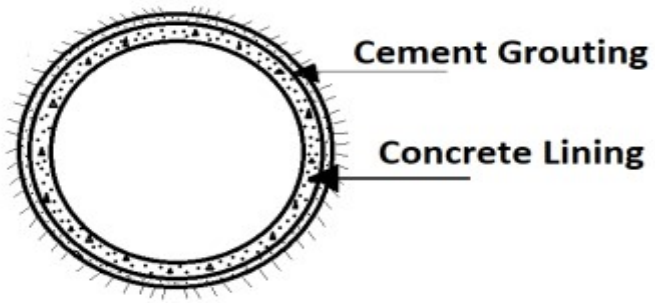

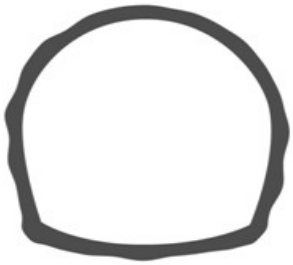

(a) Circular Section **(b) Horse Shoe Section**

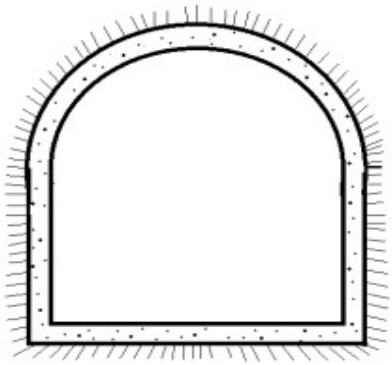

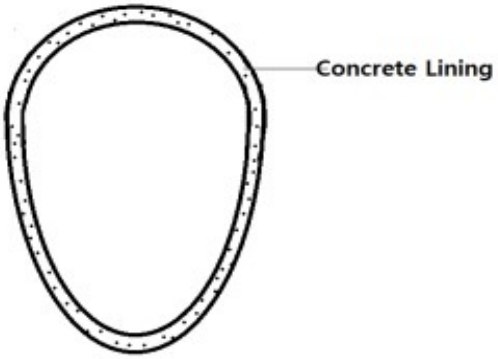

(c) D section or Segmental section (d) Egg Shaped Section

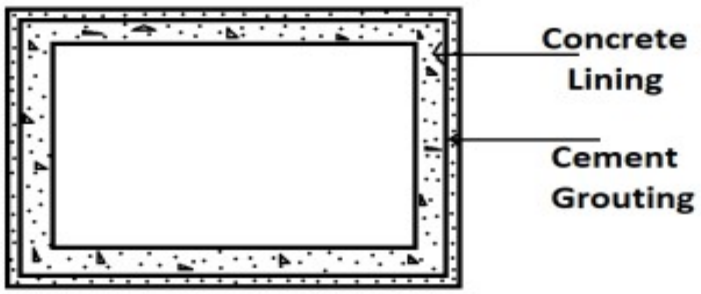

(e) Rectangular Shaped Section

Fig. 2.3 Various types of tunnel sections (Ramamurthy, 2015).

2.3.3 D-Shaped or Segmental Section

This type of tunnel section is also known as a segmental tunnel. This type of tunnel section is generally required for tunnelling in hard rocks. The type of section is similar to the English alphabet “D”. This section consists of two straight walls and one arched roof. The load is directly imposed on the segmental-arched section which further transfers the load to the side walls which are vertical in shape. In case of heavy overburden pressure, the side walls are constructed with reinforced concrete. This type of tunnel section is also known as a segmental tunnel section.

2.3.4 Egg Shape Section

This type of tunnel section is used for carrying sewage as it provides self-cleansing velocity in weather flow also. The egg-shaped section can resist both external and internal pressures due to its circular walls geometry. This type of section is not recommended for traffic purposes as the construction process of the egg shape section is quite difficult.

2.3.5 Rectangular Shaped Section

A rectangular type of tunnel section is highly used in the case of hard rock strata. This type of section is also used for pedestrian traffic. The disadvantage of a rectangular type of section is that it is very costly to construct and also the cost of constructing a rectangular section is also very high.

2.4 Method of Tunneling

During the construction of tunnels, different types of ground conditions have to face.

Sometimes tunnels are constructed in soft ground conditions, where the construction of tunnels

is relatively easy. In some cases, tunnels are excavated through hard rock having a high value of compressive strength. In such cases, the excavation of tunnels becomes a challenge. The method of excavation of tunnels mainly depends upon the types of ground conditions through which the tunnels pass. Some methods of construction of tunnels are discussed below.

1. Full Face Method
2. Heading and Benching Method
3. Drift Method
4. Pilot Tunnel Method
5. Perimeter Method

2.4.1 Full Face Method

The full-face method is used for short tunnels i.e. less than 3metres length tunnels. In this method, a lot of holes are drilled after placing vertical columns at the face of the tunnel section as shown in Fig. 2.4. After the explosive is kept in these holes and ignited. The removal of muck is done after that. This method is suitable for tunnels having a diameter of less than 6metres.In this method of tunnelling, minimum equipment is required and it is easy to operate as the extent of the magnitude of surface disturbance s also less in this method.

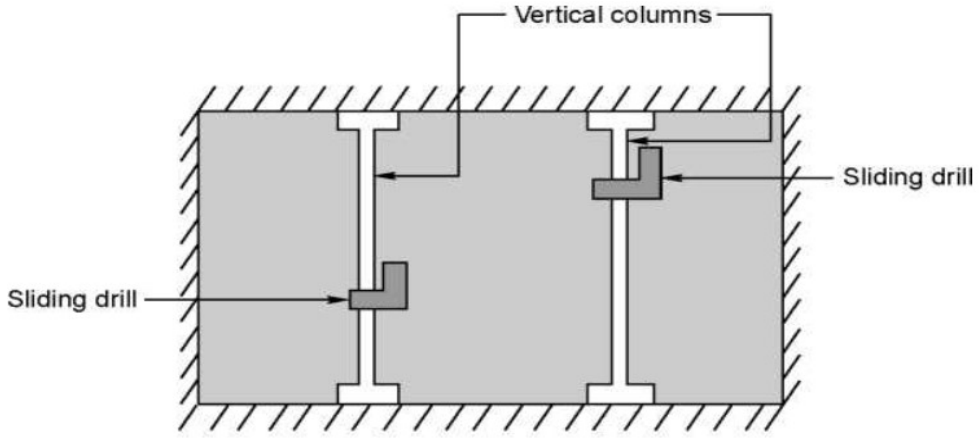

Fig. 2.4 Full Face Method

2.4.2. Heading and Benching Method

The heading and benching method is commonly used for the excavation of railway tunnels. In the heading and benching method, the top portion known as the heading is ahead of the bottom portion by 3.70 to 9.6 metres. In the case of tunnelling in hard rock, the heading will be bored first and then the drilled holes will be driven for the bench as shown in Fig. 2.5. This method requires very less explosive as compared to the full-face method. The use of this method has decreased nowadays because of the development of drill carriage.

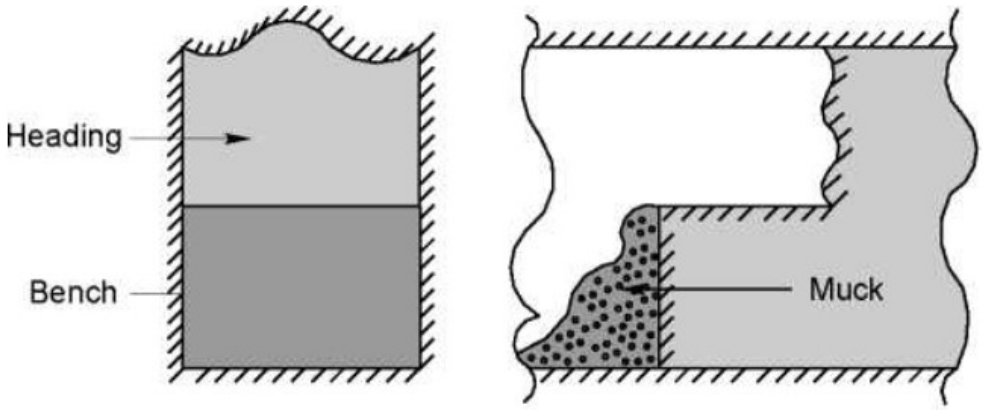

Fig. 2.5 Heading and Benching Method

2.4.3. Drift Method

Adrift is 3x3 meter tunnels excavated into the rock, the portion of which gets extended in consecutive procedures until it becomes equal to the tunnel. In this method, holes are created around the drift with the help of the drilling process. After that these drilled holes are injected with explosives which are further ignited. As a result of which the size of the drift increases which can be further matched to the size of the tunnel section required as shown in Fig. 2.6. The placement of the drift is determined by local factors, and it could be in the centre top,

bottom or side. The central drift is the greatest alternative, according to practical experience, because it provides ventilation and needs minimal explosives. On the other hand, the side drift has the advantage of allowing timber to be used as roof support.

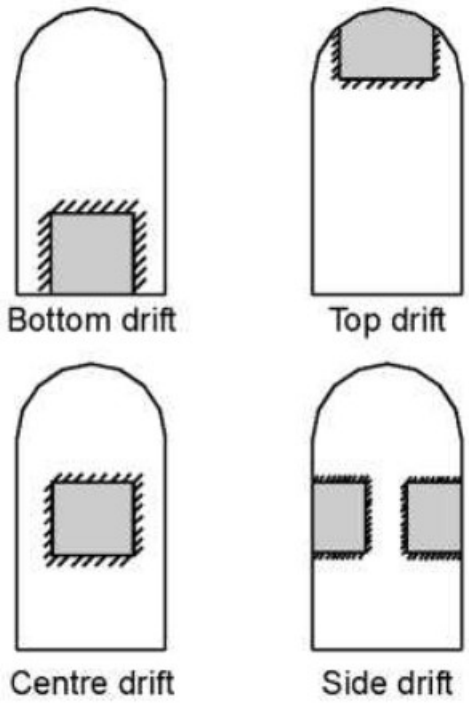

Fig. 2.6 Drift Method

2.4.4. Pilot Tunnel Method

In this method, two tunnels are dug one is known as the main tunnel and the other is known as the pilot tunnel. The cross-section of the pilot tunnel is approximately 2.4 m x 2.4 m. In this method, the main tunnels and pilot tunnels run parallel to each other and are connected to the main tunnel's centre line through many crosscuts. The main tunnel is then excavated from several points as shown in Fig. 2.7.

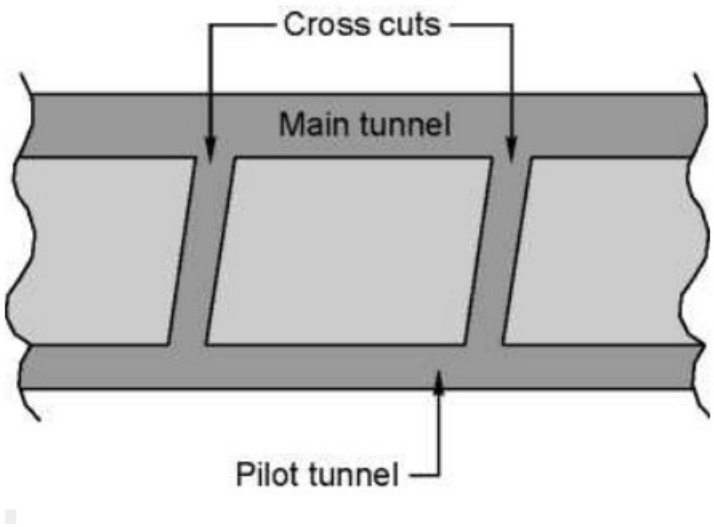

Fig.2.7 Pilot Tunnel Method

2.4.5. Perimeter Method

This method is also known as the German method. In this method, the excavation is done along the periphery of the tunnel cross-section.

2.5 Stresses around an underground opening

The study of the stresses acting on the underground structure is very essential as it gives an idea about the general deformation behaviour of the tunnels which is helpful in deciding the design parameters of the tunnel for safe and economical design. During the designing of the tunnel, evaluation of stresses and displacement around the circular opening is a primary requirement. There are various methods are available which are helpful in determining the stress distribution and displacement behaviour of tunnels when they are subjected to different loading conditions. Numerous solutions have been given for the distribution of stresses around the circular opening. A lot of researchers had given their theories and solutions for the stresses acting around the underground structures. Kirsch was the first who had given the analytical solution for the stress

and displacement around the circular opening in plain strain conditions in 1898 as shown in Fig. 2.8. According to Kirsch, for a circular opening of radius "a" and radial distance "r", the expression for radial, tangential and shear stress are given.

$$\sigma_r=1/2.(\sigma_x+\sigma_z).(1-a^2/r^2)+1/2.(\sigma_x-\sigma_z).(1+3a^4/r^4-4a^2/r^2).\cos2\theta \quad (1)$$

$$\sigma_\theta=1/2.(\sigma_x+\sigma_z).(1+a^2/r^2)-1/2.(\sigma_x-\sigma_z).(1+3a^4/r^4).\cos2\theta \quad (2)$$

$$\tau_{r\theta}= -1/2.(\sigma_x-\sigma_z).(1-3a^4/r^4+2a^2/r^2).\sin2\theta \quad (3)$$

where, σ_r= radial normal stress

σ_θ= tangential normal stress

$\tau_{r\theta}$ =shear stress

σ_z= γ.h= overburden pressure

σ_x= K.σ_z = horizontal pressure

a= radius of the opening

r = radial distance from the centre of opening

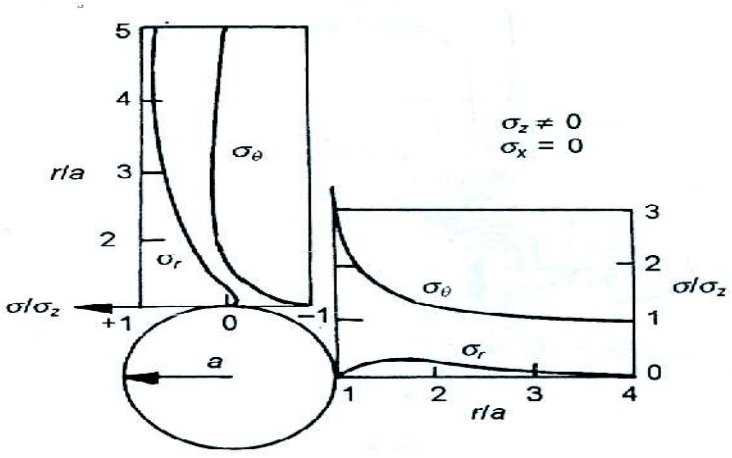

Fig.2.8: Tangential and radial stresses around circular openings

2.6 Factors affecting the stability of Tunnels

2.6.1 Type of Tunnel Section

Khan et al. (2015) conducted a study on the interaction behaviour of tunnel lining with its surrounding rock mass with change in stresses. In this study different tunnels section i.e. circular, semicircular and horseshoe were considered in both fractured and unfractured rock as shown in Fig. 2.9. Stress and deformation are analyzed in all three sections and the most suitable section is determined. Numerical modelling using FEM was done for modelling and meshing of the tunnel in 2D. From the results, it was concluded that the semicircular section is the best type of tunnel section as it experienced minimal deformation whereas, in the case of plain rock, the horseshoe type of tunnel section is the best section from a vertical stress point of view. For fractured rock, the most suitable section from both points of view is a semicircular section.

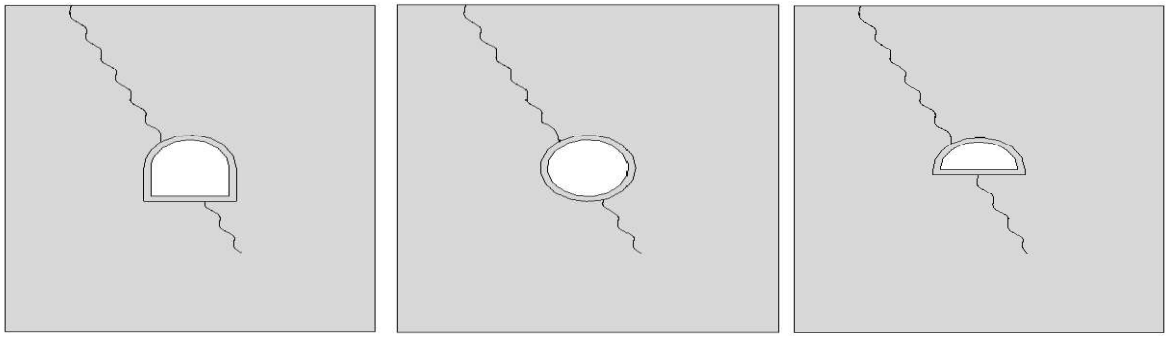

Fig. 2.9 Shapes of different tunnel sections (Khan et al. 2015)

Elshamy et al. (2013) conducted a study to determine the effect of different shapes of the tunnel on its deformation behaviour. In this study, a plain strain numerical model is generated with the help of software. The variation in the displacement of the tunnel, internal forces acting along the length of the tunnel and stress acting nearby the vicinity of the tunnel section are studied and their variation with change in the thickness-radius ratio (t/r) is also investigated. The study

is conducted on circular, rectangular and elliptical types of tunnel sections as shown in Fig. 2.10. The displacement experienced along the ground surface is noticed for various types of shapes and sizes of the tunnel section. From the result obtained from the study, it is noticed that the circular tunnel is the best shape of twin tunnels as it experienced the minimum displacement as compared to the other type of tunnel sections.

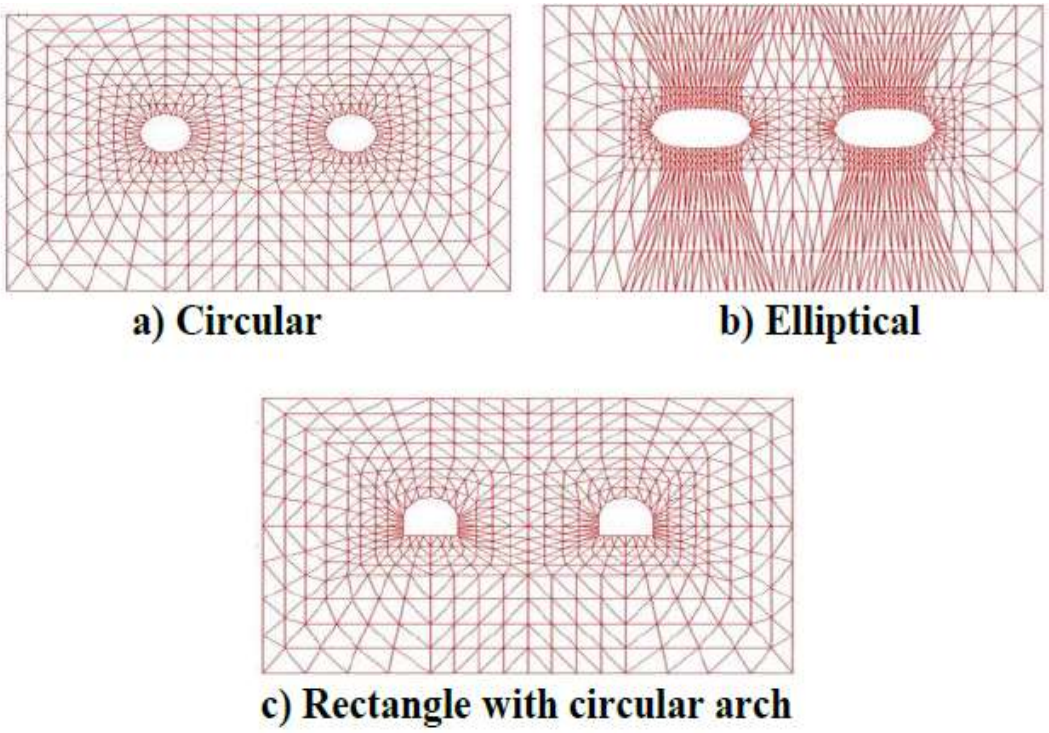

Fig. 2.10 Layouts of different shapes of Twin Tunnel (Elshamy et al. 2013)

2.6.2 Effect of Overlying Strata

Nunes and Meguid (2009) made an attempt to investigate the effect of the stresses acting in the tunnel lining with the change in the thickness of the above lying strata. An experimental investigation is done to achieve the objective of the study. The effect of stiffness ratio and effect of layer thickness is also studied. Numerical modelling is also done by using Plaxis V8 software. The meshing given to the soft soil layer and stiff layer is shown in Fig 2.11. From the

results obtained from the study, it can be concluded that the deformation behaviour of tunnels and stresses acting along the length of the tunnel mainly depends upon the stresses coming from the above lying strata. The thickness and location of the overlying layer above the tunnel also have a significant effect on the stresses acting on tunnels.

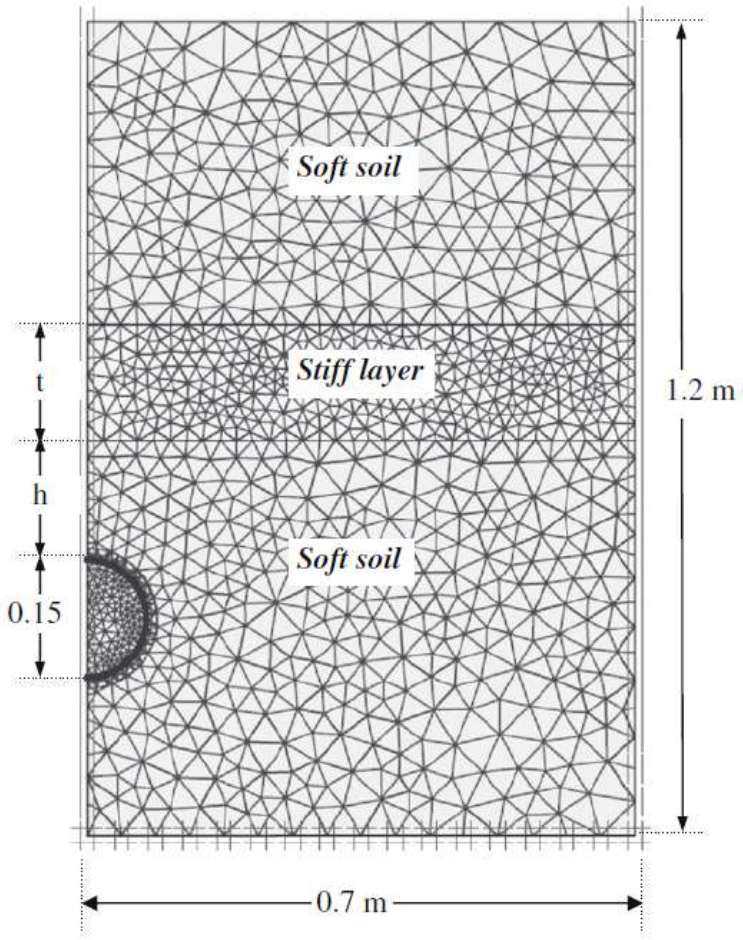

Fig. 2.11 Finite element mesh in the study (Nunes and Meguid, 2009)

2.6.3 Type of Loading

Hosseini et al. (2010) conducted a study to analyze the effect of dynamic loading occurring due to earthquakes on the tunnel structures. The effect of forces created due to the dynamic loading on the deformation behaviour of tunnel structures is studied. Horseshoe type tunnel section is taken into consideration. The result of the study shows that, when the dynamic stress due to an

earthquake is applied, the stress and displacement in the tunnel periphery are increased as shown in Fig 2.12. It was also noticed that among all elastic waves, love waves are the most dangerous for the stability of the underground structures. Therefore, for the stability of the tunnel, it is important that the support system must be reinforced. It was also concluded that the flexibility of the tunnel structure decreases with an increase in the thickness or stiffness of the support system.

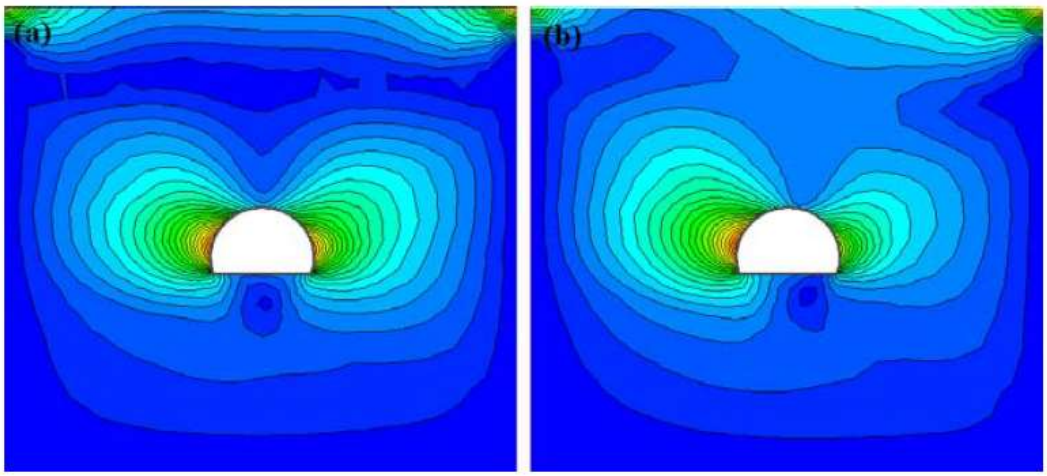

Fig. 2.12 Displacement obtained in (a) static loading and (b) Dynamic loading.

Mishra et al. (2016) made an attempt to understand the damage to shallow tunnels under static and dynamic loading with the help of numerical modelling. In this study, two synthetic materials (mix material and POP) were to simulate the soft rock conditions. The results obtained from numerical modelling were then validated experimentally. From the results, it was concluded that the length of the cracks in case of static loading is large as compared to dynamic loading and the zone is fully crushed in case of dynamic loading.

2.6.4 Effect of joints in tunnel

Jia and Tang (2008) conducted a study on the deformation of the tunnel in jointed rock mass using numerical software. The study deals with the influence of different dip angles of the

layered joint on the stability of the tunnels. Dimensions of the model are kept 40meter x 40 meters. Five models were prepared with dip angles of 0°,30°,45°,60° and no joint in the first model. From the results, it can be noticed that the dip angle and lateral pressure have a considerable effect on the failure of the tunnel. As the dip angle of the joint increases, the displacement of the sidewall also increases.

Sakurai (2014) investigated the analysis of jointed rocks strengthened by rock bolts in tunnelling. Physical tests were performed in the laboratory to investigate the reinforcement effect of rock bolts. According to the findings, rock bolt placement enhances the value of young's modulus and compressive strength, particularly for hard rock. Bolts have a lower reinforcement effect on soft rock than on hard rock. Zhu et al. (2015) conducted a study to determine the effect of above lying stresses on the deformation behaviour of tunnels. For that, three typical tunnel models are prepared and the materials used for tunnel model formation are cement mortar and sandstone. The first one is a regular tunnel model loaded with various orientation principle stresses. The second one is a tunnel with various inclination cracks. And the third one is a tunnel with a fixed angle crack loaded by various orientation principle stresses. A cement mortar tunnel model and its loading device are shown in Fig. 2.14.

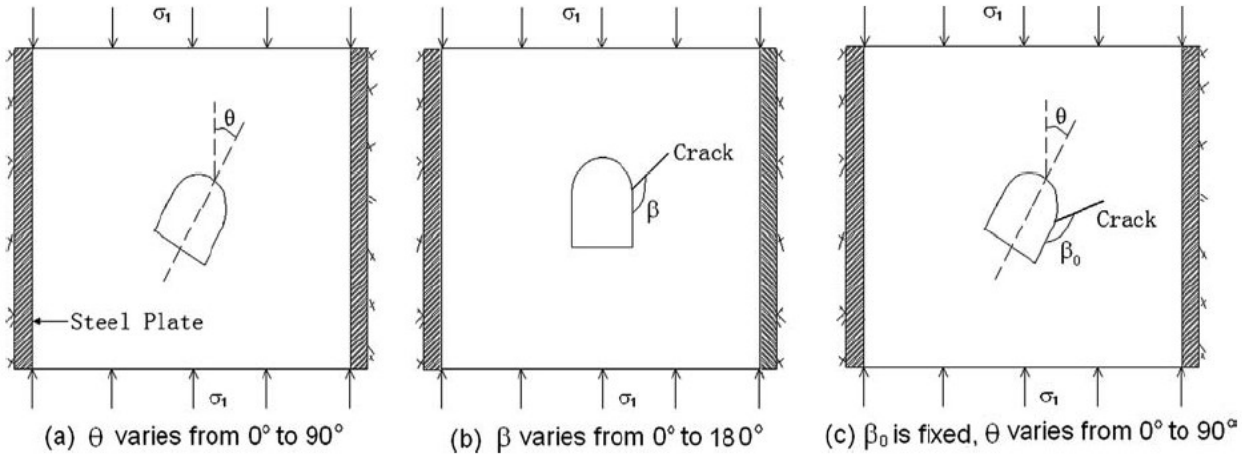

Fig.2.13 Test model of tunnel (Zhu et al. 2015).

.

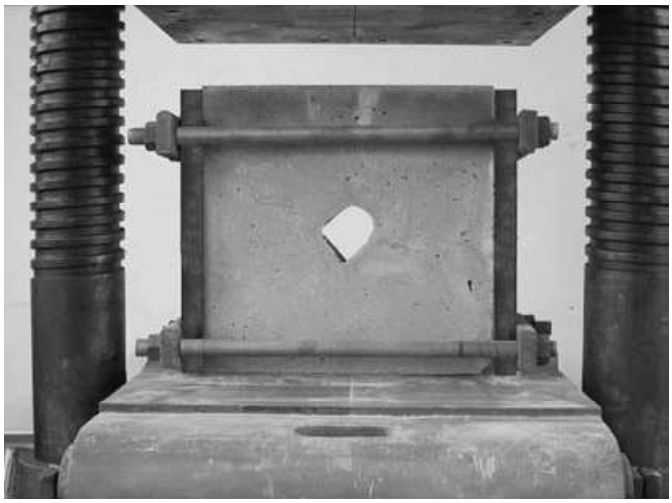

Fig. 2.14 A cement mortar tunnel model and its loading device (Zhu et al. 2015)

In this study, an attempt is made to find out the effect of the crack inclination angle on the tunnel stability. A 5cm radial crack with different inclination angles β at tunnel spandrels is made as shown in Fig.2.13. The angle β varies from 0° to 180° and the interval is 10°. The relationship between the compressive strength and the crack inclination angle β is obtained. The results show that the critical compressive stress varies with the angle of inclination of the crack. The critical stress lowers as β increases from 0° to 135° and the critical stress is lowest when β is about 135 ° As an increase in the angle of inclination β from 135° to 180°, the critical stress increases. For the regular tunnels under compression, when the inclination angle between the tunnel axis and major principle stress is 45°, the tunnel stability is low.

2.6.5 Effect of Alignment of tunnels

Oliaei and Manafi (2015) and Moussaei et al. (2019) conducted a study on twin tunnel interaction under static loading conditions. The study is conducted on horizontal, vertical and inclined tunnels as shown in Fig.2.15. From the results, it has been noticed that vertically

aligned tunnels experienced the maximum settlement whereas the settlement is recorded as a minimum in the case of horizontally aligned tunnels. It is also concluded that with an increase in distance between the tunnels, the settlement decreases. 9

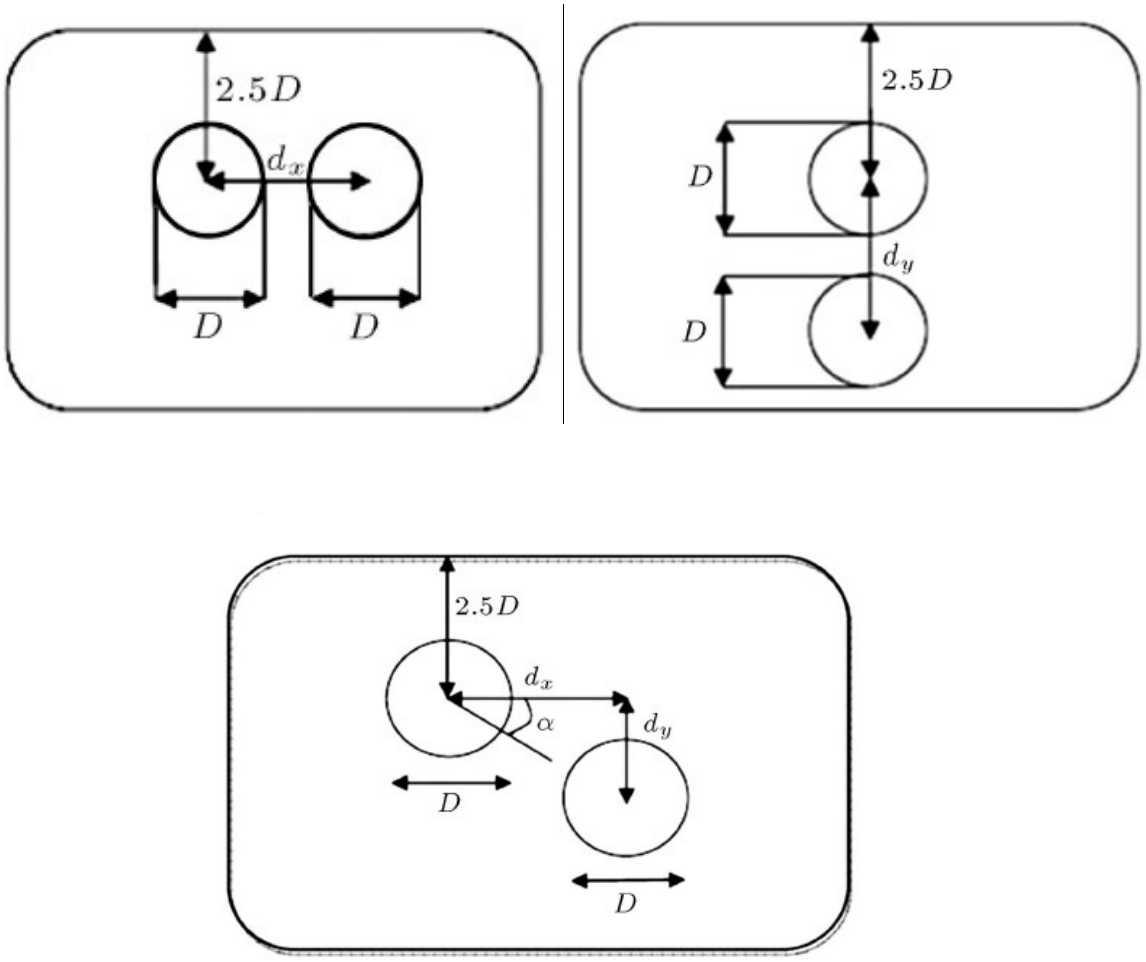

Fig. 2.15 Geometric alignment used in the study (Oliaei and Manafi 2015)

Chehade and Shahrour (2008) conducted a study on the interaction behaviour of twin tunnels with the help of numerical software. The effect of the construction procedure of twin tunnels and their relative position on the settlement behaviour is investigated. Three different types of tunnel alignment are used in the study i.e. horizontally aligned tunnels, vertically aligned tunnels and inclined tunnels as shown in Fig.2.16. From the results, it can be concluded that

higher settlement will occur if the upper tunnel is constructed first and it can also be concluded that in the case of vertically aligned tunnels, the extent of the settlement will be more as compared to horizontally aligned tunnels. The interaction behaviour between the twin tunnel and underground parking is studied by Nematollahi and Dias (2020) and Shaofeng et al. (2018) and the result showed that there is a significant effect of the construction procedure of the tunnel on its stability behaviour.

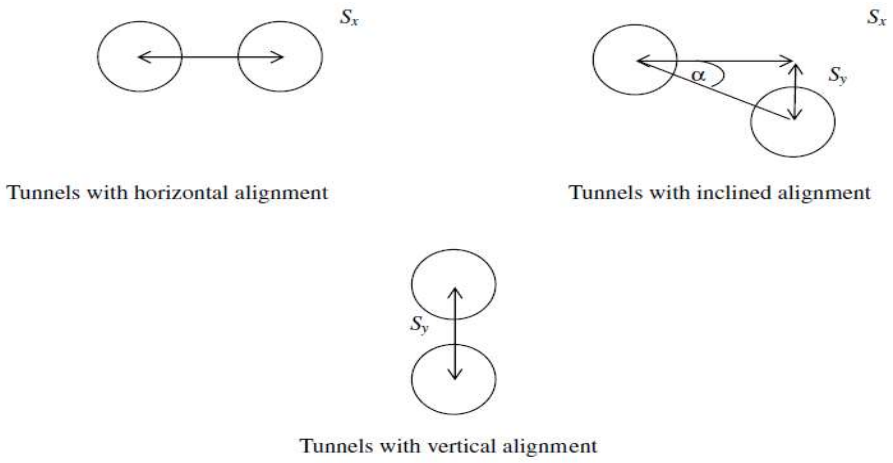

Fig. 2.16 Different alignments of Twin tunnels adopted for the study

(Chehade and Shahrour, 2008)

2.7 Physical Modelling of tunnels

Atkinson and Potts, (1977) conducted a study on the stability of a shallow circular tunnel. An experimental and theoretical study on the stability behaviour of a circular tunnel is investigated in the present study. Small-scale model experiments in the laboratory were used in the experimental inquiry. All model tests were conducted in plane strain with Leighton Buzzard sand, with experiments with and without surcharge loading being reported. The upper and

lower bound theorems are used in the theoretical analyses, and predictions of collapse pressures based on these theoretical results are demonstrated to closely match the values found in the model testing. Li et al. (2005) conducted a study to investigate the effect of displacement, yield zone and stresses on underground structures. Then the results of the physical and numerical models were compared the results show that the effect of physical model tests was more satisfactory as compared to numerical simulation. It was also concluded that the horizontal displacement for the two methods was quite the same but the vertical displacement in numerical simulation is a little less than in the physical model. The yield zone of the model test was larger than those of the numerical simulation. Stress concentration was almost the same in range and magnitude. Fig. 2.17 shows the photograph of the three-dimensional geomechanical model test platform.

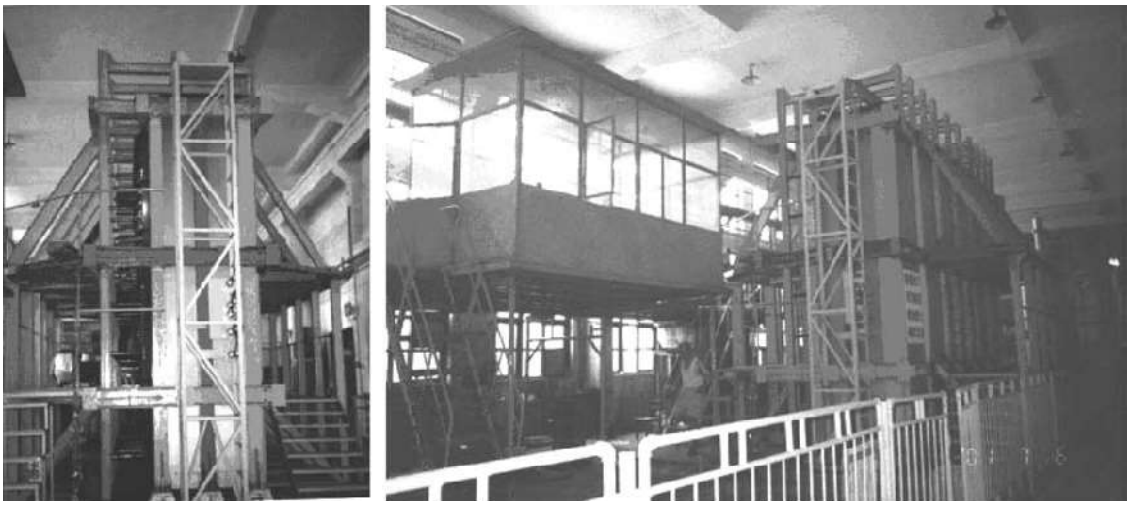

Fig.2.17 Photograph of 3-dimensional geo-mechanical model test platform (Li et al. 2005)

Li et al. (2009) investigated the mechanical behaviour of rock under the effect of static loading. From the results, it is noticed that the strength of rock under the effect of static-dynamic loading is more as compared to the individual static and dynamic strength. Rock strength under paired loads increases with increasing strain rates at the same axial pre-stress. Rock falls in tensile mode when subjected to combined static and dynamic loads. Sagong et al. (2011) conducted a

study to determine the effect of fracture in rock on tunnel stability behaviour with the help of experimental and numerical studies. A jointed rock model is prepared in the laboratory having dip angles of 30°, 45° and 60° as shown in Fig.2.18. From the results, it can be concluded that tensile cracks are observed in the tunnel model under a low joint angle. The experimental results are further compared with the numerical results and it can be concluded that the results obtained from both experimental and numerical analysis are in close agreement with each other.

Fig. 2.18 Jointed rock tunnel model prepared in laboratory (Sagong et al. 2011)

Yingjie et al. (2014) investigated the failure process of weak rock surrounding the tunnel using physical and computational methods. The displacement and collapse behaviour of the weak rocks that surround a tunnel is investigated. According to the findings, the weak rocks surrounding the tunnel fail predominantly due to shear wedge failure in the minimal principle stress direction, causing the tunnel arch to collapse as seen in Fig. 2.20. Shear strain also caused a shear wedge in the middle of the tunnel and a crack surrounding the tunnel arches, and the

arches collapsed as a result of the combined effects of shear stress and tensile stress, as illustrated in Fig. 2.19.

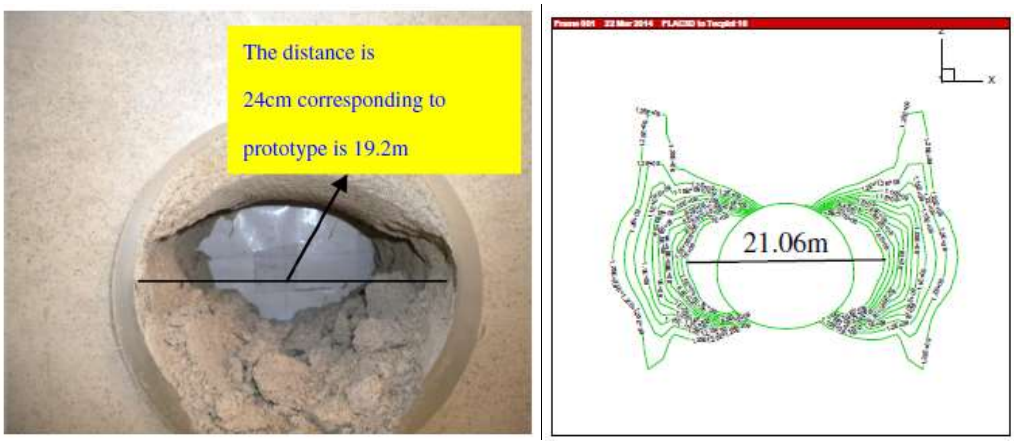

Fig.2.19 Damage zone from the numerical and experimental results.

Fig. 2.20 Experimental results of gradual failure.

Yang et al. (2019) conducted a study on the effect of non-persistent joints on the stability behaviour of circular opening. The study is conducted with the help of experimental analysis further the results are compared with numerical modelling. Different tunnel models having joint inclination angles as 0, 15°, 30°, 45°, 60°, 75° and 90° are prepared and tested under compression loading as shown in Fig.2.21. From the result, it can be concluded that the joint provided at an inclination of 90° has the least effect on the mechanical behaviour of the tunnel model.

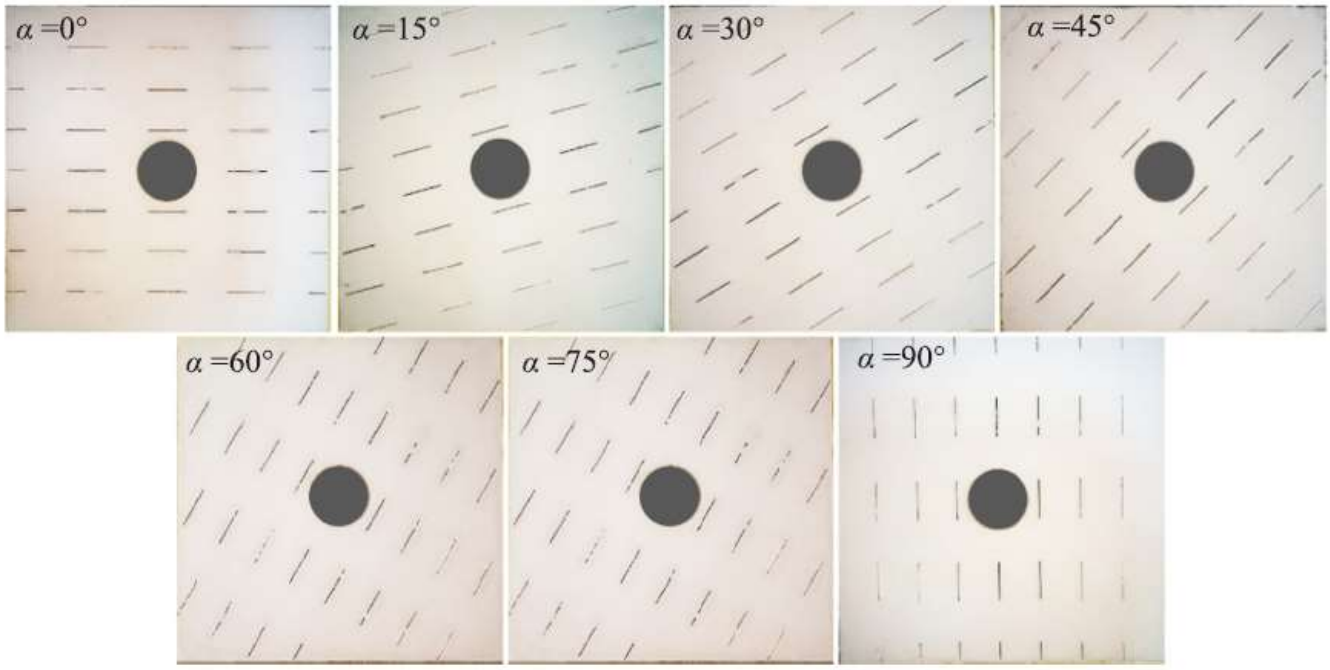

Fig.2.21 Joints given in tunnel mode at different inclinations (Yang et al. 2019)

The stability behaviour of the face of a tunnel largely depends upon the cover depth and diameter of the tunnel opening in the case of circular tunnels as investigated by Ahmed and Iskander (2012), Kumar and Shrivastava (2019a) and Zaid et al. (2019). A study conducted by Shrivastava and Rao (2015) and Shrivastava and Rao (2018) concluded that the shear behaviour of infilled rock joints depends upon the thickness of the infill material. The presence of asperity also affects the shear behaviour of rock joints Shrivastava and Rao (2011). Rathod et al. (2012) conducted a three-dimensional stability assessment of jointed rock using a numerical modelling

technique and concluded that the presence of discontinuities in the rock mass has a significant effect on the stability behaviour of rock slope. Nguyen and Nguyen (2015) made an attempt to evaluate the stand-up time of the surrounding rock mass of the tunnel using analytical solutions. An attempt is made to study the influence of tunnel depth, rock mass quality and maximum displacement on the stand-up time of the rock mass. From the results, it can be concluded that the stand-up time decreases with an increase in the tunnel depth. It can also be observed that in the case of deep tunnels, the stand-up time of the surrounding rock mass is less as compared to the shallow tunnels. The stand-up time will increase with an increase in the increase in maximum allowable displacement of the rock mass. Kumar and Shrivastava (2017) and Kumar and Shrivastava (2019b) reviewed the various factors which affect the stability of underground structures. It was concluded that the stability of tunnels depends upon many factors such as types of tunnel section, crack inclination angle and stress caused on tunnels due to overlying strata.

Chen et al. (2016) conducted a study to determine the deformation behaviour of brick-lined tunnels under the effect of extreme loading. The study is conducted with the help of physical modelling and further validated with numerical modelling. A series of small scale physical tunnel model tests are conducted under static uniform and concentrated load. Numerical modelling is done using UDEC and Flac. Then the Numerical results are compared to the physical model test results to assess the overall stability of the tunnel. The results show that the model tests under concentrated load showed more brittle behaviour than under uniform load. It can also be concluded that with an increase in the depth the concentrated load acting at the centre of the arch fails easily. The effect of uniform loading is experienced along the tunnel arch. The comparison of the deformation obtained from numerical modelling with the deformation obtained from physical modelling is shown in Fig. 2.22.

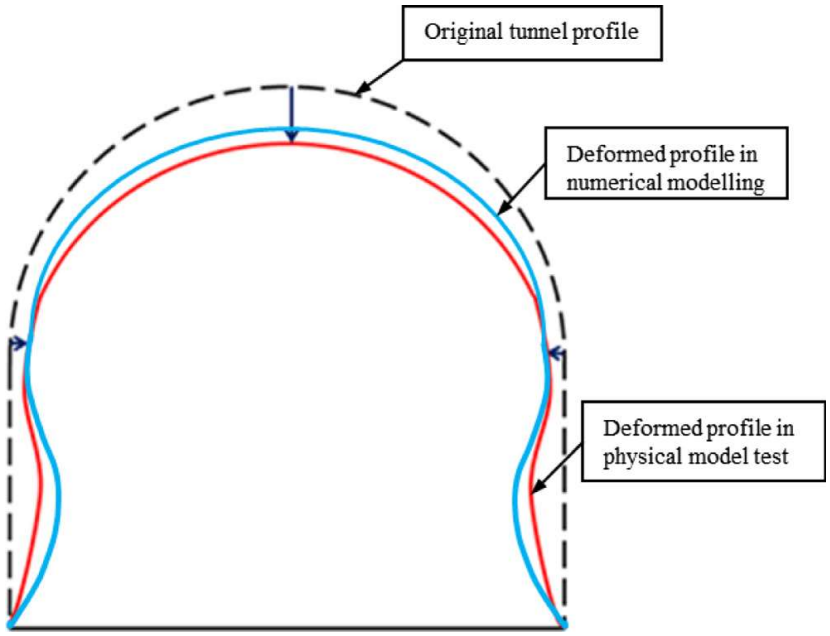

Fig. 2.22 The comparison of the deformation obtained from numerical modeling with the deformation obtained from physical modelling (Chen et al. 2016).

Kusui al. (2016) investigated the deformation behaviour of tunnels under the effect of high stresses. The tunnel models were constructed by drilling into (400W X 400H X 200D mm) blocks of sandstone having a UCS ranging from 50 to 120 MPa. The block was loaded vertically at a constant loading rate. From the results, it can be concluded that the tunnel is very unstable in the case of high loading conditions. When high stresses are applied the tensile cracks are noticed on the crown and floor of the tunnel. Rao et al. (2016) conducted a study to determine the effect of different loading conditions on tunnel lining in soft rocks. From the results, it was concluded that the length and shape of the fracture zone in tunnels depend upon the type of loading and depth of the tunnels

Mishra et al. (2017) made an attempt to study the deformation behaviour of lined and unlined tunnels at shallow depths. The objective of the study was to simulate the in-situ conditions with

physical modelling. For the testing purpose, a synthetic model material is proposed, which consists of 50% Plaster of Paris, 35% sand and 15% clay. From the results, it can be concluded that It is observed that the displacement at the loading surface increases with an increase in the number of cycles Therefore the number of cycles required for the damage of the unlined tunnel is less as compared to the lined tunnel. It is also concluded that the strain in the lined tunnel is less than the strain in the unlined tunnel because of the resistance offered by the tunnel lining. Mishra et al. (2018) discuss the effect on the shallow tunnel under static and dynamic loading. The result shows that the strength of the rock plays an important factor in stability behaviour. It is also observed that the extent of damage is maximum at the centre of the tunnel axis and it keeps on reducing towards the face of the tunnel.

Mishra et al. (2021) conducted a study to investigate the stability behaviour of a single tunnel in soft rock. The experimental results are validated with the numerical results and it is found that they are in good agreement with each other. Single tunnel rock models of different cover depths are prepared in the laboratory. Then these models are tested under dynamic loading conditions. From the results, it is concluded that the deformation in tunnels depends upon various factors such as the cover depth of the tunnel, the mechanical strength of the rock mass and the intensity of the drop load. Sharma et al. (2018) conducted a study to determine the effect of the cover depth of the tunnel on its stability behaviour under the effect of impact loading. The study is conducted with the help of physical modelling. Rock tunnel models are casted in the laboratory having three different cover depths i.e. 25mm, 35mm and 50mm as shown in Fig. 2.23. The size of the rock tunnel model is kept at 350x300x300mm (LxWxH).LVDTs are used to take deformation in different positions along the tunnel axis. The photograph of the experimental setup used in the study is shown in Fig. 2.24. From the results, it can be concluded that the cover depth of the tunnel plays an important role in the stability behaviour of the tunnel. Rock

tunnel models having the lowest cover depth i.e. 25mm are subjected to the highest deformation whereas the extent of deformation in the case of the tunnel having the highest cover depth i.e. 50mm is the lowest.

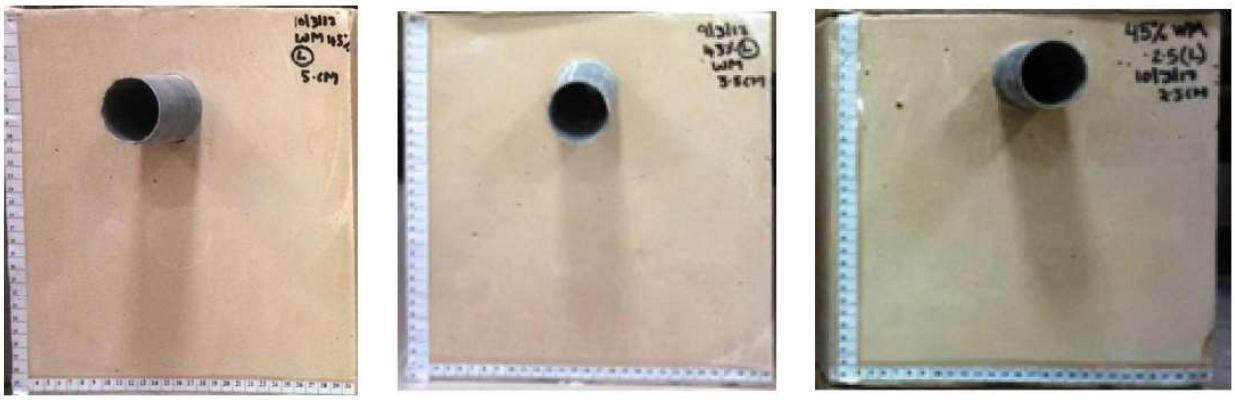

Fig.2.23 Rock Tunnel models having different coverdepths (Sharma et al. 2018

Fig.2.24 Photograph of the experimental setup used in the study (Sharma et al. 2018)

Chen et al. (2019) conducted a study to develop an analytical solution for the developing stresses and deformation occurring in twin tunnels at greater depths. The effect of various

factors such as the geometrical design of tunnels, spacing between the twin tunnels, and diameter of the tunnels on stress and displacement behaviour is also studied. The effect of the installation of liner material and the interaction of liner material with the geometrical is also investigated. In the study, the main focus is on computing the stresses and deformations occurring in the geo-materials and lining material. Then the analytical solution is compared with the numerical solutions for the general case. From the results, it is concluded that the analytical solutions are in good agreement with the numerical solutions. It is also concluded that there is a significant effect of the spacing between the tunnels on its stress deformation behaviour. In the case of twin tunnels, the effects of deformation become zero if the spacing between the tunnels is greater than six times the radius of the tunnel.

He et al. (2019b) conducted a study on the interaction behaviour of twin tunnels under dynamic loading conditions in multi-layered half-space. In this study, a semi-analytical model is developed to study the interaction between the twin tunnels. Then the comparison of the existing model is done with the existing numerical model for proper validation. From the numerical results, it is concluded that there is a significant effect of the ground vibration on the existence of the surrounding tunnel. It is also concluded that the stiffness of the layer lying above the tunnel has a great effect on the dynamic behaviour of the twin tunnel whereas the effect of the stiffness of soil beneath the tunnel has very less effect on the dynamic interaction of twin tunnels. He et al. (2019a) conducted a study to determine the effect of seismic interaction of two neighbouring tunnels on the vibration-induced from railways under saturated conditions. The simulation of the twin tunnel is done with the help of Flugge shell theory. From the results, it is concluded that the neighbouring tunnels have a very significant dynamic interaction on vibration which is induced from underground railways. It is also concluded that the geometrical dimension of the neighbouring tunnels has a significant impact n the dynamic

interaction between the adjacent tunnels. With an increase in the radius of neighbouring tunnels, there is a significant effect on the interaction behaviour of two adjacent tunnels.

Rahaman et al. (2020) conducted a study to determine the stability behaviour of single and twin unlined tunnels of horseshoe shape in the rock mass. The tunnels are subjected to overlying stresses. The effect of the C/D ratio and spacing between the twin tunnels is also studied. From the results, it is concluded that with an increase in spacing between the tunnels the deformation effect will decrease. It is also concluded that in the case of railways and road tracks, circular tunnels are more expensive than horse-shoe tunnels. Elwood et al. (2016) conducted a study to determine the deformation effects in twin tunnels which are excavated close to each other. From the results, it is concluded that in the case of materials having the same properties, the damage risk to the surrounding structures is minimum when the pillar width is 0.5 times the diameter of the tunnel.

Sohaei et al. (2020) conducted a study to determine the settlement of the ground surface on the construction of the tunnel. An experimental set is also developed for this study as shown in Fig. 2.25. A box of dimension 600x600x500mm (LxWxH) is fabricated in the laboratory. Aluminium liner is used for tunnel lining. Four LVDT are also used to record the displacement in the transverse and longitudinal directions. The relative density of sand varies as 30, 50 and 75% and the cover to diameter ratio is kept at 3. From the results, it can be concluded that with an increase in the relative density of sand, there is a decrease in the settlement of the surface.

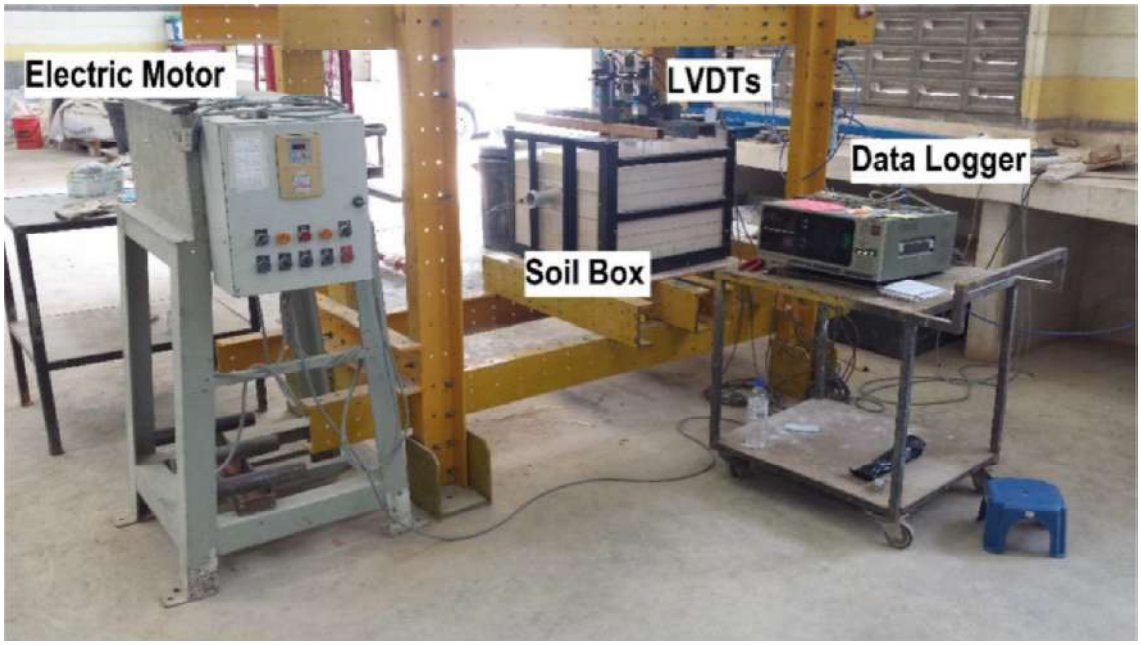

Fig.2.25 Photograph of the experimental setup (Sohaei et al. 2020).

Zheng et al. (2021) conducted a study on the uplift behaviour of twin tunnels under seismic loading. The uplift movement of twin tunnels under different positions and spacing are studied. From the results, it is concluded that the liquefaction around the tunnel and the generation of excess pore water pressure are essential for the uplift. Wang et al. (2020a) conducted an analytical study on the interaction behaviour of the existing tunnels and newly constructed tunnels at shallow depths. An analytical solution is given for the stress developing in the ground and the displacement occurs due to the interaction of the newly constructed and exiting tunnel. The various factors such as the size of the tunnel, various arrangements of the tunnel and ground rheology are taken into consideration. Then the analytical results are compared with numerical modelling results for proper validation. From the results, it is concluded that the time required for excavating a new tunnel affects the displacement around the existing tunnel. Wang et al. (2020b) used empirical solutions and computational modelling to demonstrate how the excavation of a new tunnel influences the deformation behaviour of an existing tunnel and

found that if a new tunnel is excavated near an existing tunnel, the excavation period of the new tunnel affects the displacement encountered in the existing tunnel. Wang et al. (2020) explain the effect of dynamic loading on the cross tunnel lining with the help of experimental tests and further validate the results with numerical modelling. For the experimental test, a hydraulic loading system is developed which consists of a test box of size 400x300x250mm (LxBxH). The deformation that occurs in the tunnel lining is computed with the help of strain gauges. The results show that the value of the deformation is maximum at crossing positions of tunnel lining and is significantly affected by the magnitude and intensity of the loading. Cheng et al. (2021) explained the effect of loading on the longitudinal deformation that occurs in the tunnel lining with the help of experimental and analytical study and observed that as the ground conditions change the deformation in the tunnel also gets affected. Singh et al. (2017) conducted a study to determine the behaviour of metamorphic rock in the Rohtang tunnel. The study was conducted on three types of rocks which are extracted from the site i.e. Phyllitic Quartzite, Quartzitic Phyllite and Migmatic gneiss. The conclusion obtained from the study is helpful in designing the safe and economical design of the tunnel structures. Yang et al. (2019) conducted a study to determine the failure characteristics of the deep tunnel in rock strata. For that, a large scale experimental set-up is developed in the laboratory. The experimental setup mainly consists of three components i.e. loading frame, hydraulic servo control system and computer control setup as shown in Fig. 2.26. The results obtained from physical modelling are then compared with the numerical analysis and it is found that both are in good agreement with each other.

(a) Loading Frame (b) Hydraulic system (c) Computer system

Fig.2.26 Components of experimental setup used in the study (Yang et al. 2019)

Kumar and Shrivastava (2021) conducted a study on the deformation behaviour of a single tunnel under static loading conditions and concluded that in the case of tunnels at shallow depths the extent of the damage along the tunnel axis depends upon the strength characteristics of the rock. In the case of weak rock, the extent of damage will be more as compared to the hard rock. Kumar and Shrivastava (2022) conducted a comparative study on the deformation behaviour of single and twin tunnels under static loading conditions and concluded that the extent of deformation in tunnels mainly depends upon the unconfined compressive strength of the model material.

2.8 Numerical Modelling of tunnels

Meguid et al. (2003) conducted a 3D analysis of unlined tunnels excavated in the rock and are subjected to high stresses. The study is conducted on the stability of the face and the stresses developed on and around the face of the tunnels having large diameters. The effect of the

strength characteristics of rock mass and high stresses acting in the horizontal direction on the deformation behaviour of the tunnel is also determined. From the results, it is concluded that the amount of deformation that occurs during the construction of a tunnel is very large. It is also observed that the pattern of failure at the face of the tunnel in weak and strong rock is very different. In the case of strong rock tensile failure occurs at the tunnel face which is due to the tensile stresses acting on the tunnel face. Whereas in the case of weak rocks, the failure occurs due to the overstresses of the rock mass at the tunnel face. Pakbaz and Yareeband (2005) conducted a 2D numerical study on the interaction between the tunnel lining and the ground. Then the numerical results are compared with an analytical close form solution. From the results, it is concluded that the interaction between the ground and tunnel under earthquake loading depends upon various factors such as the magnitude and duration of an earthquake, peak acceleration and the rigidity of the tunnel and ground. It is also suggested that in the case of circular tunnels subjected to earthquake loading, a close form solution can be used for the analysis process. Hashash et al. (2005) studied the deformation behaviour of circular tunnels in full slip and no-slip conditions between the ground surface and tunnel lining under the effect of seismic loading with the help of an analytical solution and further validated the results with numerical modelling. The results obtained from numerical modelling are in close agreement with the analytical results in the case of full slip conditions between the ground surface and the lining of the tunnel.

Idris et al. (2008) conducted a study on the numerical modelling and mechanical behaviour analysis of ancient tunnel masonry structures by using UDEC. The experimental design was proposed for various factors like masonry block cohesion, tensile strength and friction angle. From the study, it can be concluded that the effect of cohesion and friction angle on the mechanical behaviour of tunnels is very significant. Masonry strain lightly increases due to an

increase in the Young's Modulus. Idris et al. (2009) proposed an experimental design to determine the effect of ageing on old tunnels. The effect of joint tensile strength, joint cohesion and joint friction angle is taken into consideration. The results obtained from the experimental investigation are further validated with numerical analysis with the help of UDEC software. From the results, it can be concluded that these factors have a considerable effect on the deformation behaviour of old tunnels. It can also be noticed from the study that the effect of joint cohesion is greater on the stability behaviour of old tunnels as compared to the other factors. Scussel and Chandra (2013) proposed a new method in which the polyaxial state of stress can be incorporated into the analysis. The method employs modified angle of friction and cohesion values that may be derived using the provided equations, and the analysis is simplified to the same form as the Mohr-Coulomb theory.. Scussel and Chandra (2014) describe a new approach to designing the tunnel in squeezing ground conditions using the equivalent angle of friction and cohesion of the rock mass surrounding the tunnel.

Chakeri et al. (2011) conducted a study on the interaction between the tunnels in soft ground conditions. Numerical Modeling is done with the help of Flac 3D software. From the results, it can be concluded that as the horizontal distance between the tunnels increases, the settlement decreases in the central part of the twin tunnels. It can also be concluded that change in the sequence of excavation also has a minor effect on the settlement of the surface of the tunnel. Naggar and Steele (2012) conducted a study to investigate the effect of the stiffness of the tunnel lining on the distribution of stress in tunnels having shallow depths. The effect of the quality of compaction of backfill material on the stability of tunnel liner is also studied. The study is conducted on Plaxis software. The concrete material is used as a tunnel liner in this study as it has a high elastic modulus. From the results, it is concluded that there is a significant effect of the quality of compaction on the stress-induced in the tunnel lining.

Do et al. (2014) conducted a study on a 2D investigation of twin tunnel interaction using the FLAC finite difference element program. The influence of segment joints and tunnel distance on the structural lining force induced in twin tunnels is studied. The Plane strain model used in the study is shown in Fig. 2.27. The findings indicate that the construction process of the second tunnel has a significant impact on the structural ling forces created in the first tunnel. Whereas it is also found that the joint distribution in the second tunnel has no effect on the structural forces created in the first tunnel.

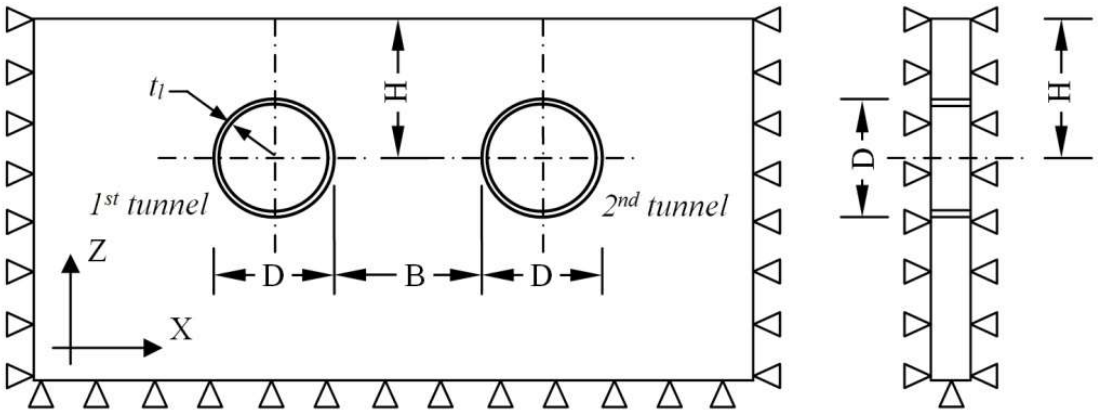

Fig. 2.27 Plane strain model under consideration (Do et al. 2014)

Shaalan et al. (2014) conducted a numerical study on stability analysis of two adjacent tunnels using Finite element based software ADINA. The effect of different spacing between tunnels and tunnel lining thickness is studied. From the results, it has been concluded that as the clay stiffness increases there is a slight difference between the different tunnel lining thicknesses is noticed. Bayoumi et al. (2016) determine the effect of the construction of a twin tunnel on the structure with the help of PLAXIS 2D software. The study is conducted on vertically and horizontally aligned tunnels as shown in Fig. 2.28. From the results, it has been concluded that the construction procedure affects the settlement of vertical twin tunnels and it is also

concluded that when the upper tunnel first is constructed first it will cause greater displacement. Do et al. (2016) studied that in the case of a twin tunnel, the lagging distance affects the surface settlement behaviour of the tunnel. With an increase in the spacing between the tunnels when they are closely spaced, ground loss percentages caused by the second tunnel decrease, as studied by Fang et al. (2016). A study conducted by Fu et al. (2019) shows that in the case of two crossing tunnels, the surface settlement caused due to excavation is more when the second tunnel is excavated above the first tunnel. The construction of a new tunnel significantly affects the settlement behaviour of the existing tunnel explained by Jin et al. (2018), Do et al. (2014), Gao et al. (2017) and Wu and Zou (2020). Liang et al. (2016) explained that various factors such as clearance distance, advancing distance and the influence of multiple new tunnels significantly affect the stability behaviour of the existing tunnel. The elastic modulus of the ground has a significant effect on the settlement of the tunnel structures concluded by Liang et al. (2018).

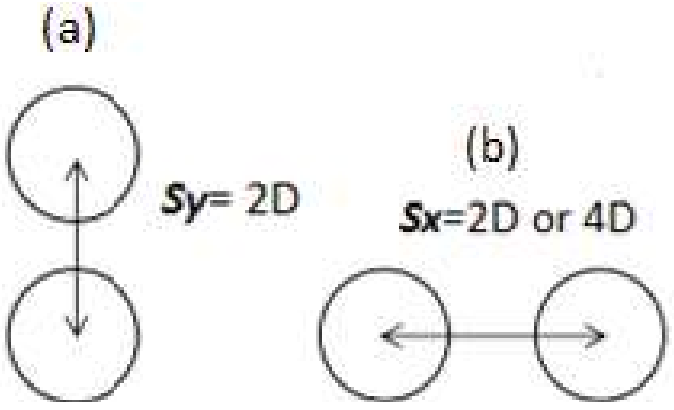

Fig.2.28 Alignments of tunnels used in the study (Bayoumi et al. 2016)

Channabasavaraj and Visvanath (2013) studied the settlement behaviour of twin tunnels using numerical modelling. The effect of change in the alignment of tunnels and relative position of

the tunnel is studied. Three different types of alignment are used in this study i.e. horizontal, vertical and inclined as shown in Fig.2.29. From the results, it can be concluded that the maximum settlement is experienced in vertically aligned tunnels whereas the lowest settlement is recorded in horizontal tunnels. It can also be concluded that the extent of settlement is more if the upper tunnel is constructed first.

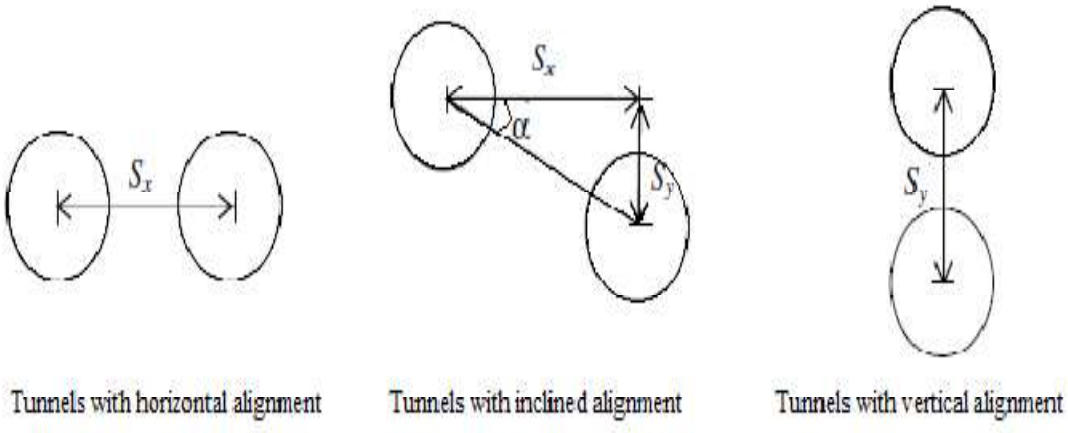

Fig.2.29 Different alignments of twin tunnel (Channabasavaraj and Visvanath 2013)

Shirinabadi and Moosavi (2016) made an attempt to study the behaviour of twin tunnels under static and dynamic load with the help of UDEC. The results show that under the effect of static and dynamic loading, the twin tunnels are not fully stable and therefore require a support system. It can also be concluded that under the effect of static loading, the variation in the displacement experience along with the tunnel length and velocity variations experienced in the roof of the tunnel is larger as compared to the value of displacement and velocity noticed on the rest of the tunnel section. The increase in the unbalanced forces was more in the dynamic loading conditions. The value of displacement and change in velocity experienced on the floor of the tunnel is greater than the rest of the tunnel section. Tiwari et al. (2016) conducted a study to determine the stability behaviour of twin tunnels with concrete lining under the effect of blast

loading. Numerical modelling is done using ABACUS. Pressure in the RC lining caused by the explosive induced shock wave has been studied for both tunnels. From the results, it can be concluded that the damage that occurs in concrete lining depends upon the distance between the tunnel and the surcharge weight. Paternesi et al. (2017) conducted a numerical study on the analysis of twin tunnels at shallow depths using the numerical tool Plaxis 3D. The deformation behaviour of the shallow twin-tube tunnel is analyzed. The study is conducted on the construction of twin tunnels at shallow depth which is excavated in fine-grained and stiff deposit. From the results, it is concluded that the settlement behaviour of the tunnel mainly depends upon the shape and the magnitude of loading. Muhammad (2017) conducted a study on circular tunnels under static and dynamic loads at different depths. A numerical investigation is conducted with the help of a finite element software tool. It was noticed that the depth of the tunnel has a significant effect on the stability behaviour. Shalabi (2017) carried out a numerical investigation on the interaction between twin circulars at shallow depth with the help of FE analysis. The study is conducted on the change in the deformation behaviour of twin tunnels as the spacing between the tunnels varies. It was concluded that as the spacing between the tunnels decreases, the interaction effect increases. Singh et al. (2018) conducted a numerical investigation to analyze the spacing and diameter effect on the stability of twin tunnels and concluded that the minimum spacing for twin tunnels should be 0.8 times the diameter of the circular opening. The geometry used in the twin tunnel simulation is shown in Fig.2.30. The displacement decreases with an increase in spacing between the tunnels.

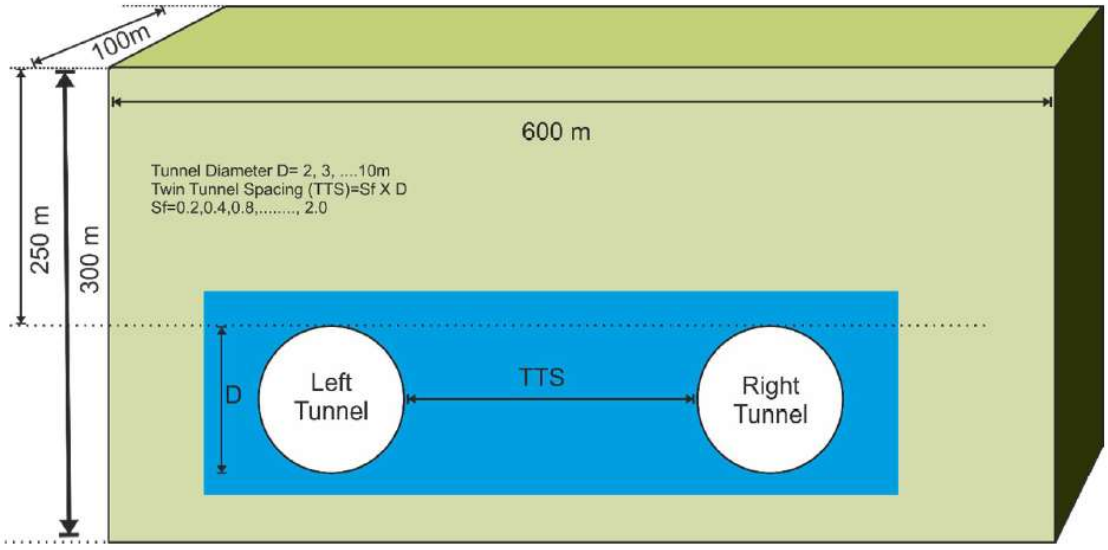

Fig.2.30 Geometry used in twin tunnel simulation (Singh et al. 2018).

Varma et al. (2019) conducted a study on the numerical investigation of the tunnel in jointed rock subjected to seismic loading. The study is conducted on UDEC software. From the results, it is concluded that with an increase in lateral stress coefficient the deformation around the tunnel increases. It is also concluded that tunnels in the jointed rock are highly susceptible to earthquake loads. Alagha and Chapman (2019) conducted a numerical study to investigate the behaviour of face stability of tunnels when excavated in homogenous soft ground. The study is conducted with the help of Midas GTS NX software. The pressure requires to damage the face of the tunnel is determined. The effect of various factors such as strength characteristics, cover depth add the diameter of the tunnel on the deformation behaviour is also analyzed. From the results, it is concluded that with an increase in the diameter of the tunnel there is an increase in face collapse pressure. It is also observed that there is a significant effect of cohesion on the collapse pressure of the face. Liu et al. (2019) analyze the effect on the mechanical behaviour of the existing tunnel due to the construction of a new tunnel. The study is based on the analytical model using MATLAB software which is further validated numerically with

ABAQUS software. The results obtained from the study show that with a decrease in the vertical distance between the newly constructed and already existing tunnel, the magnitude of the deformation increases. Also with a reduction in the coefficient of subgrade reaction, there is an increase in deflection. Zhang et al. (2019) studied the stability behaviour of dual circular tunnels with the help of numerical modelling. In this study, the tunnels are modelled under plain strain conditions as shown in Fig.2.31. It is assumed that the rock is homogenous and isotropic. From the results, it can be concluded that the failure in dual tunnels can be divided into two parts. The first one can be represented by a cross-shaped zone which is located at the centre portion of the dual tunnels. This failure depends upon the L/B parameter. The other failure is represented by two large slip surfaces. These slip surfaces start from the outside of the tunnels and extend up to the ground surface. This failure depends upon the H/B parameter.

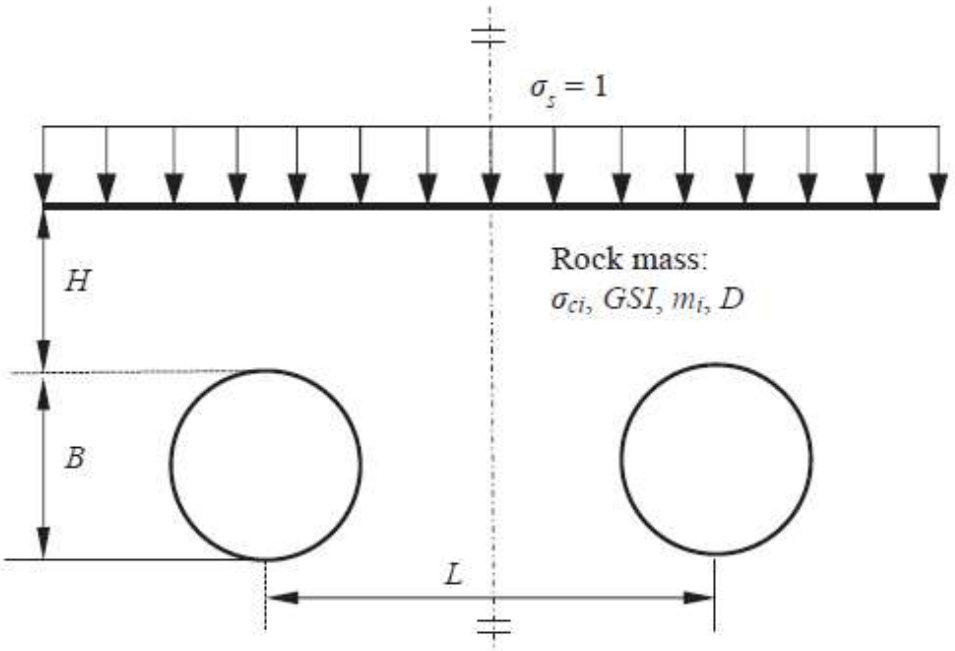

Fig.2.31 Plane-strain model used in the study for dual circular tunnels (Zhang et al. 2019).

Lv et al. (2020) explained the effect of pile reinforcement on the deformation behaviour of tunnel lining and surface settlement with the help of numerical simulation. The study is based on the deformation of tunnel lining and ground settlement. The effect of the isolation pile on the construction is analyzed and then compare to the actual field data. From the results, it can be concluded that the presence of reinforcement significantly influences the settlement of ground and tunnel lining. With the introduction of reinforcement, the deformation will reduce. The results obtained from numerical modelling are in good agreement with the on field results.

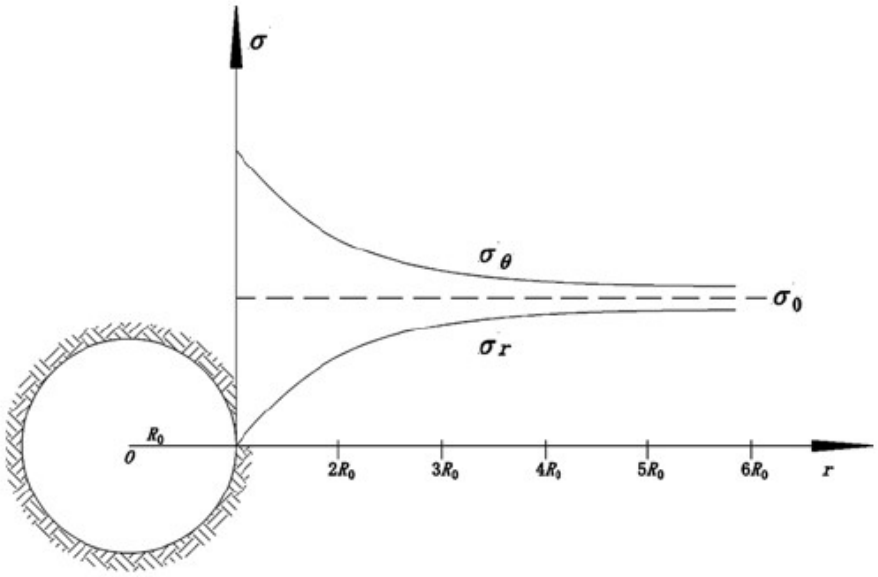

Fig.2.32 Distribution of stresses around the tunnel (Lv et al. 2020)

Huang et al. (2020) explained the effect of change in the strength parameters on the settlement behaviour of existing tunnels with the help of numerical analysis. FLAC 3D is used in this study. In the present study, the effect of variation in the sensitivity of strata on the deformation of already existing tunnels is determined. The result indicates that the settlement of the tunnel and surface is dependable on the strength of the layer. It can also be concluded that when a new

tunnel is constructed close to the existing tunnel, then a large settlement is experienced at the face of the existing tunnel.

Zhang et al. (2015) conducted a numerical study based on the analysis of face stability of tunnels at shallow depths with the help of FLAC 3D software. The study is based on the three-dimensional analysis of circular tunnels in a cohesion soil medium. On the basis of the numerical study, a 3D failure mechanism is proposed which is based on kinematic theory. The failure zone obtained from numerical modelling and the proposed failure mechanism are compared. From the results, it can be concluded that the results obtained from the proposed mechanism are more accurate and reliable Kumar and Shrivastava (2021) conducted a numerical study on the deformation of a single tunnel under the effect of static loading and concluded that as the cover increase the effect of deformation will decreases.

Yang et al. (2020) studied the importance of soil properties in transferring the load caused by the traffic in metro tunnels. The study is conducted with the help of numerical modelling software FLAC 2D. From the results, it can be concluded that the structure and anisotropy of the soil affect its dynamic response caused due to the traffic load in metro tunnels.

Mahalakshmi et al. (2012) conducted a study to determine the effect of various factors such as variation in ground loss, depth of the tunnel and relative spacing between the tunnels. The study is conducted on the basis of numerical modelling using Plaxis software. From the results, it can be concluded that with an increase in the ground loss, there is an increase in the settlement also. As the spacing between the tunnels in the case of the twin tunnel increases, the effect of settlement reduces. Fig. 2.33 shows the deformed shape of the tunnel.

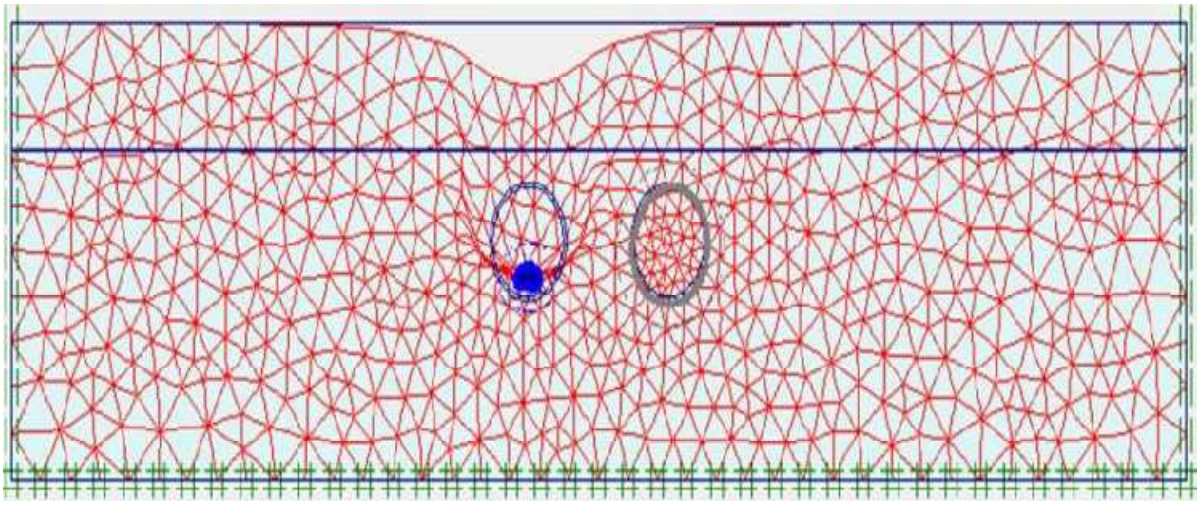

Fig.2.33 Deformed Shape of Ground Surface after Excavation of Tunnel

(Mahalakshmi et al. 2012)

Du et al. (2020) conducted a study to determine the effect of surcharge loading on horseshoe-shaped tunnels excavated in soft rocks. The study is conducted with the help of the Hyperstatic reaction method and the result obtained is further validated with numerical modelling. The effect of water pressure and groundwater level is also studied. The result shows that the bending moment and radial displacement induced in the horseshoe tunnel are highly sensitive to water pressure, surcharge loading and groundwater level. Chen et al. (2020) conducted a study to determine the deformation behaviour of segmental rings in shield tunnels. The study is conducted with the help of numerical modelling software. From the results, it can be concluded that the reason behind the failure mechanism of the segmental ring is the development of plastic hinges which are formed in joints. Chou and Bobet (2002) studied the deformation behaviour of tunnels at shallow depth in the clayey medium. Stress and displacement induced in tunnel lining were determined and from the results, it is concluded that the vertical displacement value obtained in the tunnel section is very large as compared to the horizontal deformation. Sahoo

and Kumar (2012) study the behaviour of long tunnels under seismic loading and found that the deformation behaviour depends upon the variation in the stability number and nodal velocity pattern. Qian et al. (2021) studied the deformation behaviour of utility tunnels under the effect of surface explosion conditions. The study is done through numerical modelling using LS-DYNA software. From the results, it can be concluded that with an increase in the primary reinforcement ratio of utility tunnels, there is a decrease in the deflection response of the tunnel as a result it will increase the blast resistance of the utility tunnel. It can also be concluded that with an increase in the wall thickness and depth of the tunnel there is a decrease in the extent of damage in the utility tunnels. Panji et al. (2016) studied the stability behaviour of tunnels at shallow depth under the effect of eccentric loading. The study is performed with the help of the direct boundary element method. The cross-sectional shape of the tunnel is considered a circular, square and horseshoe shape. From the results, it can be concluded that there is a significant effect of eccentric loading on the stability behaviour of the tunnel. It can also be concluded that with an increase in the width and eccentricity of shallow footing, there is an increase in the stress values. The minimum buried depth required for the circular and horseshoe section tunnel is 6R whereas for the square cross-section tunnel the minimum buried depth is 7R. Zaid et al. (2020) conducted a study to determine the effect of the shear zone on the seismic behaviour of the tunnel. The study is conducted with the help of FEM based software i.e. ABAQUS. The results obtained from the numerical analysis are further compared with the experimental results obtained from various studies in past and it is found that they are in good agreement with each other. The results show that the orientation of the shear zone plays an important role in the stability and serviceability of the tunnel under the effect of loading.

Singh and Shrivastva (2000) conducted a study to determine the appropriate method for the construction of twin tunnels. Three methods are compared in this study i.e. simultaneous excavation, alternate excavation and simultaneous sequential excavation. From the conclusion of the study, it is found that the third method i.e. simultaneous sequential excavation method is the best method for the construction of twin tunnels. Dhamne et al. (2018) conducted a study to investigate the response of different shapes of the tunnels under the effect of dynamic loading. Geometric models of D shaped and Circular sections are taken into consideration. Numerical analysis is conducted with the help of ABAQUS software. The effect of loading conditions on tunnel lining and the crown of the tunnel is also investigated. From the results, it can be concluded that D-shaped tunnel sections experienced more deformation as compared to circular tunnel sections. Therefore it can be concluded that the circular tunnel section is more suitable. Yoo et al. (2018) conducted a study to determine the effect of joints on the stability behaviour of circular tunnels under the effect of seismic loading. A set of joint parameters are decided in the study. Vertical and horizontal joints are developed in the circular tunnel section. The joint orientation provided in the circular opening is shown in Fig. 2.34. From the results, it can be concluded that there is a significant effect of joints on the deformation behaviour of tunnel lining. It is also noticed that in the case of vertical and horizontal joints, the tunnel response is highest whereas it is lowest in the case of 45 degree joint dip angle. The disturbance is 20 times more in jointed rock as compared to intact rock.

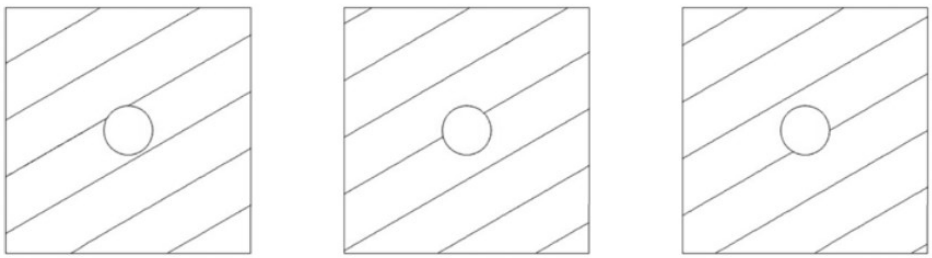

Fig.2.34 Joint orientation provided in the circular opening (Yoo et al. 2017)

Jose and V (2018) conducted a study to determine the behaviour of tunnels with the help of numerical modelling software i.e. ANSYS. The study is conducted on the different cross-sectional shapes of the tunnel i.e. circular sections and semi-elliptical shape tunnels. From the results, it can be concluded that the circular tunnel shows less deformation as compared to the semi-elliptical shape tunnel section. Mohammed et al. (2017) conducted a numerical analysis of circular tunnels excavated at different depths under the effect of static and dynamic loading with the help of MIDAS GTS NX software. The effect of displacement and stresses acting on the tunnel lining is noticed. From the results, it can be concluded that the effect of displacement is more in the case of dynamic loading as compared to static loading. The displacement is 20 times more in dynamic loading as compared to static loading.

Manouchehrian et al. (2017) conducted a study to investigate the importance of discontinuities present in the tunnel under the effect of static loading. Numerical analysis is done with the help of ABAQUS software. Various tunnel models with and without discontinuities are built and tested under the effect of static and dynamic loading. From the results, it can be noticed that there is a significant effect of discontinuities on the stability behaviour of the tunnel structures. With the presence of discontinuities in the tunnel structures, the effect of deformation will be more. Zhang et al. (2013) conducted a study to determine the effect of displacement occurring in a tunnel due to the construction of another tunnel section adjacent to it. A semi analytical method is used in this study to predict the settlement behaviour of the tunnel section. From the results, it can be concluded that the displacement in the tunnel will decrease rapidly with an increase in the distance between the two tunnels and it becomes almost zero when the distance between the tunnels is more than 5D, where “D” is the diameter of the tunnel.

Yang et al. (2010) carried out a numerical analysis to study the response of metro tunnels with the help of ANSYS software. The effective stress and displacement developed in the tunnel

lining due to the blast is studied. From the results, it can be concluded that the upper part of the tunnel lining section is more vulnerable and the effect of the explosion is negligible below 7-meter depth. Heidarzadeh et al. (2021) explained the best suitable criteria for the determination of damage in tunnels using numerical techniques and it is concluded that for the tunnels excavated in hard rock, the non-linear elastoplastic model is the best option. Rashiddel et al. (2020) studied the effect of explosive loading on the segmental tunnel lining and concluded that in the case of explosive conditions the curved jointed segmental lining is very efficient. Wang et al. (2012) studied the settlement behaviour of tunnels in clay at shallow depth using FEM techniques and found that settlement depends upon the creep behaviour of clay. Li et al. (2018) studied the response of the tunnel and found that in the case of blast loading the maximum deformation is experienced at the roof and floor of the tunnel. Shahin et al. (2019) stated that a three-dimensional finite element study of the tunnel behaviour is very essential for determining the exact tunnel design parameters. Shiau et al. (2020) explained the importance of various factors such as cohesion, unit weight, and surcharge loading on the displacement. Sun et al. (2020) investigated the behaviour of tunnels under the effect of seismic loading. The study is conducted with the help of numerical software i.e. FLAC. The results show that the effect of deformation under the effect of the seismic load is very significant.

2. 9 Gaps in Literature Review

From the review conducted by various researchers in past, it is clear that the stability behaviour of single and twin tunnels under static loading conditions depends upon various factors. So for the safe and economical design of the tunnels, it is very essential to assess the extent of deformation in the tunnel under the effect of static loading. From the literature review, the following gaps can be summarized.

i. While going through the literature review, it is seen that experimental work done by changing the cover depth of tunnels and strength characteristics of the surrounding rock mass of the tunnel and its validation with the numerical modelling is very limited.

ii. The experimental work done on the effect of variation in the spacing between the tunnels on its deformation behavior in case of twin tunnel is very limited.

iii. A lot of work is done on the stability analysis of a single tunnel under different loading conditions. Not much experimental work is done on twin tunnels in rock masses.

iv. Limited work is done on the validation of results obtained from experimental and numerical modeling of single and twin tunnels under the effect of static loading.

v. While going through literature review. It can be observed that work done to determine the deformation of tunnel under the effect of static loading is very limited, The majority of the study is conducted for dynamic and impact loading.

Although advances in computational methodologies have allowed for extensive numerical and analytical tunnelling research, geotechnical engineering researchers still rely heavily on physical modelling to understand various tunnelling phenomena such as deformation patterns and failure mechanisms. However, relatively few studies have been conducted in this area. Until now, there have been no guidelines or analytical solutions illustrating damage generated in tunnels and linings through small scale basic static tests. Inspite of being the easiest way to formulate deformations inside a tunnel under static load, physical modelling is found to be very scanty in the studies so far. Therefore, keeping the above limitations in the physical and numerical modelling in view, the objectives for the present study were set. It was decided to fabricate an automatic compression testing facility with an LVDT data acquisition system. A detailed parametric study is planned and carried out to understand the deformation behaviour

and fracture propagation of tunnels under static load. Finally, the physical modelling is validated with numerical analysis.

The next Chapter describes the development of an automatic compression testing facility and details of a physical study carried out. A digital compression testing apparatus is developed in the present study to determine the deformation behaviour of single and Twin Tunnels. The detail of the development of the equipment is discussed in the next chapter.

Chapter 3

EXPERIMENTAL SETUP

3.1 General

Accurate measurement of the compressive strength and deformation behaviour of tunnels is very essential for assessing the stability behaviour of tunnels in rock mass which can be very useful for proposing safe economical design parameters. For that, a specialized compression testing facility is required in the present study to check the deformation behaviour of tunnels under static loading conditions. Various initial trial testing was conducted to finalise the design parameters of newly developed the compression testing machine. An LVDT transducer unit is also attached to the compression testing machine to record the deformation occurring along the tunnel axis.

From the previous studies, many researchers have used various numerical and experimental techniques to determine the strength of rock tunnels under static loading conditions. In the past various numerical and analytical solutions have been given by various researchers to study the effect of static loading on the deformation behaviour of tunnels. Limited work has been done to determine the deformation of tunnels under the effect of static loading. In the field conditions, it becomes very difficult to assess the tunnel deformation behaviour due to various adverse conditions. Hence in the present study, there is a need to design equipment which can control these limitations and difficulties.

3.2 Design and Fabrication of Compression testing machine

A compression testing machine is developed in the present study to determine the deformation behaviour of single and twin tunnels under static loading conditions. In a compression test, the test model is normally placed between two plates and load is applied with the help of a pressure sensor as a result a uniform force is transferred in the form of load on the top surface of the specimen. After the application of load, the platen of the compression testing machine will move towards each other (Mishra et al. 2018). As a result, of this, the sample will get pressed which further causes the flattening of the sample subjected to loading conditions. In general, compressed specimens contract in the direction of applied forces and expand in the orthogonal direction. A compression test is the completely opposite of the more common tension test. Compression testing is a method of determining the deformation behaviour of material or its response to a compressive force acting on it by measuring key parameters such as stress, strain and deformation. Compressive strength, elastic modulus, elastic limit, ultimate strength and yield strength are the major parameters that can be determined by assessing a material in compression. The knowledge of these components and their working will help in finding the durability of the material whether it is appropriate for a particular practice or if it will deform when specified stress is applied to it.

In this study, a compression testing unit is designed and developed to study the tunnel behaviour under static loading conditions. To obtain an accurate idea of the extent of damage which is occurred in the tunnel, it is very essential to have an advanced compression testing facility in the laboratory. Although the deformation which is caused due to the effect of static loading can be less than the dynamic and impact loading, it is very essential to determine that damage. Hence in the present study to test the rock tunnel models of single and twin tunnels

under varying static loads, a digital compression testing machine with a data acquisition system is designed. This apparatus can operate on varying static loads. The size of the various sections of the testing machines is fixed according to the size of the testing tunnel models. The platen size and the vertical clearance of the loading platen are fixed according to the dimensions of the tunnel sections. In the present chapter, a detailed discussion about the design, development and fabrication of the experimental setup is made. The apparatus is made up of three primary units i.e. loading frame, a pumping unit and a data acquisition system for measuring the deformation that occurred in the tunnel section. On the right side of the loading frame, the pumping unit is placed. The complete schematic diagram of the loading unit is shown in Fig. 3.1. The detailed information about each working component is discussed below.

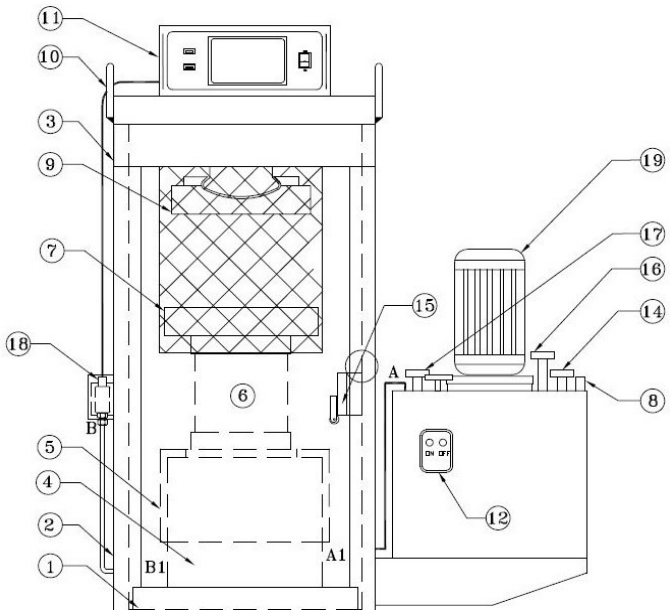

S. NO.	D E S C R I P T I O N
01	BASE PLATEN
02	SIDE PLATEN
03	UPPER HEAD
04	JACK
05	JACK COVER
06	SPACER
07	LOWER PLATEN
08	RELIEF KNOB
09	SPHERICAL SEATING
10	HOOK
11	ELE. DISPLAY UNIT
12	ON/OFF SWITCH
13	
14	FLOW CONTROL KNOB
15	LIMIT SWITCH
16	BOOSTER LEVER
17	RELEASE VALVE
18	PRESSURE SENSOR
19	MOTOR

Fig. 3.1 Schematic diagram of the loading unit.

3.2.1 Frame and the Loading Unit

This is the most important and biggest part of the system which consists of various components such as lower and upper platen, spherical seating, spacer, hydraulic ram etc. A new frame is purchased from Hydraulic & Engineering Instruments (HEICO), New Delhi. The frame is fabricated in Industrial Estate, Rai plant, Sonipat of Hydraulic & Engineering Instruments (HEICO).The loading frame is made up of mild steel material. This frame is designed to resist several times of complete repetitions of loading without any failure or buckling effect. The weight of this frame is very light. At the base of the loading frame, a lower platen along with a hydraulic ram is attached whereas at the top of the plate a spherical seating is provided. The function of this spherical seating is to make sure that there may be no irregularity in the sample. It also keeps the specimen at the central position and takes care of the misplacement of the sample. The loading frame is covered with the help of an expanded sheet which acts as the front cover to protect the operator and it also gives an undisturbed view of the sample during the testing process. Fig. 3.2 shows the compression testing machine with an electronic display unit and a Pumping unit.

Fig. 3.2 Compression testing machine with an electronic display unit and pumping unit.

3.2.1.1 Base Platen and Side platen

The base platen is provided at the bottom of the loading frame. The whole loading frame is rested on the base platen. The function of the base platen is to provide a firm foundation sitting on the loading frame. As the load frame is a very heavy structural unit, so it is very essential to provide it with a strong and balanced footing. The weight of the loading frame is transferred to the base platen. The base platen is fabricated with mild steel material. The base platen is supported with the help of side platens. The loading frame is covered with the help of a side platen from both sides. The function of the side platen is to provide support to the base platen and whole structural member i.e. loading frame.

3.2.1.2 Upper Head

The upper heat is provided at the top of the loading platen. It acts as the top surface of the loading frame. It is supported with the help of side platens. The upper head is further connected to the spherical seating which is in a circular shape.

3.2.1.3 Jack and Jack Cover

Jack is fixed at the bottom of the loading frame. The function of the jack is to apply the bottom load. When the switch is turned ON and load is applied to the sample, the pressure starts rising in the pumping unit. As a result of this, the jack started moving in the upward direction and start applying the load on the tunnel sample which is placed on the lower platen surface. The Jack cover is fixed at the top of the jack. Its function is to protect the jack from any type of damage. Hence it acts as a shield for Jack.

3.2.1.4 Spacer

The spacer is kept below the lower platen. The function of the spacer is to decrease the gap between the lower and upper platen. The spacer is provided to adjust the vertical clearance distance during the testing of the samples. They are used to adjust the samples of different sizes and shapes in the loading frame. They are made up of mild steel material and are painted to protect them from corrosion. The diameter of the spacer which is used in the present study is 150mm and its height is 200mm. In this study, large-sized samples of the single and twin tunnel are fixed inside the loading frame with the help of these spacers.

3.2.1.5 Lower Platen

The machine's lower platen sits on the spacer, which is held in place by a catering pin. The inward movement of the lower platen available in compression testing machines is used to load the machine. In this designed loading frame, the size of the lower platen is kept according to the dimensions of the single and twin tunnel samples. The size of the lower platen is fixed as 500x500mm (LxW) and the thickness is kept at 50mm. The lower platen is again made up of hard mild steel material.

3.2.1.6 Spherical Seating

The angular displacement of the top of the specimen with respect to the loading axis of machines is accommodated by spherically seated compression seats. This is accomplished through the self-aligning action of the seat. Spherical seating is attached to the upper head of the loading unit. Spherical seating can be of different diameters depending upon the size of the sample which is to be tested. The main function of spherical seating is to ensure the exact placement of the specimen which is to be tested. Spherical seating is also used for applying the

uniform load on the sample. These are also made up of mild steel material. Spherical seating is provided in various diameters which are used to test different types of material.

3.2.1.7 Electronic Display Unit and ON/OFF Switch

The electronic display unit is kept at the top surface of the loading frame. It consists of 4 channels. One of its channels is connected to the pressure sensor cord and the remaining three channels are for strain measurement. The electronic display unit is fully microprocessor-based and it also consists of a built memory. This unit is used to record the load and stress values during the testing of the sample. It also records the strain value. The ON/OFF switch is provided on the pumping unit which is placed on the right side of the loading frame. The function of this switch is to start and stop the functioning of the compression testing unit.

3.2.1.8 Booster Lever and Limit Switch

The booster lever is fixed at the top surface of the pumping unit. The booster lever's job is to raise the lower platen rapidly. It gives the bottom platen an extra push to get to an appropriate position. The limit switch is fixed with the side platen of the loading frame towards the inward direction. The limit switch is an electro-mechanical device used for restricting the movement of the loading hanger during the application of static load.

3.2.1.9 Release Valve

A release valve is provided on the top surface of the pumping unit. The function of the release value is to control the pressure developed during the process of loading. Release value act as a safety valve without which the excessive pressure may develop as a result, the failure of an instrument may also occur. The design of the release valve is made in such a way, that it can

work at a predefined set pressure. During the process of testing, when the load is applied to the sample of the tunnel which is kept inside the loading frame, pressure is developed due to the pumping unit. Due to this developed pressure, the lower platen moves in the upwards direction to apply the load on the sample. When the sample is crushed or failed, the release value is open to release the pressure developed in the loading unit. As the release valve is opened, the lower platen will start moving in the downwards direction and the pressure is release from the sample.

3.2.1.10 Pressure Sensor

The purpose of fixing the pressure sensor is to control the pressure of fluids. The force necessary to restrict fluid from expanding is known as pressure, and it is measured in force per unit area. In this loading frame, the pressure sensor is attached to the left side of the side platen. Its cord is connected to the electronic display unit which reflects the reading of pressure when the load is applied to the specimen. A transducer works as a pressure sensor. The function of the transducer is to generate a signal when the pressure is applied. The purpose of the pressure sensor is to control various similar applications. Pressure sensors are also used to monitor various parameters such as speed, the flow of fluid and gas and the level of water. The function of a pressure sensor is to convert pressure into an analogue electrical signal. The pressure transducers are designed in such a way that they generate a linear output on the application of pressure. A constant-area sensing device is used in pressure transducers to respond to the force applied by fluid pressure. The diaphragm of the pressure transducer will deflect as a result of the applied force. The deflection obtained in the internal diaphragm is controlled and transformed into an electrical output. As a result of this, the pressure is controlled by computers, programmable controllers, microprocessors and other electronic devices. The close up of the rear view of the electronic box is shown in Fig. 3.3.

Fig. 3.3 Close Up of Rear View of Electronic Box

3.2.1.11 Motor

Electric Motor is fixed at the top surface of the pumping unit on the right-hand side of the loading frame powered by 1.5Kw. An electric motor, unlike an electric generator, is a device that transforms into mechanical energy from electricity. The electrical motor works on the electromagnetism principle. The majority of electric motors are designed to revolve constantly or move in a straight line.

The load frame is made of steel that has been welded together. It is designed to endure several million full loading cycles without any sign of deformity and fatigue. The weight of these frames is light. The lower platen and the hydraulic ram are mounted on the base. Spherical seating is attached to the top plate. The purpose of the spherical seating is to ensure any type of unevenness and irregularity present on the surface of the specimen. It also takes care of the position of the specimen from the central spot. The other main purpose of spherical seating is to provide the standardized and uniform application of load on the surface of the sample. The

loading unit capacity ranges from 0-2000kN and its minimum count is 0.1kN up to 200Kn and 1Kn above 200Kn. The accuracy of the load applied is less than (+/-) 1% of the load indicated.

3.2.2 Pumping Unit

On the right-hand side of the loading unit, the pumping unit is connected shown in Fig. 3.4. The pumping unit has a 1.5kW powered electric motor. It is a multi-piston pump which is submerged in the tank. The hydraulic ram receives non-pulsating flow from the Powerpack. This confirms the smooth loading of the sample, which can be seen by the loading gauge/digital monitor movement. The oil flow can be controlled precisely by the strain control knob which is located at a suitable height. The indication of the load is displayed on the digital display system. With a built-in RS232 serial port, the electronic display unit is microprocessor-based. It indicates the load, peak load, and speed rate. By adjusting the flow control, the knob the pacing rate is manually achieved. The pumping unit is fabricated in Industrial Estate, Rai plant, Sonipat of Hydraulic & Engineering Instruments (HEICO).

Fig.3.4 Pumping Unit attached to the loading unit.

3.2.3 Data Acquisition and Controlling System

The AI8000+ data acquisition system, which is a multi-point data collection and control system that is microprocessor-based and device compatible, was employed at this testing facility. This device serves as a calculator as well as a monitor. With remarkable success, it is being used to analyze various analogue sensors and inputs, pulse train input and digital inputs, and control via digital and analogue outputs. It's a 12-channel system for converting mechanical and electrical impulses to digital data. Eight of the 12 channels are assigned to LVDTs, two to load sensors, and the remaining two are kept available for some other type of connection. These components are contained in a single electronic casing. The output signal is connected to the CPU through a cable wire, which is then used to transmit data in the form of load and deformation to the appropriate location of the CPU. This software can keep track of the testing procedure and save the results.

3.2.3.1 LVDT's

Linear variable deformation transducers are used to measure and monitor the distortion that develops in the tunnel specimen. It is extremely difficult to insert strain gauges inside the tunnel axis in rock tunnel samples. LVDTs are employed to measure displacement along the tunnel axis for this purpose. A total of three LVDTs are used in both single and twin tunnel samples. LVDTs are positioned at various points along the tunnel axis. LVDTs are manufactured from stainless steel, which ensures that they remain scratch-free and rust-free even after extended use. The LVDT has a 9.5mm diameter, making it ideal for applications with limited or no space. Fig. 3.5 shows the photograph of a slimline LVDT.

This sensor has a 107mm body length and a non-linearity inaccuracy of only 0.3 percent. A 28mm long spring-loaded core rod is also connected to this device. As a result, the LVDT's overall body length, including the spring core rod, is 135mm. This device has a movement limit of (+/-) 10mm, which indicates it can travel up to 10mm to accommodate the deformation. Because the extent of deformation in this study is not very much as it is a case of static loading static loading, hence LVDT with this sort of motion range is appropriate. This device's operating temperature ranges from 0 to 60 degrees Celsius.

Fig. 3.5 AC Slim Line LVDT

3.2.3.2 LVDT full connection, location and Placement arrangement

Accurate positioning of LVDTs inside the single and twin tunnel samples is the most challenging and important phase of this experiment work. As discussed earlier, the fixing of strain gauges inside the tunnel axis cannot be possible because of the large depth of the tunnel. So, it is decided to use LVDTs for measuring the deformation of the tunnel. For that purpose, the holes are drilled from the bottom of the tunnel samples with the help of a drill machine and

then the LVDT is inserted into that drilled hole in such a way so that the top endpoint of the LVDT touches the crown of the tunnel axis. The whole process of drilling the holes into the samples and fixing the LVDT into them is very time consuming and laborious.

3.2.3.3 LVDT full connection

The length of the LVDT is around 107mm, therefore careful positioning was required to guarantee that they did not touch the tunnel's top surface or lining. Even after significant static loads, the bottom lining or surface appears to be undamaged. Because the total height to which LVDTs must be embedded in the casted model to touch the top surface of the tunnel varies depending on the overburden, which is approximately 200mm, for 30mm and 180mm for 50mm cover depth, a thin mild steel rod of 5mm and various lengths corresponding to different cover depths is connected with the main LVDT. The use of double-sided clinical tape ensures a secure attachment. The close-up view of the Data acquisition system and rear view of the LVDT data logger is shown in Fig. 3.6 and Fig. 3.7 respectively. LVDTs are further connected to 16- a channel plate which is shown in Fig. 3.8.

Fig. 3.6 Close Up View of Data Acquisition System

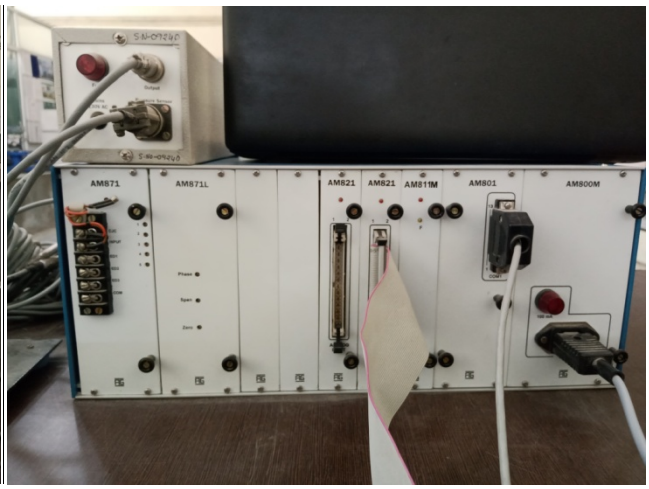

Fig. 3.7 Close Up of Rear View of LVDT Data Logger

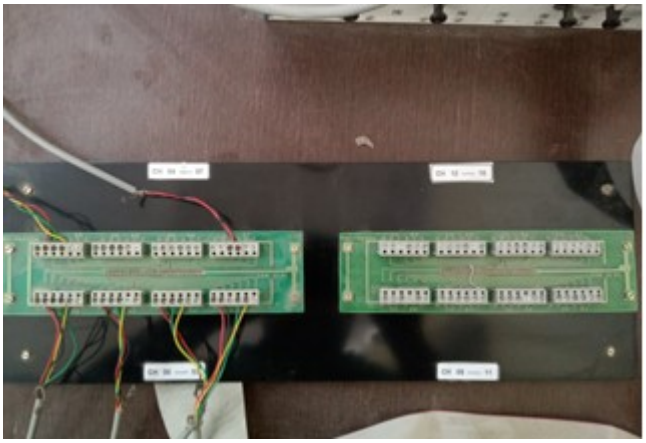

Fig. 3.8 16-Channel Plate attached with LVDT Data acquisition system

3.2.3.4 Calibration of LVDTs

Before the start of the experimental work, the LVDTs are properly calibrated. In the case of static loading, when the load is applied n the tunnel sample, a very less deformation occurs as compared to the deformation obtained in impact or dynamic loading. So it is very important to calibrate the device so that it can work properly and give a minimum error that can be considered within the permissible limit. A number of trials have been conducted with the help of a dial gauge to calibrate the LVDT's reading. From the numerous trails, it can be concluded that the error in the displacement value obtained from LDVT is under a permissible limit in comparison with the reading obtained from the dial gauge.

3.2.3.5 Location of LVDTs

The location of LVDTs inside the tunnel sample is one of the very essential aspect. The position of fixing LVDTs inside the tunnel is decided according to the extent of deformation. Various trail testing is done to fix the location of LVDT. To find out the extent of deformation on the application of load, various numerical models are run. From the various trails, three major positions are finalized to fix the LVDT to record the deformation effect in the case of a

single tunnel. The three major positions which are decided in single tunnels are L/3, L/2 and 7L/12, where “L” is the total length of the tunnel axis i.e. 300mm in the case of a single tunnel as shown in Fig. 3.9. Also in the case of a twin tunnel, as the dimension of the model is different from that of a single tunnel model so different positions are decided in the twin tunnel specimen. From the trail testing of twin tunnels samples, it was concluded that the deformation value is to be obtained at L/3, L/2 and 9L/15 where “L” is again denoted as the length of the tunnel section which is 425mm as of twin tunnel sample as shown in Fig. 3.10. Taking full advantage of the symmetry, the entire model is divided into two half, with two separate locations chosen on either side of the tunnel length that operate as mirror images of one another.

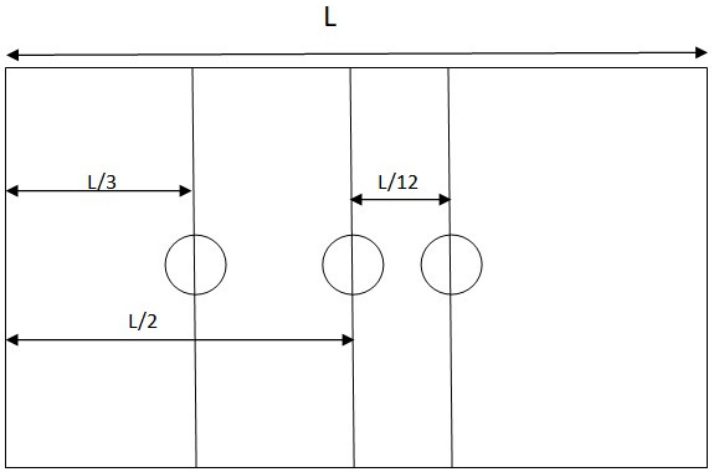

Fig. 3.9 Placement of LVDTs in the Single Tunnel Model.

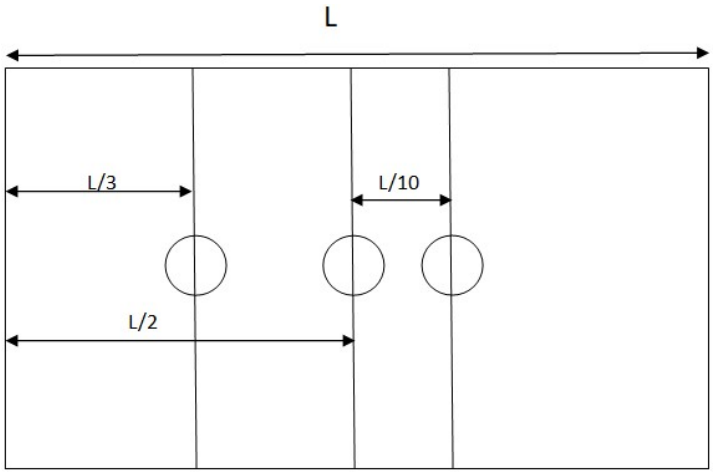

Fig. 3.10 Placement of LVDTs in the Twin-Tunnel Model.

3.2.3.6 LVDT placement arrangement

Three holes were drilled straight down the tunnel length with a drill bit that was 30cm long and 5.5mm in diameter on the opposite side of the targeted surface. A wooden I-section with three mild steel cylindrical pieces is welded at the selected positions of LVDTs, with a central flange length of about 30cm and length of two parallel plates of about 25cm. These mild steel cylindrical parts are hollow in the centre and have a slightly larger diameter than the LVDT's connecting rod (approximately 5mm) which is about 6mm shown in Fig. 3.11. The welded cylindrical component's height is kept close to 3cm so that the hole in the model can be drilled right away and all three pieces can be aligned linearly. All the casted models were drilled properly from the bottom with the help of drilling machines and drilling bits of various diameters, and after installing the LVDTs in the sample, they were kept back to the loading platform. A compact arrangement of cylindrical hollow mild steel bar with 10mm inner diameter and 20mm height with a three-sided nut system is given as shown in Fig. 3.12 in order to forcefully fix the LVDT straight to the appropriate place in the models for fixing LVDTs at the requisite position in the models. The figure depicts the tri nut system employed in the study.

After placing all three LVDTs and calibrating them, the sample is tumbled back to the loading area, and jerks were encountered due to the excessive weight of the casted model, which disrupted the LVDT's location. The placement of LVDTs inside the tunnel sample is shown in Fig. 3.13.

Fig. 3.11 Extension fixed to LVDT for fixing inside the tunnel sample

Fig. 3.12 Tri-nut system for fixing LVDT inside the tunnel sample

Fig. 3.13 Placement of LVDT inside the tunnel sample

3.3 Moulds for Preparation of Samples

The single and twin tunnel specimen of different parameters is prepared in the laboratory for which specially designed and fabricated tunnel moulds are required. For the preparation of tunnel moulds, Perspex sheet material is selected as the material. The purpose of selecting the Perspex sheet is due to its transparent surface which gives clear visibility during the casting of tunnel samples. The Perspex sheet having 16mm thickness is used for making the tunnel mould. The purpose of selecting this thickness size is so that the mould can resist the effect of vibration when it is kept on the vibrating table during the process of sample preparation. As in the present study, the deformation behaviour of lined tunnels is also studied, therefore in the case of lined samples, PVC pipe is used as the liner material. The thickness of the PVC pipe is kept at around 2mm.

3.3.1. Dimension of the Moulds

In the present study, the deformation behaviour of single and twin tunnels is determined under the effect of static loading. For that, single and twin tunnel samples of different parameters are prepared in the laboratory. The dimension of the tunnel mould is decided according to the stress distribution in tunnels. In the case of single tunnel samples, the dimensions of the tunnel mould are kept at 300x250x230mm (LxWxH) whereas, in the case of Twin Tunnel samples, the dimension of the tunnel mould is kept at 425x375x230mm (LxWxH) as shown in Fig. 3.16.To insert the circular PVC pipe which designated the shape of the tunnel, circular holes of 50mm diameter are drilled in the parallel sheets of the Perspex mould along the transverse axis of the tunnel mould. These circular shape holes are drilled from both sides of the Perspex box at different depths to cast tunnel samples with different cover depths i.e. 30mm and 50mm respectively. The present study is conducted on these two different cover depths both in single and twin tunnel models. Circular holes of a diameter of 5cm are extruded from both sides at different depths to prepare models with varying cover depths of 2.5 cm, 3.5 cm, and 5 cm respectively. The geometrical view of the single tunnel model with varying overburden along the x-x axis and lining thickness is shown in Fig. 3.14 (a and b) respectively.

In the case of twin tunnel samples, the spacing between the tunnels is varied as 1.5D, 2D and 2.5D where “D” is the diameter of the tunnel which is fixed at 50mm in all the cases. For the twin tunnel tunnels, two holes are drilled on the single side of the Perspex sheet and the other two holes are drilled on the parallel side of that. The length of the tunnel in the twin tunnel sample is kept at 425mm whereas the diameter of the tunnel is the same as in the case of a single tunnel i.e. 50mm. The geometrical view of the Twin Tunnel model having a 1.5D centre to centre spacing model with varying overburden along the x-x axis is shown in Fig. 3.15.

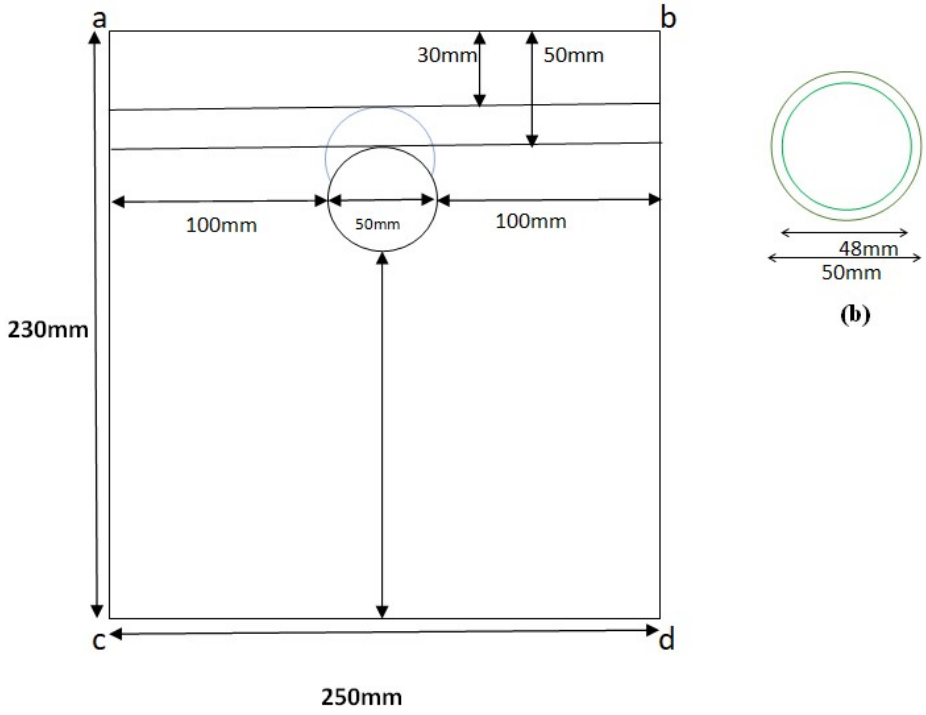

Fig. 3.14 Geometrical view of Single Tunnel Model with varying Overburden along the x-x axis; (b) Lining Thickness

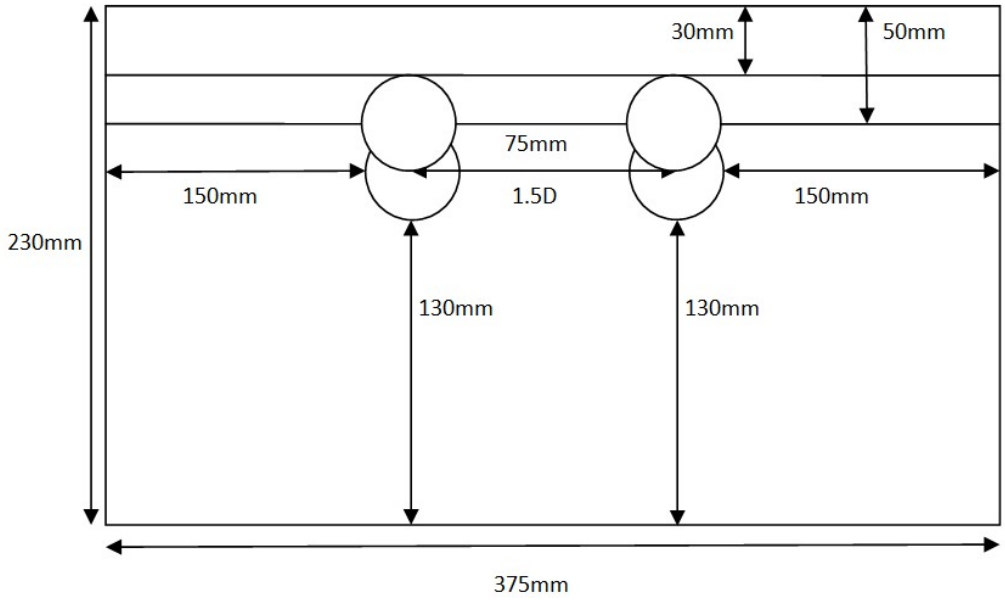

Fig. 3.15 Geometrical view of Twin Tunnel Model with varying Overburden along x-x axis

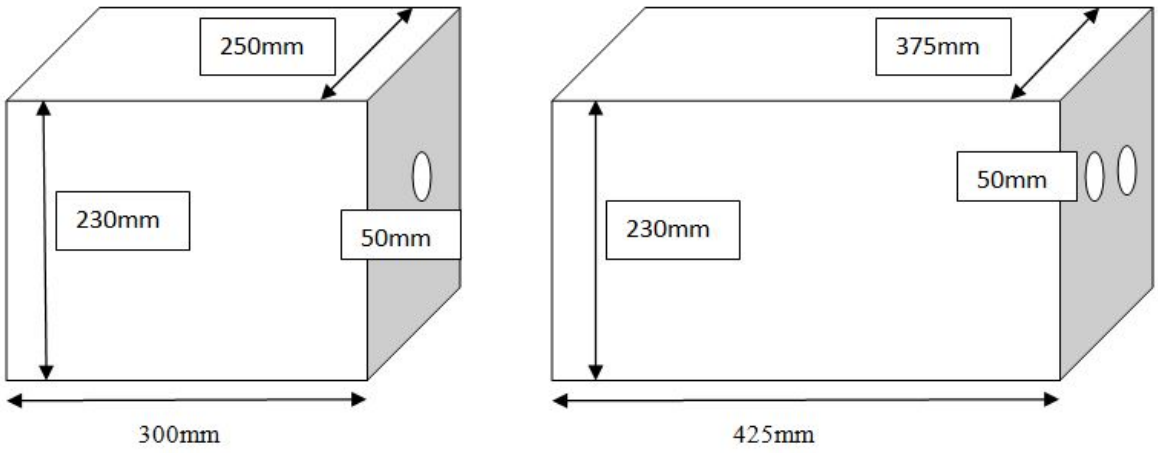

Fig. 3.16 Single Tunnel and Twin Tunnel model Dimension

3.4 Summary

The following conclusion can be drawn from this chapter.

- A digital compression testing machine along with an LVDT data acquisition system is designed and fabricated to determine the effect of static loading conditions on the tunnel's stability.
- The Perspex sheet mould which is used to cast the single and twin tunnel samples having different cover depth and spacing in between the tunnels is fabricated and designed to cast the tunnel specimens.
- The whole setup require for determining the extent of damage in single and twin tunnels is designed and developed.

The following chapter covers the selection of the model material, its characterisation, and the experimental programme.

Chapter 4

EXPERIMENTAL INVESTIGATIONS

4.1 General

The deformation behaviour of single and Twin Tunnels is investigated through a detailed and compressive method under static loading conditions. Various experiments are carried out in the laboratory with different parameters. The underground tunnel opening is subjected to various types of loading such as static load, dynamic load and earthquake load. Due to this continuous loading, the strength properties of the underground structure begin to deteriorate. As a result of the tunnel, the structure begins to crumble and failure occurs. So the prime objectives of the design engineers should be the safety of the structure under adverse loading conditions. For that various design, parameters are needed to study. An efficient way to alleviate traffic congestion in metro cities is to create underground structures. As the underground structures are exposed to different loading conditions, so it becomes very important to access the deformation behaviour of these structures. Tunnel modelling is very essential for deciding the designing parameters of tunnels to make safe and economical designs of underground structures. The purpose of the present study is to simulate in-situ conditions through experimental investigation and to identify the key factors that influence the deformation of underground structures. A novel approach is developed to resolve the challenges that come during tunnel field testing under the effect of static loading. In the present study, an experimental approach is used to examine and design tunnels under static loading conditions. For this purpose, small-scaled rock models of single and twin tunnels are prepared in the laboratory. Various geo-materials are mixed in different proportions to vary strength properties. Finally, the deformation of the tunnel under the effect

of static loading is investigated. The findings of the experiments revealed that rock stiffness, the pressure exerted, and tunnel spacing plays a significant role in the deformation of underground constructions. In the case of rock with poor strength properties, the extent of damage is greater.

A series of tests were conducted to determine the deformation behaviour of single and twin tunnels under static loading conditions. For that various tunnel models were casted in the laboratory for experimentation work. The tunnel models were prepared without any joints or cracks in them. In the case of the single tunnel, 36 models were prepared with varying parameters whereas, in the case of the twin tunnel, 36 models were prepared having different spacing and cover depth. The whole testing program consists of more than 72 tests over single and twin tunnel models.

In this chapter a detailed discussion about the selection of model material, its characterization, the composition of various components for preparing the models, preparation of single and twin tunnel models, the methodology adopted for testing and complete testing set up and the application of tunnel structures in actual field conditions is made.

4.2 Testing Program of Single Tunnels

4.2.1. Selection of Model Material

The major difficulty which is faced during the experimentation process is to find a model material which can be used to simulate actual rock conditions because it is very difficult in the laboratory to incorporate all the challenges which are to be faced in actual field conditions. Therefore to solve this problem, a material is found that can be used to prepare rock tunnel samples and can be simulated to actual field situations. Three geo-materials are modelled in the laboratory which represent the weak rock properties. These materials are selected according to

their stress-strain behaviour. As the rock has an unconfined compressive strength of more than 1MPa, therefore the selection of model material is done keeping in mind the strength characteristics of the rock. Plaster of Paris is chosen as the model material because it is commonly available and has the ability to mould into any shape when mixed with water. (Mishra et al. 2021) used plaster of paris as a model material in creating rock tunnels models. The compressive strength plaster of paris is around 8MPa which is greater than 1MPa therefore it represents the rock behavior. According to Deere Miller classification (1968) the classification of plaster of paris is done as EM (Medium Elastic). Therefore the structure of rock mass can be simulated with the actual tunnel engineering structure excavated in weak rock. Along with Plaster of Paris, Sand and Kaolinite clay are also added as constituents to make models as shown in Fig.4.1. The proportion of the constituents is varied in different tunnel models to change the strength characteristics of rock so that the effect of strength characteristics on the deformation of a single tunnel can be determined. In the laboratory, a number of single tunnel samples were casted by combining a specific amount of water into Plaster of Paris material. To decide the quantity of water which is to be added to the Plaster of Paris, various trial testing is conducted and it is observed that the desired strength is obtained at 60% water content Shrivastava and Rao (2013) and Niktabar et al. (2018). The quantity of water is kept the same for GM-2 and GM-3 tunnel models. In order to change the strength characteristics of rock, different compositions of Plaster of Paris, Sand and Clay are decided after a number of trial testing. The composition of these three materials is shown in Table 4.1.

4.2.2 Characterization of Geo-materials

In the present study, various types of constituents materials are used to prepare the rock tunnel models. These constituents are mixed in different proportions to make a rock tunnel model. The purpose of adding these constituents is to vary the strength parameters of the rock mass and to

examine the effect of change in the rock mass properties of the tunnel on its deformation behaviour. To characterize the various engineering of these geo-materials, an extensive experimental program is framed and conducted. Various trail testing is done to determine the properties of the geo-materials**.** The detailed characterization and engineering behaviour of selected geo-materials have been determined through different tests.

Table 4.1 Composition of the Synthetic Material used for making single tunnel models.

Synthetic Material	Plaster of Paris (POP)	Sand	Clay	Water Content
GM-1	100%	-	-	60%
GM-2	50%	40%	10%	60%
GM-3	50%	30%	20%	60%

a)Plaster of Paris **b) Sand** **c) Kaolinite Clay**

Fig. 4.1Various constituents for preparing synthetic rock.

The unconfined compressive strength and the dry density of the kaolinite clay is determined as per IS 2720 (Part-10), 1991 and IS 2720 (Part-7), 1980 and found to be 8.7KPa and 13.5 KN/m^3 respectively whereas the value of liquid limit and the plastic limit is determined as 56% and 28% respectively as per IS 2720 (Part-5),1985. The properties of kaolinite clay are discussed in Table 4.2. To classify the sand type, grain size analysis is carried out and the fineness modulus of the sand is determined as 2.754, which means the sand is classified as medium sand. The basic properties of sand is classified in Table 4.3. These three materials are mixed in different proportions to make a synthetic material. In the case of the twin tunnel sample, only Plaster of Paris material is used as model material and the water powder ratio is kept at 0.6 in all the types of composition.

Table 4.2 Properties of Kaolinite Clay

Property	Value	Testing Method
Specific Gravity (G)	2.64	IS:2720 (Part-3)-1980
Liquid Limit (W_L)	33.8%	IS:2720 (Part-5)-1985
Plastic Limit (P_L)	25.3%	IS:2720 (Part-5)-1985
UCS (kPa)	8.7	IS:2720 (Part-10)-1991

Table 4.3 Properties of Sand

Property	Value	Testing Method
Specific Gravity (G)	2.69	IS:2386(Part-3)-1963
D10	0.1	IS:2386(Part-1)-1963
D30	0.4	IS:2386(Part-1)-1963
D60	1.2	IS:2386(Part-1)-1963
C_u	12	IS:2386(Part-1)-1963
C_c	1.33	IS:2386(Part-1)-1963
Fineness Modulus	2.756	IS:383-1970
Water absorption	1.21	IS:2386(Part-3)-1963

4.2.3 Engineering Properties

To perform the basic test and for classification of the engineering properties, cylindrical samples are prepared in the laboratory. The cylindrical samples having (L/D= 2.0) ratio are prepared by adding the prescribed amount of water to it. As decided earlier, the water powder ratio is kept at .60. For GM-1 i.e.100% POP material, water is mixed with POP and mixed well for 1 to 2 minutes to make a uniform paste. Then the resultant paste is poured into the cylindrical moulds of size 38 mm in diameter and 76mm in length according to specimen size recommendation given in ISRM (1979). After 30 minutes, the cylindrical samples are removed from the moulds as they get sufficiently hardened. After then theses cylindrical samples are kept for air curing for 14 days. Initially, the diameter of these samples is 38mm and the length is 76mm. Then these samples are cut into other sizes desired for various other tests. Similarly, the cylindrical samples are prepared for GM-2 and GM-3 material. The samples prepared from

different geomaterials are shown in Fig. 4.2 and Fig. 4.3. The stress-strain behaviour of the model material is shown in Fig 4.4. The scale effect is considered by selecting the dimension of the model as compared with the size of the tunnel to eliminate the effect of boundary conditions.

Fig. 4.2 Prepared specimens of different Geomaterials.

Fig. 4.3 Specimens of different Geomaterials prepared for Brazilian test to determine the indirect tensile strength.

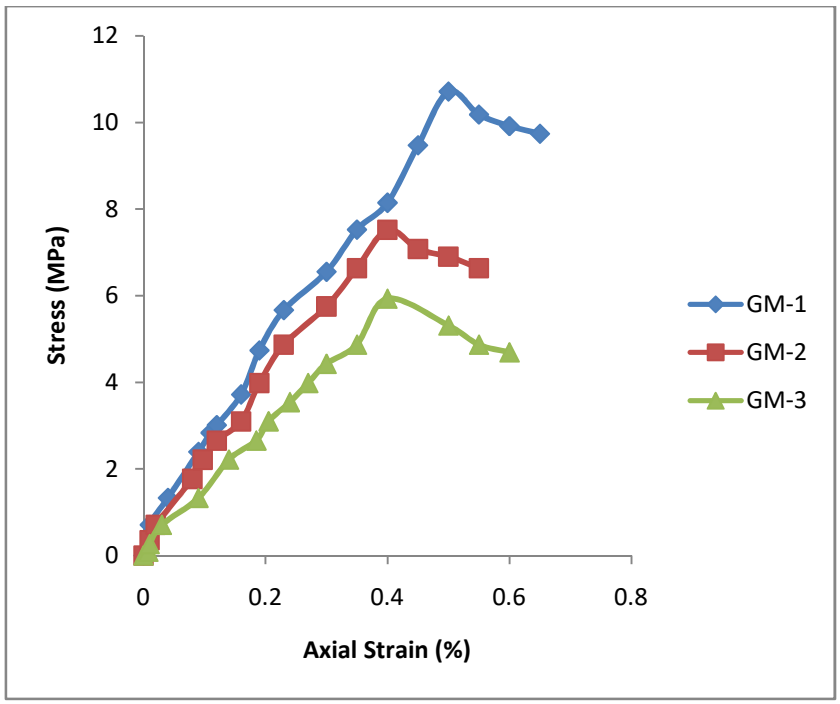

Fig. 4.4 Stress-strain Curve for all three model materials.

For the present study, three different geo-materials are selected to prepare the rock tunnel models and are named GM-1, GM-2 and GM-3. The model material is selected according to its stress-strain behaviour. For the preparation of these tunnel models Plaster of Paris, Kalonite Clay and Sand are used in different proportions as discussed in Table 4.1. Kalonite clay used in this study is characterized in the laboratory and its basic engineering properties are determined. After the preparation of cylindrical samples of all three types of materials, the basic engineering properties of the material are determined. Various tests such as dry density, unconfined compressive strength, tensile strength etc are conducted for the engineering classification of the materials. Fig. 4.5 and Fig. 4.6 show the deformed sample after UCS and Brazilian tests.

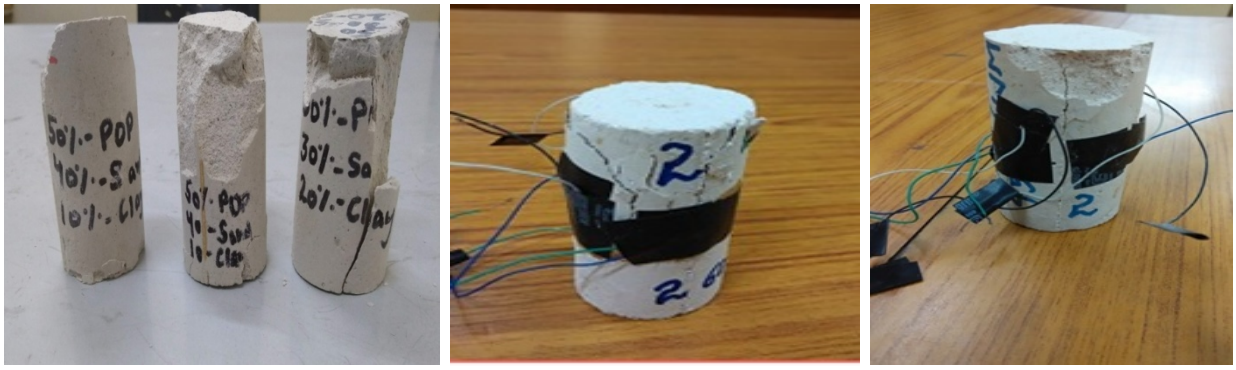

Fig. 4.5 Deformed UCS specimens after testing

Fig. 4.6 Specimen tested for indirect tensile strength

After selecting the composition of the model material, the engineering properties of the model material are determined. Various cylindrical samples of diameter 38mm and a length of 76mm are casted in the laboratory and these samples are tested to determine the engineering properties. The average uniaxial compressive strength of GM-1 material is found to be 10.5MPa.Similarly, for GM-2 and GM-3 materials, various samples are casted, and it is found that the average uniaxial compressive strength of GM-2 and GM-3 materials are 7.5 MPa and 5.9 MPa, respectively.

Various tests are conducted to determine the indirect tensile strength of the model materials. It is found that the average value of tensile strength for GM-1 is 0.78MPa, whereas, for GM-2 and GM-3, the average value is found to be as 0.56MPa and 0.38MPa respectively. The average

value of Young's Modulus for GM-1 is found to be as 2500MPa, whereas, for GM-2 and GM-3, the average value of Young's modulus is found to be as 1700MPa and 1300MPa. The engineering properties of the model material are determined according to the standards procedure for the rock mechanics laboratory. The different engineering properties of all three model materials are discussed below in Table 4.4. The flowchart of the experimental program for the present study is shown in Fig. 4.7.

According to Deere Miller classification (1968) the classification of GM-1, GM-2 and GM-3 is done as EM (Medium Elastic).As the unconfined confined strength of all the three model materials is greater than 1MPa where represent a rock structure. Therefore the structure of rock mass can be simulated with the actual tunnel engineering structure excavated in weak rock. The engineering properties of the model material are determined according to the standards procedure for the rock mechanics laboratory.

Table 4.4 Parameters determined for different Geo-materials

Properties	**GM-1**	**GM-2**	**GM-3**	**Testing Method**
Dry Density (kN/m^3)	12.20	11.6	10.3	ISRM (1972)
UCS (MPa)	10.7	7.5	5.9	ISRM(1979)
Modulus E_{t50} (MPa)	2500	1700	1300	ISRM (1979)
Tensile Strength (MPa)	0.78	0.56	0.38	IS:10082(1981)
Deere–Miller Classification (1968)	EM	EM	EM	Deere Miller classification (1968)

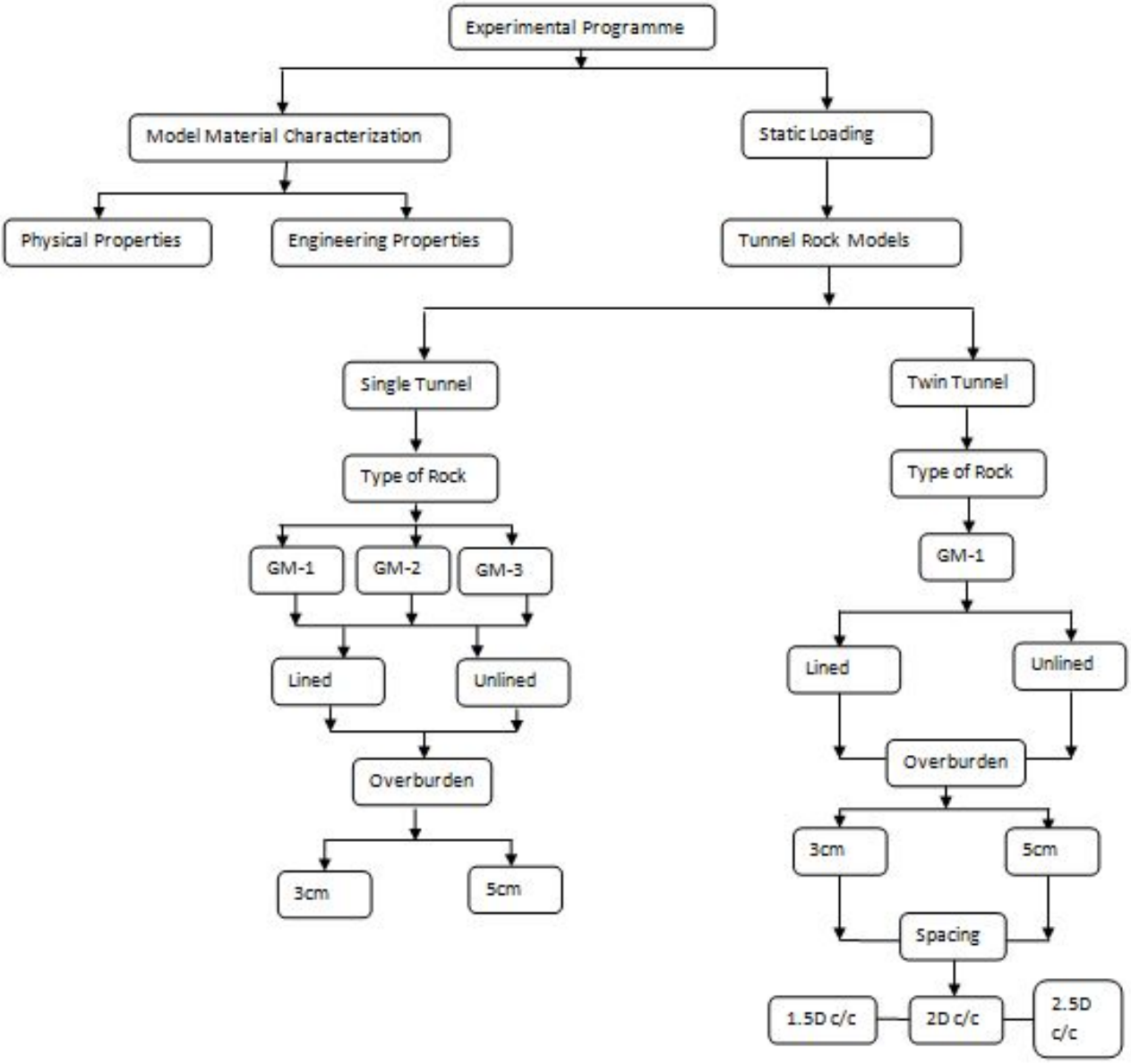

Fig. 4.7 The flowchart of the experimental program

4.3 Rock Tunnel Model

After modelling the synthetic rock in the laboratory which represents in-situ weak rock mass and soil, the rock-tunnel model was casted. In order to study the deformations in tunnel lining of weak rock mass, it is important to record the exact distribution of deformations in the underground tunnel when subjected to static loading. For a better assessment of stresses coming over lining and surrounding rock masses, field experiments are proven to be very expensive and are difficult to repeat. Henceforth ground response can be well understood by reduced physical models from the prototype.

Physical modelling in the laboratory is one of the liable methods in determining lining stresses and cracks propagated inside the tunnel and replicating the same with the in-situ condition. It is desirable to commence the testing of small-scale models before actual field investigations, for safety and economic factors. In order to examine the deformation of shallow urban tunnels and their failure under static loading conditions, a series of extensive small scale physical tunnel models were casted in the laboratory.

4.3.1 Fixing dimension of tunnel models

The geometry of both single and twin tunnel models is decided according to the boundary conditions. The dimension of the single tunnel model is kept at 300x250x230mm (LxWxH). The cover depth of the tunnel is decided as 30mm and 50mm. The diameter of the tunnel is kept at 50mm in all cases, which is decided according to the ease of workability. The width of the tunnel sample is kept at 250mm (r=4a, where “a” is the radius of the tunnel and “r” is the radial distance). For lined samples, PVC pipe is used as a liner material. The thickness of the PVC pipe is 1.74mm, and its length is kept at 300mm, i.e., the length of the tunnel sample. The

dimension of the twin tunnel sample is kept at 425x375x230mm (LxWxH). The width of the twin tunnel is decided according to the boundary conditions (i.e., r=4a, where "a" is the radius of the tunnel. Twin tunnel samples are tested for three different spacing, i.e., 1.5D, 2D, and 2.5D (where 'D' is the diameter of the tunnel). The cover depth of the tunnel is kept at 3cm and 5cm from the top of the model surface. The diameter of the tunnel is kept at 5cm the same as in the case of a single tunnel sample. In the case of twin tunnel models, again PVC pipe is used as a liner material in the case of lined tunnels. Both Lined and Unlined samples of twin tunnels are prepared in the laboratory.

4.4 Casting of models

For the preparation of single and twin tunnel samples, firsts of all the total volumes of the Perspex box is calculated. According to the calculated volume of the Perspex box, the quantity of the materials required to make the tunnel specimen is determined. In the case of 100% POP samples of a single tunnel, around 20kg of Plaster of Paris is taken in powder form in a large container so that it can be mixed thoroughly with water. After deciding the quantity of Plaster of Paris, the prescribed quantity of water is added to it i.e. 12 kg. Then the mixing of the sample is done in such a way that it should form a uniform paste and there should be no lumps in it. After mixing the model material for about 10 to 15 minutes, it is poured into the single tunnel Perspex mould and the mould is kept on the vibrating table stand for 4 to 5 minutes. The purpose of keeping the Perspex box on the vibrating table is to make sure that there should be no air bubbles that got entrapped because of the heat of the hydration of Plaster of Paris. After the process of vibration, the sample is kept undisturbed for about 30 to 40 minutes so that it gets hardened. After that, the tunnel sample is removed from the mould and kept for air curing for 28 days time span. In the case of mixed samples, sand and kaolinite clay is added to the Plaster

of Paris material and mixed thoroughly before adding the prescribed quantity of water into it. For unlined samples, the greasing and oil is done on the PVC pipe so that it can be removed easily once the sample gets hardened whereas in the case of the lined samples the PVC is not removed from the samples as it acts as the liner material for lined tunnels and the final sample is shown in Fig. 4.8. About 36 samples of the singles tunnel of three different material compositions with varying cover depths are prepared in the laboratory shown in Fig 4.9. Similarly, twin tunnel samples are prepared of different spacing and cover depths. The twin tunnel samples are prepared from Plaster of Paris material. In the case of twin tunnel samples, about 36 tunnel samples are casted out of which 18 samples are unlined tunnel samples as shown in Fig 4.10. In total, more than 72 tunnels specimen of single and twin tunnels are casted for experimentation as shown in Fig. 4.11. After the preparation of the tunnel sample, they are kept undisturbed in air curing conditions for 28 days and are tested under static loading conditions after they get sufficiently hardened.

Fig. 4.8 Final sample prepared

Fig. 4.9 Single lined and unlined tunnel samples with different cover depths

Fig. 4.10 Twin Tunnel Samples having different c/c spacing and cover depth

Fig. 4.11 Rock Tunnels Model prepared for experimental analysis.

4.5 Marking the dimensions and Drilling

After the preparation of single and twin tunnel models, the models are kept for air curing for the time period of 28 days so that they become sufficiently hardened. Then the marking is done on the tunnel surface from the bottom side to fix the LVDTs inside the tunnel samples as shown in Fig.4.12. In single tunnel samples, three LVDTs are fixed inside the tunnel model. For that holes are drilled at three different positions. The points selected for drilling holes inside the tunnel samples are L/3, L/2 and 7L/12. Firstly the dimension is marked on the bottom surface of the tunnel sample and then the centre line is plotted. On this centre line, three points are marked for drilling the holes. Similarly, In the case of the twin tunnel samples, six LVDTs are fixed inside the two tunnels three LVDTs in each tunnel. For that, six holes are drilled to insert

the LVDT inside the samples. For twin tunnel samples, the points selected for fixing LVDTs are L/3, L/2 and 9L/12 where “L” is again the length of the tunnel. After marking the positions on twin tunnel samples, the holes are drilled with the help of a drilling machine as shown in Fig. 4.13. The diameter of the drill bit is 10mm which is the same as the diameter of the LVDT used in the testing process.10mm drill bit is used so that the LVDT can be inserted inside the tunnel sample easily. A small hole of the diameter of 2mm mm is also drilled nearby to the 10mm hole. This 2 mm hole is used to fix the tri nut inside it as shown in Fig. 4.14.

Fig. 4.12 Marking the dimensions on the bottom of the tunnel sample

Fig. 4.13 Drilling holes inside the tunnel sample

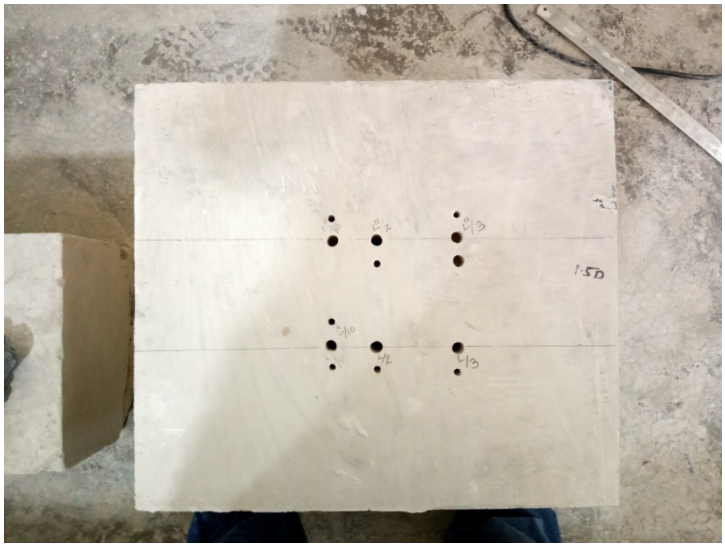

Fig. 4.14 Holes drilled in the twin tunnel model for fixing LVDT's

4.6 Physical modelling of single and twin tunnel

Physical Modelling is a very useful method to simulate the field conditions in the laboratory because, in field conditions, it is not possible to conduct all the tests. Because in field conditions there are many unfavourable conditions under which the ideal testing can not be done properly. For practical reasons, the field experiments are difficult to conduct and hence physical model tests have to be used. In this study, physical modelling of a single tunnel and twin tunnel is done under static loading conditions. The load is applied on the top surface of the tunnel model in the form of point loading. The effect of the presence of liner material, overburden, the strength of rock, and spacing between the tunnels in the case of twin tunnels on the deformation of the tunnel is also studied. In the case of the single tunnel, the test has been performed on all three types of material i.e., GM-1, GM-2 and GM-3 material. All three model materials are characterized in the earlier stage. More than 36 models of the lined and unlined tunnel are prepared in perspex mould. The size of the tunnel model is kept at 30x25x23cm which is considered to be three-dimensional modelling. (LxWxH). The experimental study is conducted on two different cover depths, i.e., 3cm and 5cm. Polyvinyl Chloride pipe is used as a liner material. After the preparation of the models, three LVDTs are fixed along the length of the tunnel. For fixing LVDTs, three different locations are selected to take the deformation in the tunnel. After the marking of locations to fix LVDTs in the model, the hole is drilled with the help of a drill machine up to the bottom lining of the tunnel. After drilling holes, three LVDTs are fixed at three different locations i.e, L/3, L/2 and 7L/12 where "L" is the length of the tunnel model. After placing the LVDTs, the tunnel model is kept inside the compression testing unit, which is attached to the 16-Ch LVDT data logger. Then the load is applied to the top surface of the tunnel sample in the form of point loading with the help of a compression testing machine. The schematic diagram of point load applied on a single tunnel model is

shown in Fig. 4.15. After the failure of the sample, it is removed from the platen. LVDT is then removed gently from the tunnel sample.

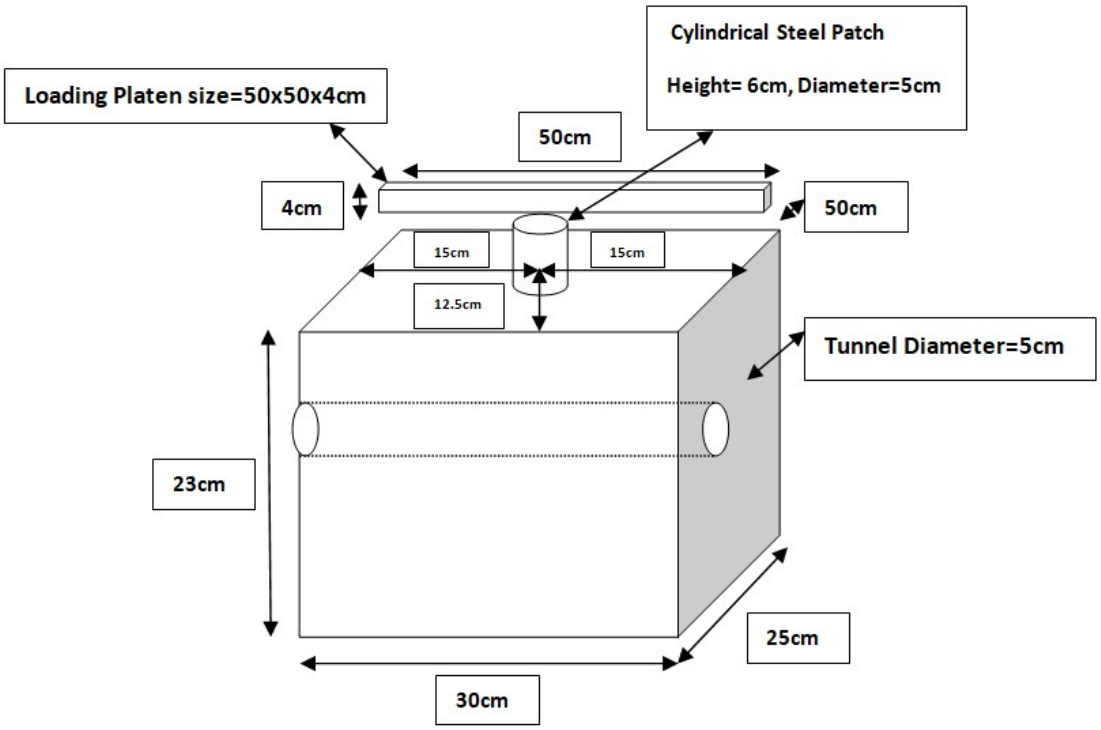

Fig. 4.15 Schematic diagram of the static load acting on a single tunnel model.

In the case of the Twin tunnel, the sample is made of GM-1 material i.e 100% Plaster of Paris material at 60% water content. The dimension of the twin tunnel sample is kept at 42.5x37.5x23cm (LxWxH). Twin tunnel samples are tested for three different spacing, i.e., 1.5D, 2D, and 2.5D (where 'D' is the diameter of the tunnel). The cover depth of the tunnel is kept at 3cm and 5cm from the top of the model surface. Both Lined and Unlined samples of twin tunnels are prepared in the laboratory. To take the deformation in the tunnel sample, six LVDTs are placed at different locations. The location of placing LVDTs in the tunnel sample is chosen according to the extent of deformation that occurs in the tunnel when applied to static loading conditions. The load is applied on the top surface of the twin tunnel model by placing a

rectangular plate of size 17x5x1.5cm (length x width x thickness). The schematic diagram of load applied on a twin tunnel model is shown in Fig. 4.16. Three LVDTs are placed in each tunnel at three different locations. LVDTs are placed at a distance of L/3, L/2, and 9L/15, where 'L' is the length of the tunnel. To place the LVDTs, the same method as adopted in a single tunnel is followed. For installation, six holes of 10mm diameter are drilled from the bottom of the surface. Then the LVDT is fixed with the help of a three-pin clamped to keep it tight so that it does not move from its location. The schematic diagram of load applied on a twin tunnel model is shown in Fig. 4.16.

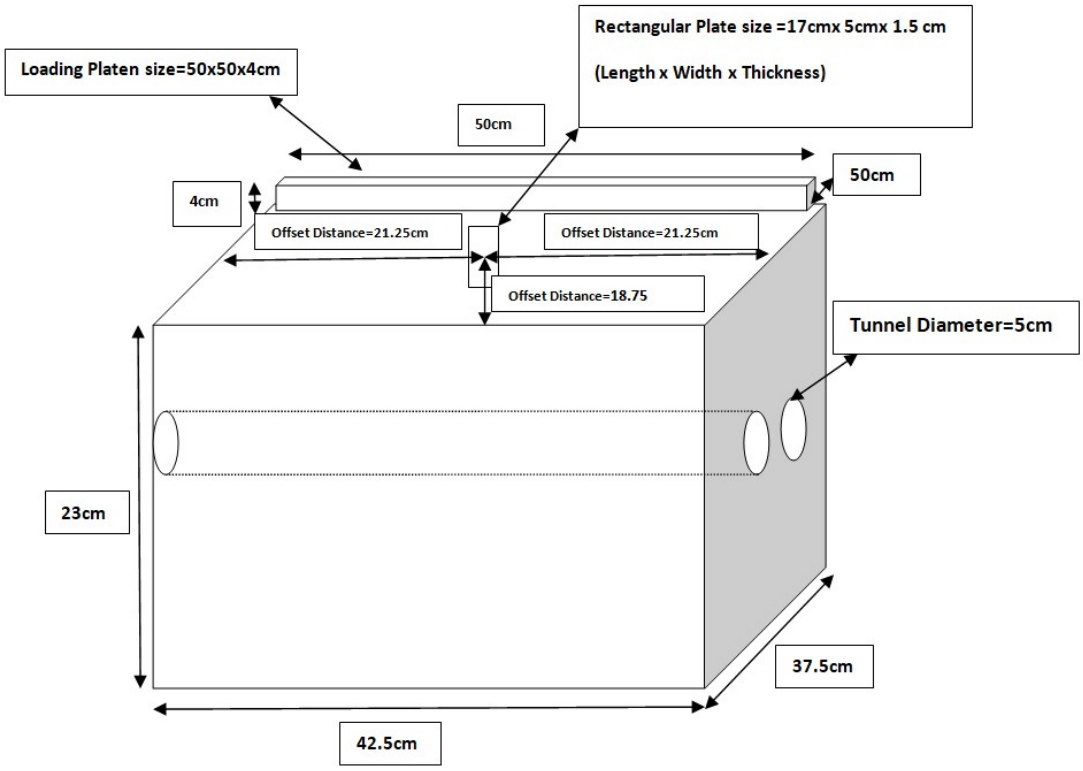

Fig.4.16 Schematic diagram of the static load acting on the twin tunnel model.

4.6.1 Deformation of the single tunnel of GM-1 material

After placing the LVDT in the single tunnel sample, the tunnel model is kept in a compression testing machine and tested under static loading conditions. The load is applied from the top of the tunnel sample with the help of the steel patch. After conducting the test on the GM-1 single tunnel sample, it has been noted that deformation is more in unlined samples as compared to lined samples. This is due to the absence of liner material in the unlined tunnel as the liner material offers resistance against the developed stresses.

In the case of 3cm cover depth unlined samples of GM-1 model material, the maximum crown deformation experienced at L/2 distance is 0.20mm whereas the deformation noticed at points L/3 and 7L/12 is 0.03mm and 0.13mm respectively obtained at 21kN load which is the maximum load at which the tunnel sample fails. The deformation obtained at L1', L2' and L3' will be the same as the deformation obtained at L1, L2 and L3. It may be stated here that L1', L2' and L3' will correspond exactly to the same distance from the centre point and hence will have the same deformation. In this case, it has been observed that the deformation obtained at the end faces of the tunnel sample is zero. Table 4.5 presents the results in terms of the deformations recorded for the case of the tunnel at a cover depth of 3cm with a diameter of 5 cm and subjected to static loading. The deformations have been reported for various positions along the tunnel axis. In the case of 5cm unlined tunnels, the crown deformation at L/2 distance is 0.16mm at 24 kN load which is the maximum load at which the tunnel sample fails, whereas the deformation is noticed at points L/3 and 7L/12 is 0.02mm and 0.09mm respectively. Table 4.6 shows the value of deformations at different locations for a 5cm cover depth unlined tunnel sample of GM-1 material. In GM-1 tunnel models, longitudinal crack length varies from 5.50cm to 5.8cm for C/D = 1.0, from 5.6cm to 6.0cm for C/D = 0.6.

Table 4.5 Deformation of Unlined Tunnel in GM-1 sample for C/D =0.6

Zones	Distance (cm)	Deformation (mm)
L1	0.0	0.0
L2	10.0	-0.03
L3	12.0	-0.13
L4	15.0	-0.20
L3’	18.0	-0.13
L2’	20.0	-0.03
L1’	30.0	0.0

Table 4.6 Deformation of Unlined Tunnel in GM-1 sample for C/D =1.0

Zones	Distance (cm)	Deformation (mm)
L1	0.0	0.0
L2	10.0	-0.02
L3	12.0	-0.09
L4	15.0	-0.16
L3’	18.0	-0.09
L2’	20.0	-0.02
L1’	30.0	0.0

In the case of 3cm lined tunnels of GM-1 model material, the crown deformation obtained at L/2 distance is 0.09mm at 32 kN load, whereas the deformation noticed at points L/3 and 7L/12 is 0.02mm and 0.06mm respectively. Table 4.7 shows the value of deformations at different locations for 3cm cover depth in GM-1. The minimum deformation is noticed in the case of a 5cm lined sample. This is due to the presence of liner material because the presence of liner material will resist the deformation in the tunnel sample as a result of that the minimum deformation is experienced in the case of a lined sample. In the case of 5cm lined samples the deformation experienced at L/3, L/2and 7L/12 is 0.01mm,0.07mm, and 0.03mm respectively at 39kN load. Table 4.8 shows the value of deformations at different locations for 5cm cover depth in GM-1. The deformation profile of GM-1 single tunnels models is shown in Fig 4.17 and the load vs. deformation graph is shown in Fig 4.18.

Table 4.7 Deformation of lined Tunnel in GM-1 sample for C/D =0.6

Zones	Distance (cm)	Deformation (mm)
L1	0.0	0.0
L2	10.0	-0.02
L3	12.0	-0.06
L4	15.0	-0.09
L3’	18.0	-0.06
L2’	20.0	-0.02
L1’	30.0	0.0

Table 4.8 Deformation of lined Tunnel in GM-1 sample for C/D =1.0

Zones	Distance (cm)	Deformation (mm)
L1	0.0	0.0
L2	10.0	-0.01
L3	12.0	-0.03
L4	15.0	-0.07
L3’	18.0	-0.03
L2’	20.0	-0.01
L1’	30.0	0.0

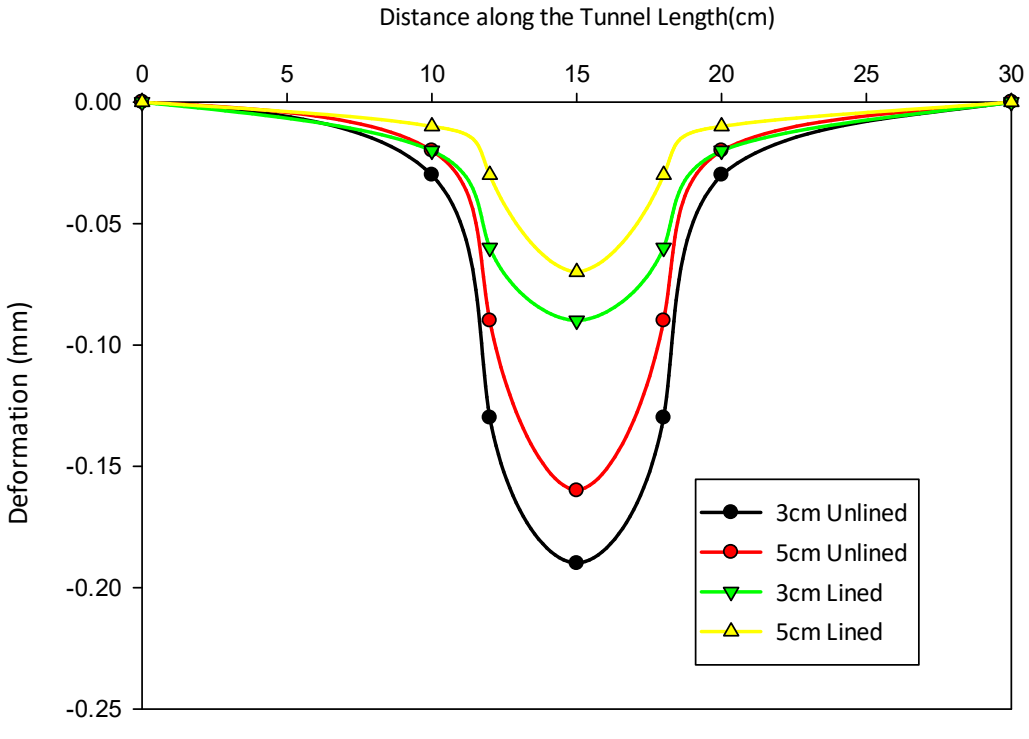

Fig. 4.17 Deformation profiles of GM-1 single tunnels models.

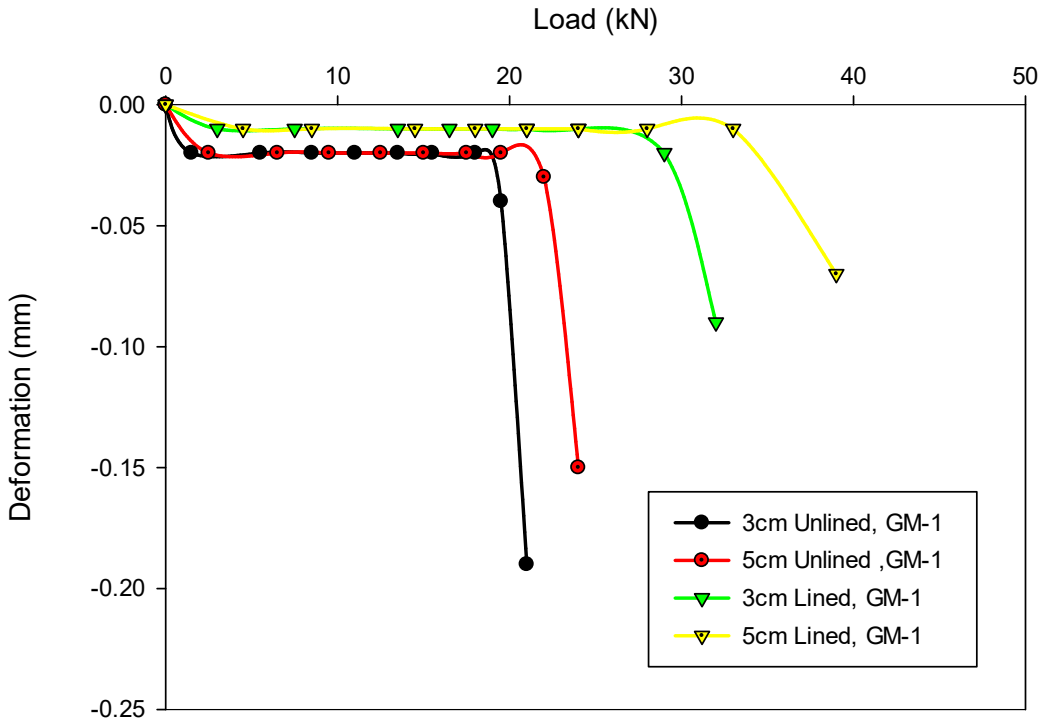

Fig. 4.18 Load vs. Deformation graph of GM-1 single tunnels models

4.6.2 Deformation of single tunnel of GM-2 material

Secondly, the tunnel samples of GM-2 material (50% POP, 40% Sand and 10% Clay) are tested under a compression testing machine. In the case of 3cm cover depth unlined samples, the maximum crown deformation experienced at L/2 distance is 0.25mm whereas the deformation noticed at points L/3 and 7L/12 is 0.04mm and 0.17mm respectively obtained at 15kN load. Table 4.9 presents the results in terms of the deformations recorded for the case of the unlined tunnel of GM-2 material at a cover depth of 3cm. In the case of 5cm unlined tunnels, the crown deformation at L/2 distance is 0.19mm at 18 kN load, whereas the deformation noticed at points L/3 and 7L/12 is 0.03mm and 0.14mm respectively. Table 4.10 shows the value of deformations at different locations for 5cm cover depth unlined tunnel sample of GM-2 material.

Table 4.9 Deformation of Unlined Tunnel in GM-2 sample for C/D =0.6

Zones	Distance (cm)	Deformation (mm)
L1	0.0	0.0
L2	10.0	-0.04
L3	12.0	-0.17
L4	15.0	-0.25
L3’	18.0	-0.17
L2’	20.0	-0.04
L1’	30.0	0.0

Table 4.10 Deformation of Unlined Tunnel in GM-2 sample for C/D =1.0

Zones	Distance (cm)	Deformation (mm)
L1	0.0	0.0
L2	10.0	-0.03
L3	12.0	-0.14
L4	15.0	-0.19
L3’	18.0	-0.14
L2’	20.0	-0.03
L1’	30.0	0.0

In the case of lined tunnels having 3cm cover depth, the crown deformation at L/2 distance is 0.12mm at 20 kN load, whereas the deformation noticed at points L/3 and 7L/12 is 0.02mm and 0.07mm respectively. Table 4.11 shows the value of deformations at different locations for 3cm cover depth in GM-2. In the case of 5cm lined samples the deformation experienced at L/3, L/2and 7L/12 is 0.01mm,0.10mm, and 0.06mm respectively at 22kN load. Table 4.12 shows the value of deformations at different locations for 5cm cover depth. In GM-2 model material, longitudinal crack length varies from 6.2cm to 6.6cm for C/D = 1.0, from 6.5cm to 6.8cm for C/D = 0.6. The deformation profile of GM-2 single tunnels models is shown in Fig 4.19 and the load vs. deformation graph is shown in Fig 4.20.

Table 4.11 Deformation of lined Tunnel in GM-2 sample for C/D =0.6

Zones	Distance (cm)	Deformation (mm)
L1	0.0	0.0
L2	10.0	-0.02
L3	12.0	-0.07
L4	15.0	-0.12
L3’	18.0	-0.07
L2’	20.0	-0.02
L1’	30.0	0.0

Table 4.12 Deformation of lined Tunnel in GM-2 sample for C/D =1.0

Zones	Distance (cm)	Deformation (mm)
L1	0.0	0.0
L2	10.0	-0.01
L3	12.0	-0.06
L4	15.0	-0.10
L3’	18.0	-0.06
L2’	20.0	-0.01
L1’	30.0	0.0

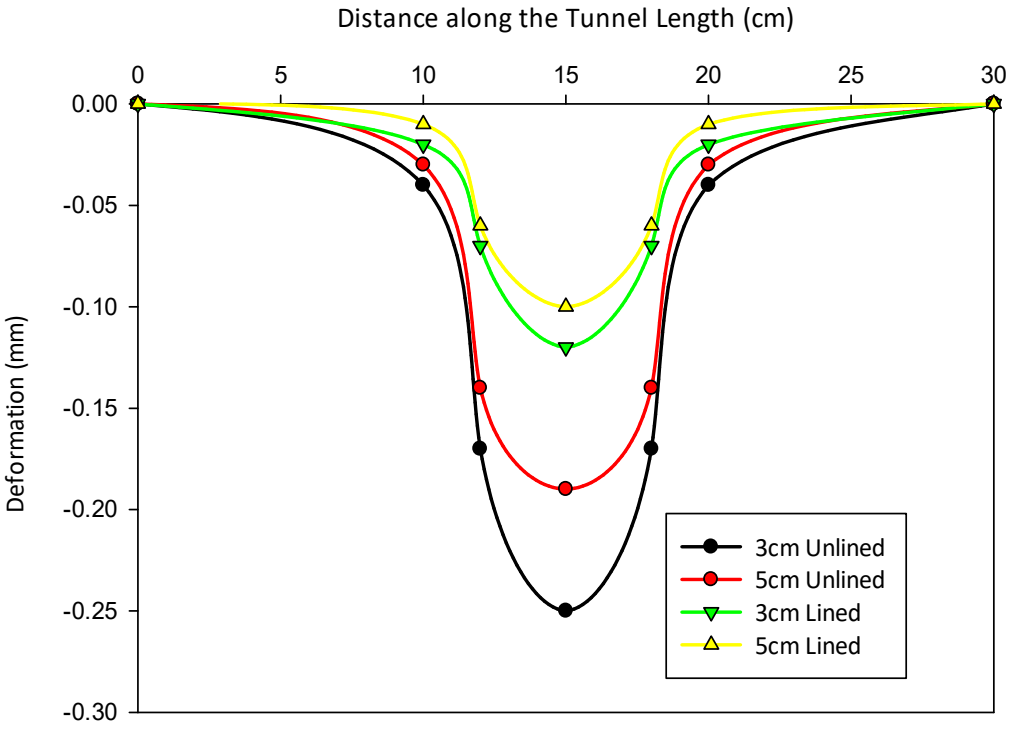

Fig. 4.19 Deformation profiles of GM-2 single tunnels models.

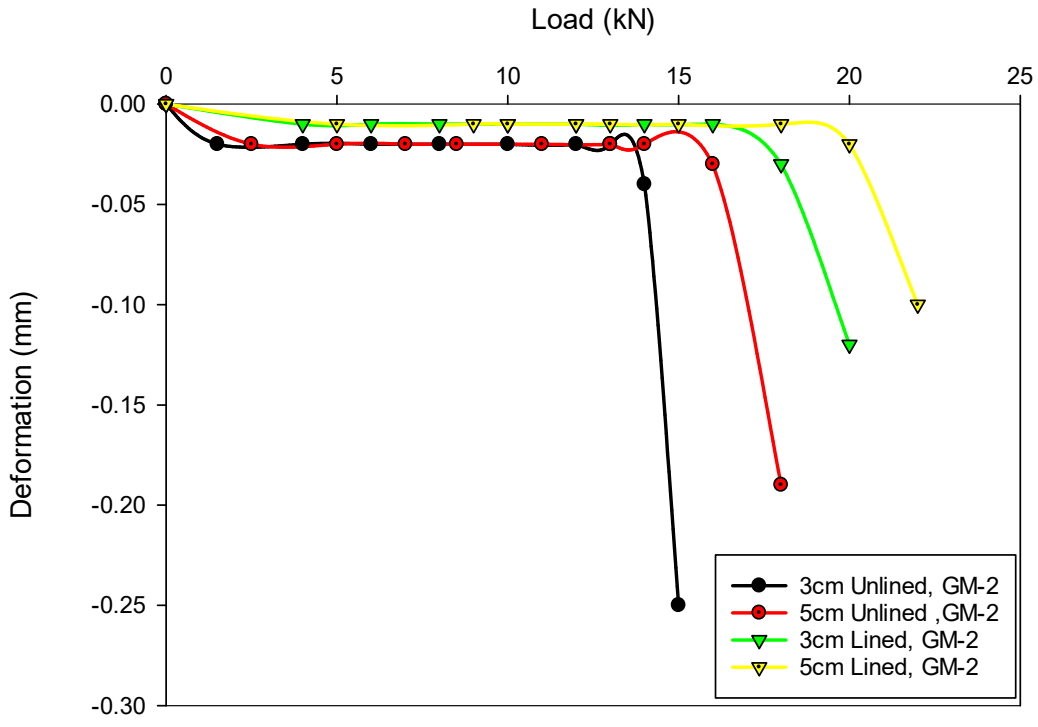

Fig 4.20 Load vs. Deformation graph of GM-2 single tunnels models.

4.6.3 Deformation of single tunnel of GM-3 material

Thirdly, the tunnel samples of GM-3 material (50% POP, 30% Sand and 20% Clay) are tested under a compression testing machine. In the case of 3cm cover depth unlined samples, the maximum crown deformation experienced at L/2 distance is 0.29mm whereas the deformation noticed at points L/3 and 7L/12 is 0.04mm and 0.20mm obtained at 11kN load. Table 4.13 presents the results in terms of the deformations recorded for the case of the unlined tunnel of GM-3 material at a cover depth of 3cm. In the case of 5cm unlined tunnels, the crown deformation at L/2 distance is 0.21mm at 14 kN load, whereas the deformation noticed at points L/3 and 7L/12 is 0.03mm and 0.15mm respectively. Table 4.14 shows the value of deformations at different locations for 5cm cover depth unlined tunnel sample of GM-3 material.

Table 4.13 Deformation of Unlined Tunnel in GM-3 sample for C/D =0.6

Zones	Distance (cm)	Deformation (mm)
L1	0.0	0.0
L2	10.0	-0.04
L3	12.0	-0.20
L4	15.0	-0.29
L3’	18.0	-0.20
L2’	20.0	-0.04
L1’	30.0	0.0

Table 4.14 Deformation of Unlined Tunnel in GM-3 sample for C/D =1.0

Zones	Distance (cm)	Deformation (mm)
L1	0.0	0.0
L2	10.0	-0.03
L3	12.0	-0.15
L4	15.0	-0.21
L3’	18.0	-0.15
L2’	20.0	-0.03
L1’	30.0	0.0

In the case of liner material tunnels having a cover depth of 3cm, the crown deformation at L/2 distance is 0.14mm at 18 kN load, whereas the deformation noticed at points L/3 and 7L/12 is 0.02mm and 0.07mm respectively. Table 4.15 shows the value of deformations at different locations for 3cm cover depth in GM-3. The minimum deformation is noticed in the case of a 5cm lined sample. In the case of 5cm lined samples the deformation experienced at L/3, L/2and 7L/12 are 0.02mm,0.11mm, and 0.05mm respectively at 21kN load. Table 4.16 shows the value of deformations at different locations for 5cm cover depth in GM-3. In GM-3 model material, longitudinal crack length varies from 6.8cm to 7.2cm for C/D = 1.0, from 7.0cm to 7.8cm for C/D = 0.6. The deformation profile of GM-3 single tunnels models is shown in Fig 4.21 and the load vs. deformation graph is shown in Fig 4.22.

Table 4.15 Deformation of lined Tunnel in GM-3 sample for C/D =0.6

Zones	Distance (cm)	Deformation (mm)
L1	0.0	0.0
L2	10.0	-0.02
L3	12.0	-0.07
L4	15.0	-0.14
L3’	18.0	-0.07
L2’	20.0	-0.02
L1’	30.0	0.0

Table 4.16 Deformation of lined Tunnel in GM-3 sample for C/D =1.0

Zones	Distance (cm)	Deformation (mm)
L1	0.0	0.0
L2	10.0	-0.02
L3	12.0	-0.05
L4	15.0	-0.11
L3’	18.0	-0.05
L2’	20.0	-0.02
L1’	30.0	0.0

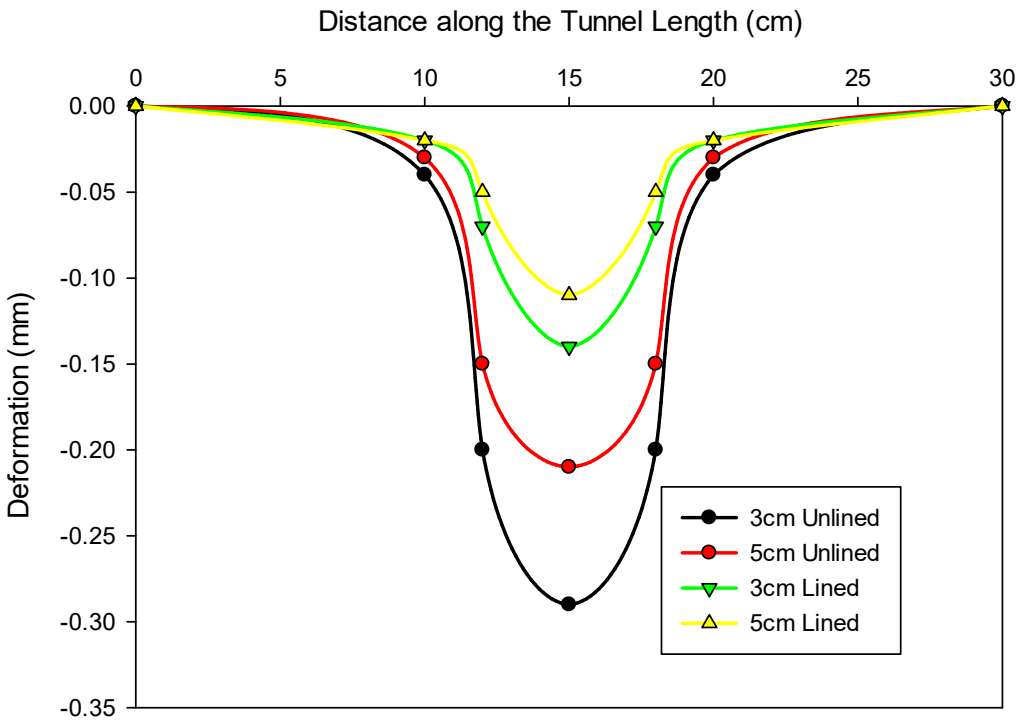

Fig. 4.21 Deformation profiles of GM-3 single tunnels models.

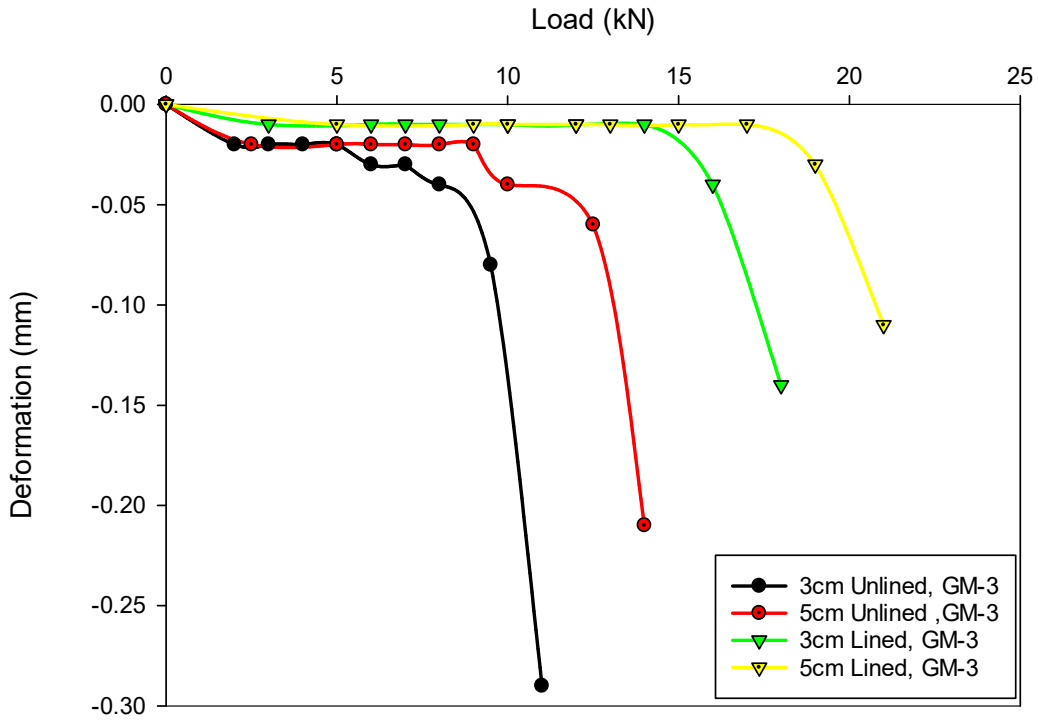

Fig 4.22 Load vs. Deformation graph of GM-3 single tunnels models.

4.6.4 Deformation of twin tunnel having 1.5D spacing

In the case of Twin tunnel samples, GM-1 material is used as the model material. The twin tunnel sample of 1.5D c/c spacing is subjected to the static loading condition. In the case of 3cm unlined tunnels, the maximum crown deformation value is 0.25mm obtained at the L/2 distance. Whereas the deformation obtained at L/3 and 9L/15 is 0.03mm and 0.16mm respectively. Table 4.17 presents the results in terms of the deformations recorded for the case of the unlined tunnel having 1.5D centre to centre spacing and a cover depth of 3cm. In the case of 5cm unlined tunnels, the crown deformation at L/2 distance is 0.20mm, whereas the deformation noticed at points L/3 and 9L/15 is 0.02mm and 0.12mm respectively. Table 4.18 presents the results in terms of the deformations recorded for the case of the unlined tunnel having 1.5D centre to centre spacing and a cover depth of 5cm.

Table 4.17 Deformation of unlined Tunnel in 1.5D c/c spacing for C/D =0.6

Zones	Distance (cm)	Deformation (mm)
L1	0.0	0.0
L2	14.0	-0.03
L3	17.0	-0.16
L4	21.25	-0.25
L3’	25.5	-0.16
L2’	28.4	-0.03
L1’	42.5	0.0

Table 4.18 Deformation of unlined Tunnel in 1.5D c/c spacing for C/D =1.0.

Zones	Distance (cm)	Deformation (mm)
L1	0.0	0.0
L2	14.0	-0.02
L3	17.0	-0.12
L4	21.25	-0.20
L3’	25.5	-0.12
L2’	28.4	-0.02
L1’	42.5	0.0

In the case of lined tunnels having 1.5D centre to centre spacing and 3cm cover depth, the crown deformation at L/2 distance is 0.12mm, whereas the deformation noticed at points L/3 and 9L/15 is 0.01mm and 0.07mm. Table 4.19 presents the results in terms of the deformations recorded for the case of a lined tunnel having 1.5D centre to centre spacing and a cover depth of 3cm. In the case of 5cm lined samples the deformation experienced at L/3, L/2and 9L/15 is 0.01mm,0.10mm, and 0.05mm respectively. Table 4.20 presents the results in terms of the deformations recorded for the case of a lined tunnel having 1.5D centre to centre spacing and a cover depth of 5cm. Deformation profiles of 1.5D c/c spacing twin tunnel models obtained from experimental results are shown in Fig 4.23.

Table 4.19 Deformation of lined Tunnel in 1.5D c/c spacing for C/D =0.6.

Zones	Distance (cm)	Deformation (mm)
L1	0.0	0.0
L2	14.0	-0.01
L3	17.0	-0.07
L4	21.25	-0.12
L3’	25.5	-0.07
L2’	28.4	-0.01
L1’	42.5	0.0

Table 4.20 Deformation of lined Tunnel in 1.5D c/c spacing for C/D =1.0.

Zones	Distance (cm)	Deformation (mm)
L1	0.0	0.0
L2	14.0	-0.01
L3	17.0	-0.05
L4	21.25	-0.10
L3’	25.5	-0.05
L2’	28.4	-0.01
L1’	42.5	0.0

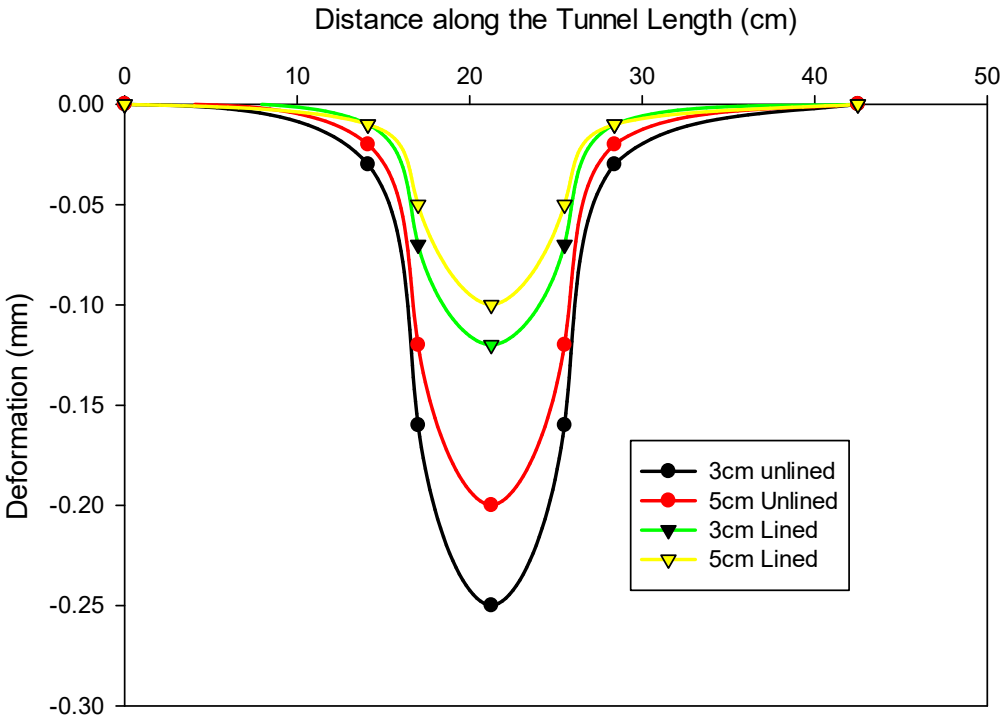

Fig.4.23 Deformation profiles of 1.5D c/c spacing twin tunnels models obtained from experimental results.

4.6.5 Deformation of twin tunnel having 2D spacing

In the case of 2D c/c spacing twin tunnels of 3cm unlined tunnels, the maximum crown deformation value is 0.22mm obtained at L/2 distance. Whereas the deformation obtained at L/3 and 9L/15 is 0.02mm and 0.14mm respectively. Table 4.21 presents the results in terms of the deformations recorded for the case of the unlined tunnel having a 2D centre to centre spacing and cover depth of 3cm. In the case of 5cm unlined tunnels, the crown deformation at L/2 distance is 0.18mm, whereas the deformation noticed at points L/3 and 9L/15 is 0.02mm and 0.11mm respectively. Table 4.22 presents the results in terms of the deformations recorded for the case of the unlined tunnel having a 2D centre to centre spacing and cover depth of 5cm.

Table 4.21 Deformation of unlined Tunnel in 2D c/c spacing for C/D =0.6.

Zones	Distance (cm)	Deformation (mm)
L1	0.0	0.0
L2	14.0	-0.02
L3	17.0	-0.14
L4	21.25	-0.22
L3’	25.5	-0.14
L2’	28.4	-0.02
L1’	42.5	0.0

Table 4.22 Deformation of unlined Tunnel in 2D c/c spacing for C/D =1.0.

Zones	Distance (cm)	Deformation (mm)
L1	0.0	0.0
L2	14.0	-0.02
L3	17.0	-0.11
L4	21.25	-0.18
L3’	25.5	-0.11
L2’	28.4	-0.02
L1’	42.5	0.0

In the case of lined tunnels having 2Dcentre to centre spacing and 3cm cover depth, the crown deformation at L/2 distance is 0.10mm, whereas the deformation noticed at points L/3 and 9L/15 is 0.01mm and 0.06mm respectively. Table 4.23 presents the results in terms of the deformations recorded for the case of a lined tunnel having a 2D centre to centre spacing and cover depth of 3cm. In the case of 5cm lined samples the deformation experienced at L/3, L/2and 9L/15 is 0.01mm,0.08mm, and 0.05mm respectively. Table 4.24 presents the results in terms of the deformations recorded for the case of a lined tunnel having a 2D centre to centre spacing and cover depth of 5cm. Deformation profiles of 2D c/c spacing twin tunnel models obtained from experimental results are shown in Fig 4.24.

Table 4.23 Deformation of lined Tunnel in 2D c/c spacing for C/D =0.6.

Zones	Distance (cm)	Deformation (mm)
L1	0.0	0.0
L2	14.0	-0.01
L3	17.0	-0.06
L4	21.25	-0.10
L3’	25.5	-0.06
L2’	28.4	-0.01
L1’	42.5	0.0

Table 4.24 Deformation of lined Tunnel in 2D c/c spacing for C/D =1.0.

Zones	Distance (cm)	Deformation (mm)
L1	0.0	0.0
L2	14.0	-0.01
L3	17.0	-0.05
L4	21.25	-0.08
L3’	25.5	-0.05
L2’	28.4	-0.01
L1’	42.5	0.0

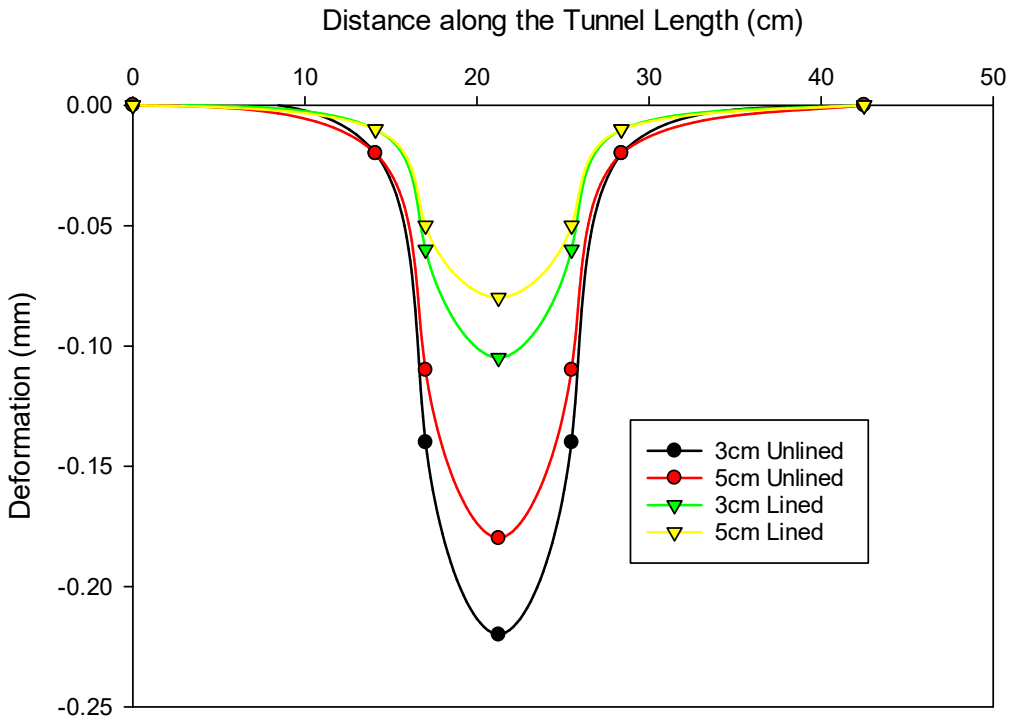

Fig. 4.24 Deformation profiles of 2D c/c spacing twin tunnels models obtained from experimental results.

4.6.6 Deformation of twin tunnel having 2.5D spacing

In the case of 2.5D c/c spacing twin tunnels of 3cm unlined tunnels, the maximum crown deformation value is 0.19mm obtained at L/2 distance. Whereas the deformations obtained at L/3 and 9L/15 are 0.02mm and 0.10mm respectively. Table 4.25 presents the results in terms of the deformations recorded for the case of the unlined tunnel having 2.5D centre to centre spacing and a cover depth of 3cm. In the case of 5cm unlined tunnels, the crown deformation at L/2 distance is 0.16mm, whereas the deformation noticed at points L/3 and 9L/15 is 0.02mm and 0.09mm. Table 4.26 presents the results in terms of the deformations recorded for the case of the unlined tunnel having 2.5D centre to centre spacing and a cover depth of 5cm. In 2.5D

c/c spacing tunnels, longitudinal crack length varies from 5.5cm to 5.8cm for C/D = 1.0, from 5.8cm to 6.1cm for C/D = 0.6 .

Table 4.25 Deformation of unlined Tunnel in 2.5D c/c spacing for C/D =0.6.

Zones	Distance (cm)	Deformation (mm)
L1	0.0	0.0
L2	14.0	-0.02
L3	17.0	-0.10
L4	21.25	-0.19
L3’	25.5	-0.10
L2’	28.4	-0.02
L1’	42.5	0.0

Table 4.26 Deformation of unlined Tunnel in 2.5D c/c spacing for C/D =1.0.

Zones	Distance (cm)	Deformation (mm)
L1	0.0	0.0
L2	14.0	-0.02
L3	17.0	-0.09
L4	21.25	-0.16
L3’	25.5	-0.09
L2’	28.4	-0.02
L1’	42.5	0.0

In the case of lined tunnels having 2.5D centre to centre spacing and 3cm cover depth, the crown deformation at L/2 distance is 0.09mm, whereas the deformation noticed at points L/3 and 9L/15 is 0.01mm and 0.04mm respectively. Table 4.27 presents the results in terms of the deformations recorded for the case of a lined tunnel having 2.5D centre to centre spacing and a cover depth of 3cm. In the case of 5cm lined samples the deformation experienced at L/3, L/2and 9L/15 are 0.01mm,0.08mm, and 0.03mm respectively. Table 4.28 presents the results in terms of the deformations recorded for the case of a lined tunnel having 2.5D centre to centre spacing and a cover depth of 5cm. Deformation profiles of 2.5D c/c spacing twin tunnels models obtained from experimental results are shown in Fig 4.25.

Table 4.27 Deformation of lined Tunnel in 2.5D c/c spacing for C/D =0.6.

Zones	Distance (cm)	Deformation (mm)
L1	0.0	0.0
L2	14.0	-0.01
L3	17.0	-0.04
L4	21.25	-0.09
L3’	25.5	-0.04
L2’	28.4	-0.01
L1’	42.5	0.0

Table 4.28 Deformation of lined Tunnel in 2.5D c/c spacing for C/D =1.0.

Zones	Distance (cm)	Deformation (mm)
L1	0.0	0.0
L2	14.0	-0.01
L3	17.0	-0.03
L4	21.25	-0.08
L3’	25.5	-0.03
L2’	28.4	-0.01
L1’	42.5	0.0

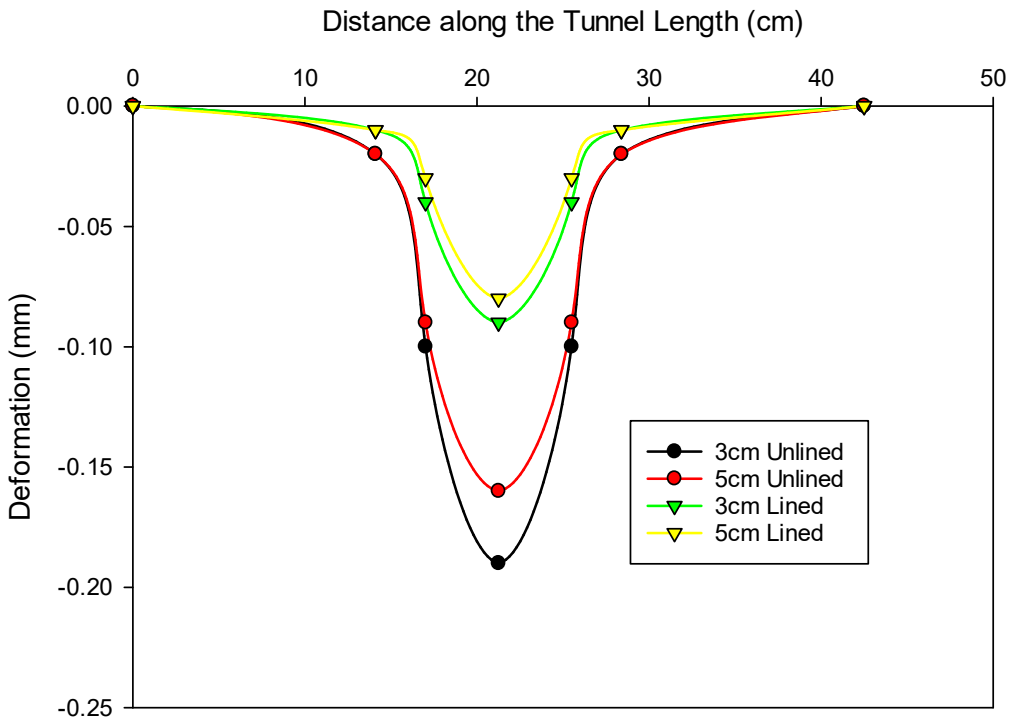

Fig.4.25 Deformation profiles of 2.5D c/c spacing twin tunnels models obtained from experimental results.

4.7 Concluding Remarks

The following conclusions can be drawn from this chapter

- The selection of model material and its characterization is done for the preparation of single and twin tunnel rock models.
- For the determination of the deformation behaviour of single tunnels, the rock tunnel models of different parameters are prepared in the laboratory.
- The preparation of Twin Tunnel samples with different spacing and cover depth is done for experimental analysis.

A detailed discussion about the results obtained from numerical analysis of single and twin tunnels has been discussed in the next Chapter.

Chapter 5

NUMERICAL MODELLING OF SINGLE AND TWIN TUNNEL

The numerical modelling of single and twin tunnels is done with the help of ANSYS software. Different methods can be used to access the deformation of underground structures subjected to static loading conditions. Numerical simulation is considered an affordable method as compared to experimental studies in engineering design and analysis. Therefore numerical simulation is done to predict the behaviour of single and twin tunnels under static loading conditions.

5.1 Load and Boundary Conditions

For the present study, the load has been applied from the top of the tunnel sample in the form of pressure (N/mm^2).To apply the load, a steel patch of diameter 50mm and a depth of 60mm is placed at the top of the tunnel sample as shown in Fig. 5.1. The boundary of the numerical model is decided according to the boundary convergence study. The base of the tunnel model is kept fixed for horizontal and vertical movement whereas all other faces are kept free for movement. In the case of the twin tunnel model, again the base of the tunnel model is kept fixed whereas all other faces are kept free for movement. The boundary conditions provided to the tunnel sample are shown in Fig. 5.2.

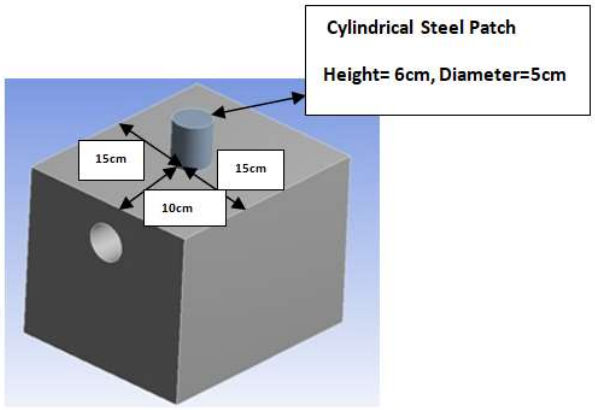

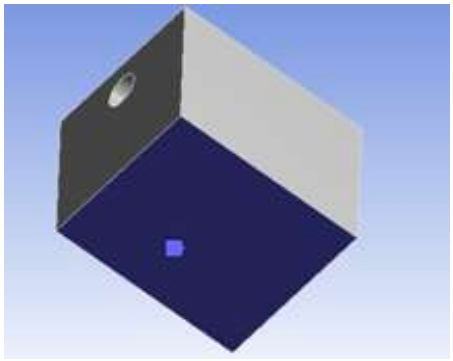

Fig. 5.1 Loading arrangement of Single Tunnel **Fig.5.2 Boundary Conditions**

5.2 Meshing

Meshing is the most important part of numerical modelling of single and twin tunnels. To decide the meshing size of the different parts of the tunnel model, a mesh convergence study is carried out. From the mesh convergence study, it becomes easy to decide mesh density. Based on the mesh convergence study, the global meshing size for rock mass is taken as 8mm in the case of a single tunnel whereas in the case of a twin tunnel sample due to its large size, the mesh size for rock mass is taken as 10mm. It has been observed from a mesh convergence study that in the case of a single tunnel sample, a mesh size finer than 8mm does not have much effect on the deformation of the tunnel. Similarly, for the twin tunnel, a mesh size finer than 10mm does have much effect on the deformation of the tunnel. The mesh density for the steel patch which is placed at the top of the tunnel model is decided as 6mm. In the case of the lined sample, the global mesh size for PVC pipe is taken as 6mm. Fig. 5.3 shows the meshing of various elements.

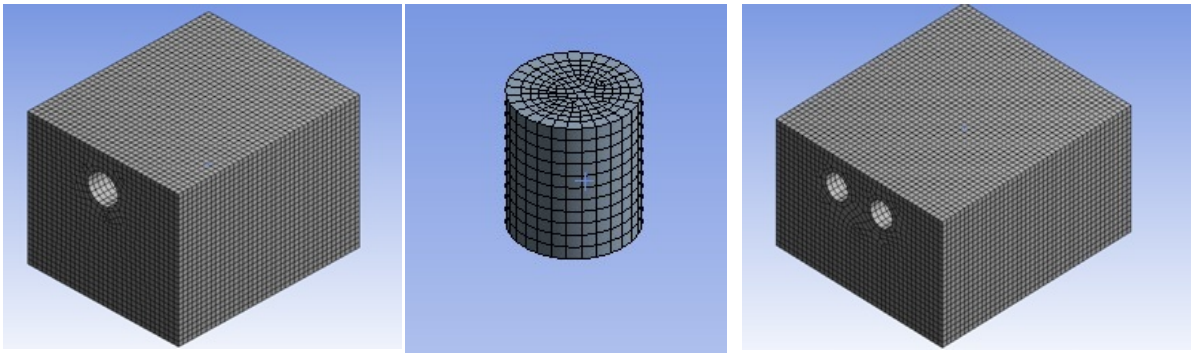

(a) Single Tunnel Model (b) Steel Patch to apply load. (c) Twin Tunnel Rock Model

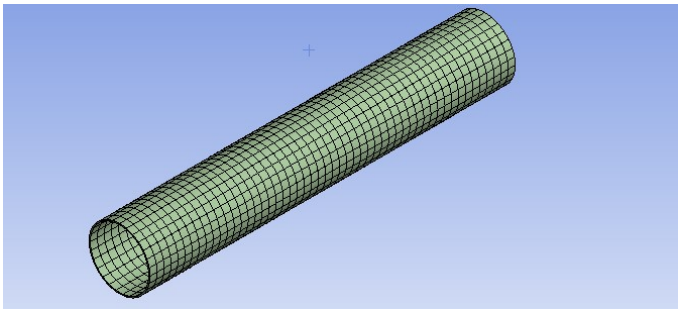

(d) Lining

Fig. 5.3 Meshing of the Elements

Meshing is an important factor for numerical analysis purposes as it decides the size and number of elements and nodes build in the tunnel sample and lining part. The rock tunnel model in the case of a single tunnel sample comprises 160578 elements and 78678 nodes, including 3658 nodes and 2200 elements for tunnel lining whereas in the case of a twin tunnel sample there are 159879 elements and 74598 nodes, including 3758 nodes and 2251 elements for tunnel lining.

5.3 Numerical analysis of Single Tunnels

5.3.1 Deformation of a single tunnel of GM-1 material

In the case of 3cm cover depth unlined samples, the maximum crown deformation experienced at L/2 distance is 0.22mm whereas the deformation noticed at points L/3 and 7L/12 is 0.05mm and 0.13mm respectively. Table 5.1 presents the results in terms of the deformations recorded for the case of the tunnel at a cover depth of 3cm. In the case of 5cm unlined tunnels, the crown deformation at L/2 distance is 0.18mm, whereas the deformation noticed at points L/3 and 7L/12 is 0.02mm and 0.08mm respectively. Table 5.2 shows the value of deformations at different locations for a 5cm cover depth unlined tunnel sample of GM-1 material.

Table 5.1 Deformation of Unlined Tunnel in GM-1 for C/D =0.6

Zones	Distance (cm)	Deformation (mm)
L1	0.0	0.0
L2	10.0	-0.05
L3	12.0	-0.13
L4	15.0	-0.22
L3’	18.0	-0.13
L2’	20.0	-0.05
L1’	30.0	0.0

Table 5.2 Deformation of Unlined Tunnel in GM-1 for C/D =1.0

Zones	Distance (cm)	Deformation (mm)
L1	0.0	0.0
L2	10.0	-0.02
L3	12.0	-0.08
L4	15.0	-0.18
L3’	18.0	-0.08
L2’	20.0	-0.02
L1’	30.0	0.0

In the case of lined tunnels of GM-1 material having 3cm cover depth, the crown deformation at L/2 distance is 0.09mm, whereas the deformation obtained at points L/3 and 7L/12 is 0.02mm and 0.06mm respectively. Table 5.3 shows the value of deformations recorded at different locations for 3cm cover depth. The minimum deformation is noticed in the case of 5cm lined samples. The deformation experienced at L/3, L/2and 7L/12 are 0.01mm,0.08mm, and 0.03mm respectively in 5cm lined tunnels. Table 5.4 shows the value of deformations at different locations for a 5cm cover depth lined tunnel in GM-1 material. The deformation profile of GM-1 single tunnel models obtained from the numerical analysis is shown in Fig 5.4.

Table 5.3 Deformation of lined Tunnel in GM-1 for C/D =0.6

Zones	Distance (cm)	Deformation (mm)
L1	0.0	0.0
L2	10.0	-0.02
L3	12.0	-0.06
L4	15.0	-0.09
L3’	18.0	-0.06
L2’	20.0	-0.02
L1’	30.0	0.0

Table 5.4 Deformation of lined Tunnel in GM-1 sample for C/D =1.0

Zones	Distance (cm)	Deformation (mm)
L1	0.0	0.0
L2	10.0	-0.01
L3	12.0	-0.03
L4	15.0	-0.08
L3’	18.0	-0.03
L2’	20.0	-0.01
L1’	30.0	0.0

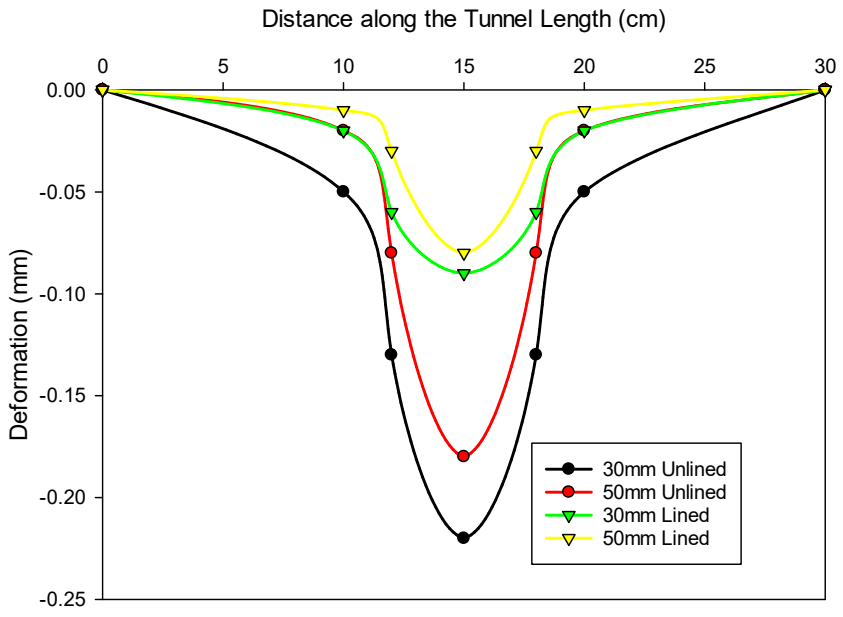

Fig. 5.4 Deformation profiles of GM-1 single tunnels models obtained from numerical analysis.

.

5.3.2 Deformation of a single tunnel of GM-2 material

Secondly, the tunnel samples of GM-2 material (50% POP, 40% Sand and 10% Clay) are subjected to static loading conditions. In the case of 3cm cover depth unlined samples, the maximum crown deformation experienced at L/2 distance is 0.27mm whereas the deformation noticed at points L/3 and 7L/12 is 0.03mm and 0.16mm respectively. Table 5.5 presents the results in terms of the deformations recorded for the case of the unlined tunnel of GM-2 material at a cover depth of 3cm. In the case of 5cm unlined tunnels, the crown deformation at L/2 distance is 0.21mm, whereas the deformation noticed at points L/3 and 7L/12 is 0.03mm and 0.14mm respectively. Table 5.6 shows the value of deformations at different locations for a 5cm cover depth unlined tunnel sample of GM-2 material.

Table 5.5 Deformation of Unlined Tunnel in GM2 sample for C/D =0.6

Zones	Distance (cm)	Deformation (mm)
L1	0.0	0.0
L2	10.0	-0.03
L3	12.0	-0.16
L4	15.0	-0.27
L3’	18.0	-0.16
L2’	20.0	-0.03
L1’	30.0	0.0

Table 5.6 Deformation of Unlined Tunnel in GM2 for C/D =1.0

Zones	Distance (cm)	Deformation (mm)
L1	0.0	0.0
L2	10.0	-0.03
L3	12.0	-0.14
L4	15.0	-0.21
L3’	18.0	-0.14
L2’	20.0	-0.03
L1’	30.0	0.0

In the case of lined tunnels having a cover depth of 3cm, the crown deformation at L/2 distance is 0.12mm, whereas the deformation noticed at points L/3 and 7L/12 is 0.02mm and 0.07mm respectively. Table 5.7 shows the value of deformations at three different locations for 3cm cover depth in GM-2. The minimum deformation is noticed in the case of a 5cm lined sample. In the case of 5cm lined samples the deformation experienced at L/3, L/2 and 7L/12 is 0.01mm,0.10mm, and 0.06mm respectively. Table 5.8 shows the value of deformations at different locations for 5cm cover depth in GM-2 tunnel samples. The deformation profile of GM-2 single tunnel models obtained from the numerical analysis is shown in Fig 5.5.

Table 5.7 Deformation of lined Tunnel in GM-2 for C/D =0.6

Zones	Distance (cm)	Deformation (mm)
L1	0.0	0.0
L2	10.0	-0.02
L3	12.0	-0.07
L4	15.0	-0.12
L3’	18.0	-0.07
L2’	20.0	-0.02
L1’	30.0	0.0

Table 5.8 Deformation of lined Tunnel in GM-2 for C/D =1.0

Zones	Distance (cm)	Deformation (mm)
L1	0.0	0.0
L2	10.0	-0.01
L3	12.0	-0.06
L4	15.0	-0.1
L3’	18.0	-0.06
L2’	20.0	-0.01
L1’	30.0	0.0

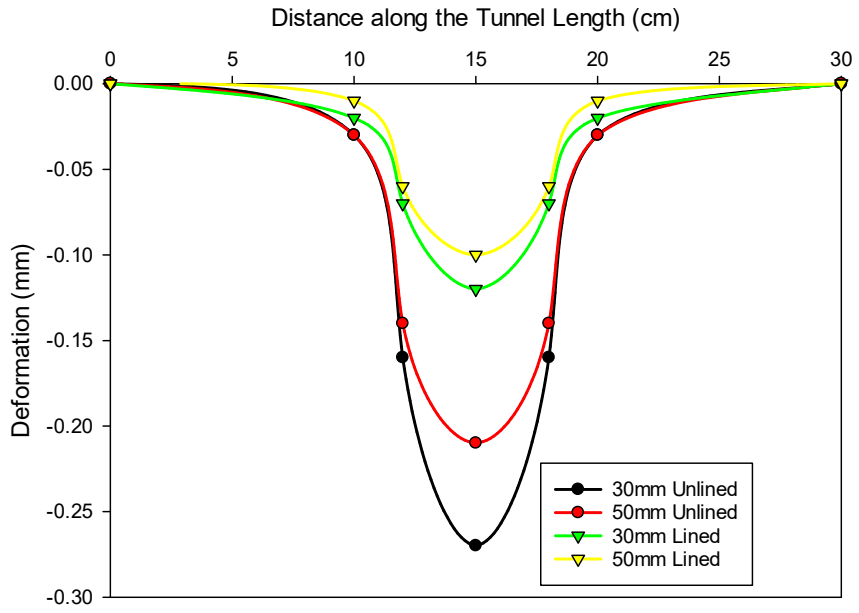

Fig. 5.5 Deformation profiles of GM-2 single tunnels models obtained from numerical analysis.

.

5.3.3 Deformation of a single tunnel of GM-3 material

In the case of 3cm cover depth unlined samples of GM-3 model material, the maximum crown deformation experienced at L/2 distance is 0.31mm whereas the deformation noticed at points L/3 and 7L/12 is 0.03mm and 0.17mm respectively. Table 5.9 presents the results in terms of the deformations recorded for the case of an unlined tunnel of GM-3 material at a cover depth of 3cm. In the case of 5cm unlined tunnels, the crown deformation at L/2 distance is 0.23mm, whereas the deformation noticed at points L/3 and 7L/12 is 0.03mm and 0.15mm respectively. Table 5.10 shows the value of deformations at different locations for a 5cm cover depth unlined tunnel sample of GM-3 model material.

Table 5.9 Deformation of Unlined Tunnel in GM-3 sample for C/D =0.6

Zones	Distance (cm)	Deformation (mm)
L1	0.0	0.0
L2	10.0	-0.03
L3	12.0	-0.17
L4	15.0	-0.31
L3’	18.0	-0.17
L2’	20.0	-0.03
L1’	30.0	0.0

Table 5.10 Deformation of Unlined Tunnel in GM3 for C/D =1.0

Zones	Distance (cm)	Deformation (mm)
L1	0.0	0.0
L2	10.0	-0.03
L3	12.0	-0.15
L4	15.0	-0.23
L3’	18.0	-0.15
L2’	20.0	-0.03
L1’	30.0	0.0

In the case of liner material tunnels having a cover depth of 3cm, the crown deformation at L/2 distance is 0.13mm, whereas the deformation noticed at points L/3 and 7L/12 is 0.02mm and 0.07mm respectively. Table 5.11 shows the value of deformations at different locations for 3cm cover depth in GM-3. In the case of 5cm lined samples the deformation experienced at L/3, L/2and 7L/12 is 0.02mm,0.11mm, and 0.07mm respectively. Table 5.12 shows the value of deformations at different locations for 5cm cover depth in GM-3. Deformation profiles of GM-3 single tunnel models obtained from the numerical analysis are shown in Fig 5.6.

Table 5.11 Deformation of lined Tunnel in GM-3 for C/D =0.6

Zones	Distance (cm)	Deformation (mm)
L1	0.0	0.0
L2	10.0	-0.02
L3	12.0	-0.07
L4	15.0	-0.13
L3’	18.0	-0.07
L2’	20.0	-0.02
L1’	30.0	0.0

Table 5.12 Deformation of lined Tunnel in GM-3 for C/D =1.0

Zones	Distance (cm)	Deformation (mm)
L1	0.0	0.0
L2	10.0	-0.02
L3	12.0	-0.07
L4	15.0	-0.11
L3’	18.0	-0.07
L2’	20.0	-0.02
L1’	30.0	0.0

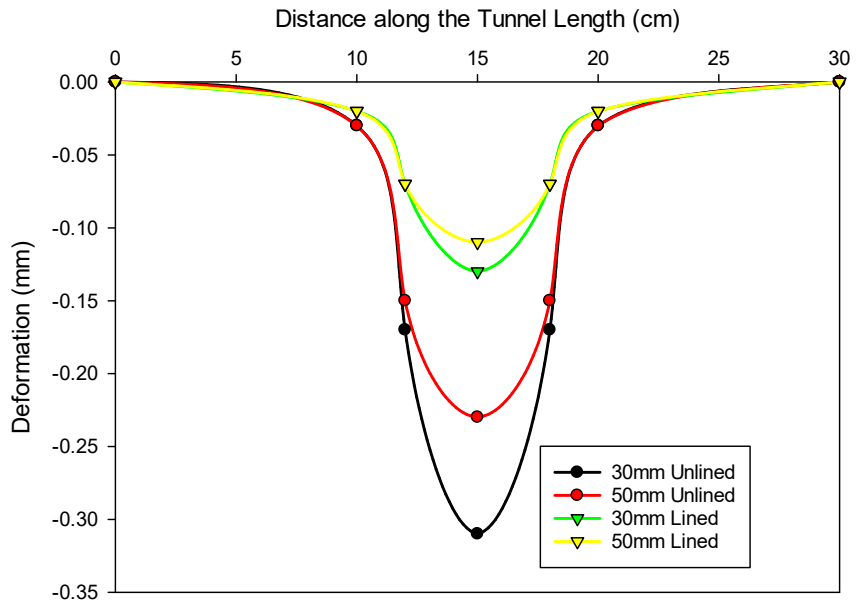

Fig. 5.6 Deformation profiles of GM-3 single tunnels models obtained from numerical analysis.

5.4 Numerical analysis of Twin Tunnels

5.4.1 Deformation of twin tunnel of 1.5D spacing

In the case of a Twin tunnel, an unlined sample having 1.5D c/c spacing and 3cm cover depth, the maximum deformation value obtained at L/2 distance is 0.28mm. Whereas the deformation obtained at L/3 and 9L/15 is 0.05mm and 0.18mm respectively. Table 5.13 presents the results in terms of the deformations recorded for the case of the unlined tunnel having 1.5D centre to centre spacing and a cover depth of 3cm. In the case of 5cm unlined tunnels, the deformation at the L/2 distance is 0.22mm, whereas the deformation noticed at points L/3 and 9L/15 is 0.03mm and 0.14mm respectively. Table 5.14 presents the results in terms of the deformations recorded for the case of the unlined tunnel having 1.5D centre to centre spacing and cover depth of 5cm.

In the case of lined tunnels having 1.5D centre to centre spacing and 3cm cover depth, the crown deformation at L/2 distance is 0.13mm, whereas the deformation noticed at points L/3 and 9L/15 is 0.02mm and 0.08mm respectively. Table 5.15 presents the results in terms of the deformations recorded for the case of a lined tunnel having 1.5D centre to centre spacing and cover depth of 3cm. In the case of 5cm lined tunnel samples, the deformation experienced at L/3, L/2and 9L/15 is 0.01mm,0.10mm, and 0.06mm respectively. Table 5.16 presents the results in terms of the deformations recorded for the case of a lined tunnel having 1.5D centre to centre spacing and cover depth of 5cm.The deformation profile of 1.5D c/c spacing twin tunnel models obtained from the numerical analysis is shown in Fig 5.7.

Table 5.13 Deformation of unlined Tunnel in 1.5D c/c spacing for C/D =0.6 and

Zones	Distance (cm)	Deformation (mm)
L1	0.0	0.0
L2	14.0	-0.05
L3	17.0	-0.18
L4	21.25	-0.28
L3’	25.5	-0.18
L2’	28.4	-0.05
L1’	42.5	0.0

Table 5.14 Deformation of unlined Tunnel in 1.5D c/c spacing for C/D =1.0.

Zones	Distance (cm)	Deformation (mm)
L1	0.0	0.0
L2	14.0	-0.03
L3	17.0	-0.14
L4	21.25	-0.22
L3’	25.5	-0.14
L2’	28.4	-0.03
L1’	42.5	0.0

Table 5.15 Deformation of lined Tunnel in 1.5D c/c spacing for C/D =0.6.

Zones	Distance (cm)	Deformation (mm)
L1	0.0	0.0
L2	14.0	-0.02
L3	17.0	-0.08
L4	21.25	-0.13
L3’	25.5	-0.08
L2’	28.4	-0.02
L1’	42.5	0.0

Table 5.16 Deformation of lined Tunnel in 1.5D c/c spacing for C/D =1.0.

Zones	Distance (cm)	Deformation (mm)
L1	0.0	0.0
L2	14.0	-0.01
L3	17.0	-0.06
L4	21.25	-0.10
L3’	25.5	-0.06
L2’	28.4	-0.01
L1’	42.5	0.0

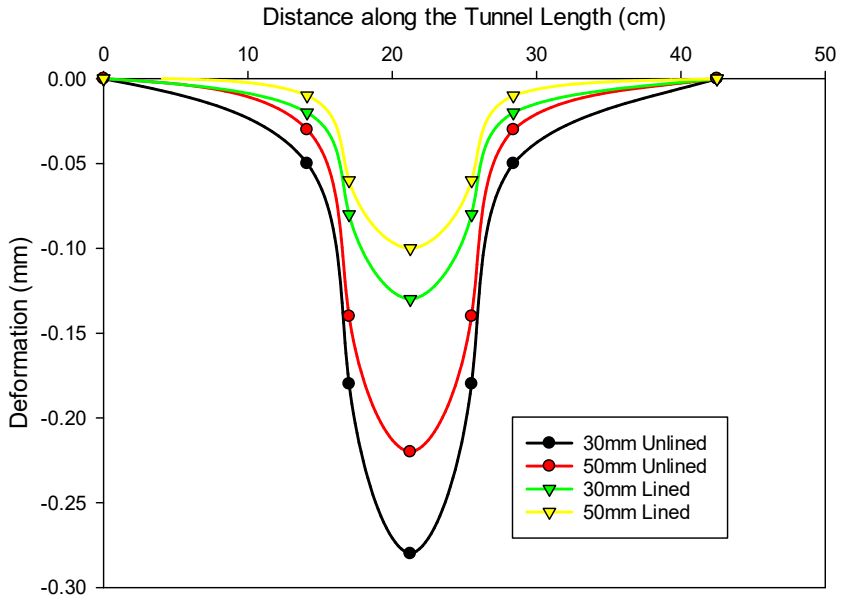

Fig.5.7 Deformation profiles of 1.5D c/c spacing twin tunnels models obtained from numerical analysis.

5.4.2 Deformation of twin tunnel of 2D spacing

In the case of 2D c/c spacing and 3cm cover depth unlined tunnels, the maximum deformation value is 0.23mm which is obtained at L/2 distance. Whereas the deformation obtained at L/3 and 9L/15 is 0.03mm and 0.16mm respectively. Table 5.17 presents the results in terms of the deformations recorded for the case of the unlined tunnel having a 2D center to centre spacing and cover depth of 3cm. In the case of 5cm unlined tunnels, the crown deformation at L/2 distance is 0.20mm, whereas the deformation noticed at points L/3 and 9L/15 is 0.02mm and 0.13mm respectively. Table 5.18 presents the results in terms of the deformations recorded for the case of the unlined tunnel having a 2D centre to centre spacing and a cover depth of 5cm.

In the case of lined tunnels having a 2D centre to centre spacing and 3cm cover depth, the crown deformation at L/2 distance is 0.12mm, whereas the deformation noticed at points L/3 and 9L/15 is 0.01mm and 0.07mm respectively. Table 5.19 presents the results in terms of the deformations recorded for the case of a lined tunnel having a 2D centre to centre spacing and cover depth of 3cm. In the case of 5cm lined samples the deformation experienced at L/3, L/2and 9L/15 is 0.01mm,0.09mm, and 0.06mm respectively. Table 5.20 presents the results in terms of the deformations recorded for the case of a lined tunnel having a 2D centre to centre spacing and cover depth of 5cm. The deformation profile of 2D c/c spacing twin tunnels models obtained from the numerical analysis is shown in Fig. 5.8.

Table 5.17 Deformation of unlined Tunnel in 2D c/c spacing for C/D =0.6.

Zones	Distance (cm)	Deformation (mm)
L1	0.0	0.0
L2	14.0	-0.03
L3	17.0	-0.16
L4	21.25	-0.23
L3’	25.5	-0.16
L2’	28.4	-0.03
L1’	42.5	0.0

Table 5.18 Deformation of unlined Tunnel in 2D c/c spacing for C/D =1.0.

Zones	Distance (cm)	Deformation (mm)
L1	0.0	0.0
L2	14.0	-0.02
L3	17.0	-0.13
L4	21.25	-0.20
L3’	25.5	-0.13
L2’	28.4	-0.02
L1’	42.5	0.0

Table 5.19 Deformation of lined Tunnel in 2D c/c spacing for C/D =0.6.

Zones	Distance (cm)	Deformation (mm)
L1	0.0	0.0
L2	14.0	-0.01
L3	17.0	-0.07
L4	21.25	-0.12
L3’	25.5	-0.07
L2’	28.4	-0.01
L1’	42.5	0.0

Table 5.20 Deformation of lined Tunnel in 2D c/c spacing for C/D =1.0.

Zones	Distance (cm)	Deformation (mm)
L1	0.0	0.0
L2	14.0	-0.01
L3	17.0	-0.06
L4	21.25	-0.09
L3’	25.5	-0.06
L2’	28.4	-0.01
L1’	42.5	0.0

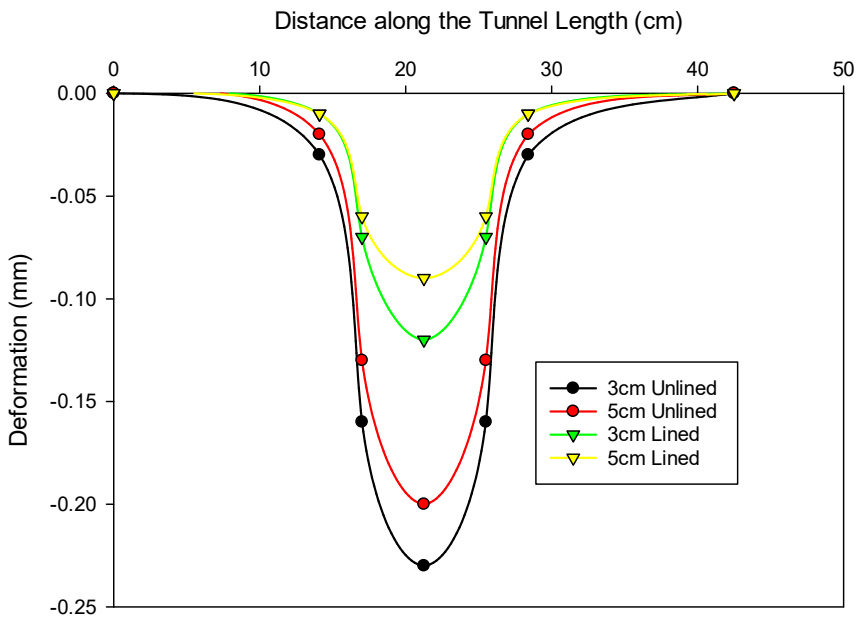

Fig. 5.8: Deformation profiles of 2D c/c spacing twin tunnels models obtained from numerical analysis.

5.4.3 Deformation of twin tunnel of 2.5D spacing

In the case of 2.5D c/c spacing twin tunnels of 3cm cover depth, the maximum deformation value is 0.20mm obtained at L/2 distance. Whereas the deformation obtained at L/3 and 9L/15 is 0.02mm and 0.13mm respectively. Table 5.21 presents the results in terms of the deformations recorded for the case of the unlined tunnel having 2.5D centre to centre spacing and a cover depth of 3cm. In the case of 5cm unlined tunnels, the crown deformation at L/2 distance is 0.17mm, whereas the deformation noticed at points L/3 and 9L/15 is 0.02mm and 0.10mm respectively. Table 5.22 presents the results in terms of the deformations recorded for the case of the unlined tunnel having 2.5D centre to centre spacing and a cover depth of 5cm.

In the case of lined tunnels having 2.5D centre to centre spacing and 3cm cover depth, the crown deformation at L/2 distance is 0.10mm, whereas the deformation noticed at points L/3

and 9L/15 is 0.01mm and 0.06mm respectively. Table 5.23 presents the results in terms of the deformations recorded for the case of a lined tunnel having 2.5D centre to centre spacing and a cover depth of 3cm. In the case of 5cm lined samples the deformation experienced at L/3, L/2and 9L/15 are 0.01mm,0.07mm, and 0.04mm respectively. Table 5.24 presents the results in terms of the deformations recorded for the case of a lined tunnel having 2.5D centre to centre spacing and a cover depth of 5cm. The deformation profile of 2.5D c/c spacing twin tunnels models obtained from the numerical analysis is shown in Fig 5.9.

Table 5.21 Deformation of unlined Tunnel in 2.5D c/c spacing for C/D =0.6.

Zones	Distance (cm)	Deformation (mm)
L1	0.0	0.0
L2	14.0	-0.02
L3	17.0	-0.13
L4	21.25	-0.20
L3’	25.5	-0.13
L2’	28.4	-0.02
L1’	42.5	0.0

Table 5.22 Deformation of unlined Tunnel in 2.5D c/c spacing for C/D =1.0.

Zones	Distance (cm)	Deformation (mm)
L1	0.0	0.0
L2	14.0	-0.02
L3	17.0	-0.10
L4	21.25	-0.17
L3’	25.5	-0.10
L2’	28.4	-0.02
L1’	42.5	0.0

Table 5.23 Deformation of lined Tunnel in 2.5D c/c spacing for C/D =0.6.

Zones	Distance (cm)	Deformation (mm)
L1	0.0	0.0
L2	14.0	-0.01
L3	17.0	-0.06
L4	21.25	-0.10
L3’	25.5	-0.06
L2’	28.4	-0.01
L1’	42.5	0.0

Table 5.24 Deformation of lined Tunnel in 2.5D c/c spacing for C/D =1.0.

Zones	Distance (cm)	Deformation (mm)
L1	0.0	0.0
L2	14.0	-0.01
L3	17.0	-0.04
L4	21.25	-0.07
L3’	25.5	-0.04
L2’	28.4	-0.01
L1’	42.5	0.0

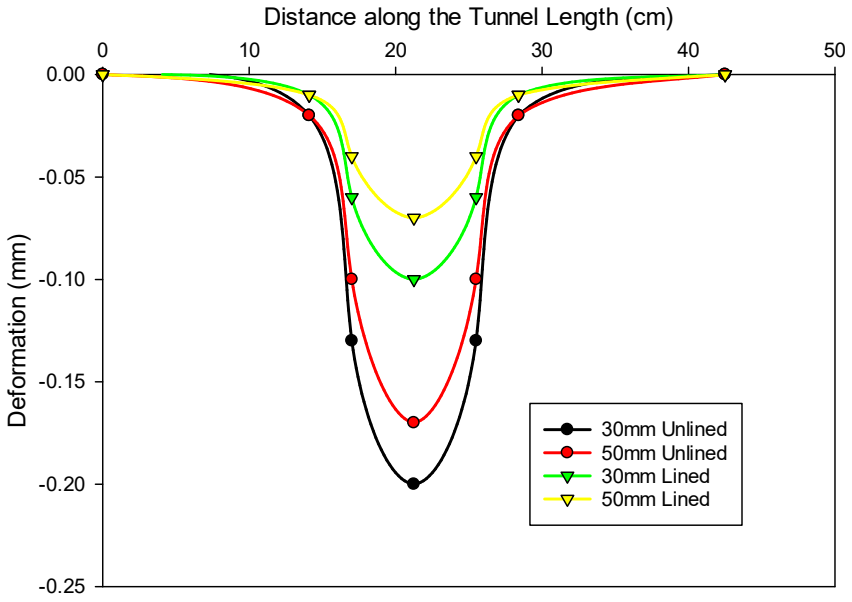

Fig. 5.9: Deformation profiles of 2.5D c/c spacing twin tunnels models obtained from numerical analysis.

5.5 Concluding Remarks

The following conclusions can be drawn from this chapter

- Numerical analysis of single tunnels under static loading conditions is done in different conditions.
- Determination of deformation behaviour of twin tunnels by changing the spacing and cover depth of the tunnel is done.

The detailed discussion and validation of results obtained from experimental and numerical analysis of single and twin tunnels have been discussed in the next Chapter.

Chapter 6

Discussion and Validation of Results

6.1 General

After conducting the experimental and numerical analysis on both lined and unlined tunnels, the results are analyzed. It has been noted that deformation is more in unlined samples as compared to lined samples. This is due to the absence of liner material in the unlined tunnel as the liner material offers resistance against the developed stresses. In the case of single tunnel samples three model materials i.e. GM-1, GM-2 and GM-3 are used to cast tunnel models. The purpose of adopting three model materials is to vary the strength characteristics of the rock. In total 36 single tunnel models are casted in the laboratory out of which 18 tunnel models are unlined and the remaining 18 are lined tunnels. After the preparation of the tunnel model, they are subjected to a compression testing machine under the effect of static loading conditions. The load is applied from the top of the tunnel model with the help of a steel patch which is placed at the top surface of the tunnel specimen. Then the deformation is measured with the help of LVDTs at three different positions. The reading is then recorded in the data acquisition system which is connected to the CPU with the help of a data cable. In the case of numerical modelling, ANSYS software is used for the analysis of the deformation behaviour of single and twin tunnels. The results obtained from experimental investigation and numerical analysis are then compared and validated. The results obtained from both modelling methods are discussed below.

6.1.1 Comparison of deformation profiles of GM-1 material

In the case of a single tunnel of GM-1 model material, the deformation profiles are obtained for 3cm and 5 cm cover depth from experimental investigation and numerical analysis. The deformation obtained in the case of a 3cm unlined sample of GM-1 model material from the experimental investigation at L/3, L/2 and 7L/12 distances is 0.03mm, 0.19mm and 0.13mm respectively along the length of the tunnel axis whereas the deformation obtained from numerical analysis in a similar case at L/3, L/2 and 7L/12 distance is 0.05mm, 0.22mm and 0.13mm respectively. Similarly, in the case of a 5cm unlined tunnel sample, the deformation obtained from the experimental investigation at L/3, L/2 and 7L/12 distance is 0.02mm, 0.16mm and 0.09mm respectively whereas the deformation obtained from numerical analysis at L/3, L/2 and 7L/12 distance is 0.02mm, 0.18mm and 0.08mm respectively. Form lined tunnels, in the case of a 3cm lined tunnel sample, the deformation obtained from the experimental investigation at L/3, L/2 and 7L/12 distances is 0.02mm, 0.09mm and 0.06mm respectively whereas the deformation obtained from numerical analysis at L/3, L/2 and 7L/12 distance is 0.02mm, 0.08mm and 0.06mm respectively. Similarly, in the case of a 5cm lined tunnel sample, the deformation obtained from the experimental investigation at L/3, L/2 and 7L/12 distance is 0.01mm,0.07mm and 0.03mm respectively whereas the deformation obtained from numerical analysis at L/3, L/2 and 7L/12 distance is 0.01mm,0.08mm and 0.03mm respectively. The Comparison of the deformation profile obtained from experimental and numerical modelling at 3cm and 5cm overburden for a single tunnel of GM-1 material is shown in Fig 6.1.

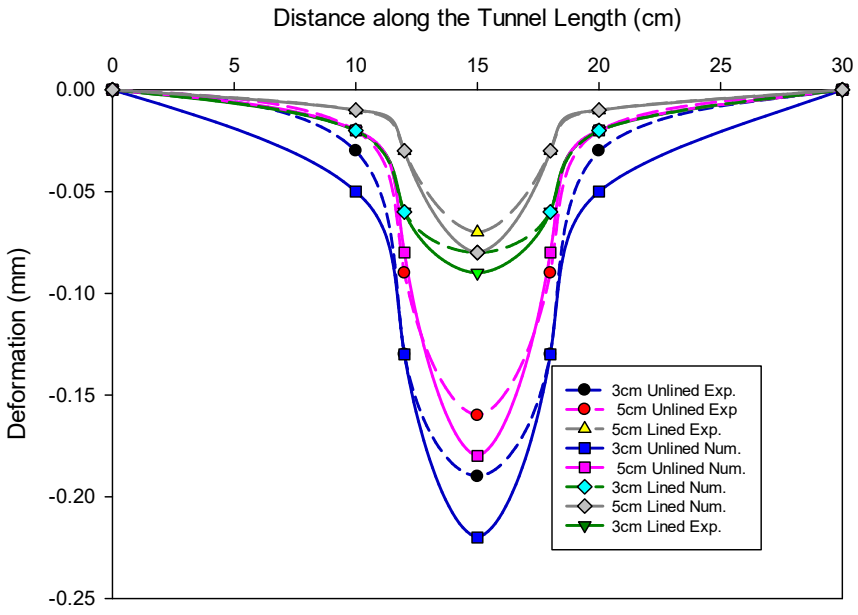

Fig. 6.1 Comparison of deformation profile obtained from experimental and numerical modelling at 3cm and 5cm overburden for a single tunnel of GM-1 material.

6.1.2 Comparison of deformation profiles of GM-2 material

In the case of a single tunnel of GM-2 model material, the deformation obtained in the case of a 3cm unlined sample of GM-2 model material from the experimental investigation at L/3, L/2 and 7L/12 distances is 0.04mm, 0.25mm and 0.17mm respectively along the length of the tunnel axis whereas the deformation obtained from numerical analysis in a similar case at L/3, L/2 and 7L/12 distance is 0.03mm, 0.27mm and 0.16mm respectively. Similarly, in the case of a 5cm unlined tunnel sample, the deformation obtained from the experimental investigation at L/3, L/2 and 7L/12 distance is 0.03mm, 0.19mm and 0.14mm respectively whereas the deformation obtained from numerical analysis at L/3, L/2 and 7L/12 distance is 0.03mm, 0.21mm and 0.14mm respectively. Form lined tunnels, in the case of a 3cm lined tunnel sample, the deformation obtained from the experimental investigation at L/3, L/2 and 7L/12 distances is 0.02mm, 0.12mm and 0.07mm respectively whereas the deformation obtained from

numerical analysis at L/3, L/2 and 7L/12 distance is 0.02mm, 0.125mm and 0.07mm respectively. Similarly, in the case of a 5cm lined tunnel sample, the deformation obtained from the experimental investigation at L/3, L/2 and 7L/12 distance is 0.01mm,0.10mm and 0.06mm respectively whereas the deformation obtained from numerical analysis at L/3, L/2 and 7L/12 distance is 0.01mm,0.105mm and 0.06mm respectively. The Comparison of the deformation profile obtained from experimental and numerical modelling at 3cm and 5cm overburden for the single tunnel of GM-2 material is shown in Fig 6.2.

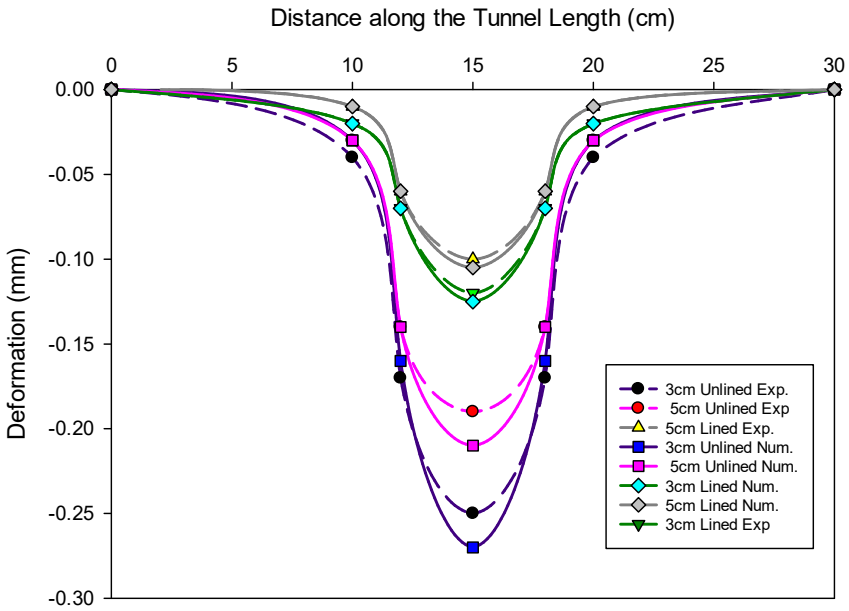

Fig. 6.2 Comparison of deformation profile obtained from experimental and numerical modelling at 3cm and 5cm overburden for the single tunnel of GM-2 material.

6.1.3 Comparison of deformation profiles of GM-3 material

In the case of the single tunnel of GM-3 model material, the deformation obtained in the case of a 3cm unlined sample of GM-3 model material from the experimental investigation at L/3, L/2 and 7L/12 distances is 0.04mm, 0.29mm and 0.20mm respectively along the length of the

tunnel axis whereas the deformation obtained from numerical analysis in the similar case at L/3, L/2 and 7L/12 distance is 0.03mm, 0.31mm and 0.17mm respectively. Similarly, in the case of a 5cm unlined tunnel sample, the deformation obtained from the experimental investigation at L/3, L/2 and 7L/12 distances is 0.03mm, 0.21mm and 0.15mm respectively whereas the deformation obtained from numerical analysis at L/3, L/2 and 7L/12 distance is 0.03mm, 0.23mm and 0.15mm respectively. Form lined tunnels, in the case of a 3cm lined tunnel sample, the deformation obtained from the experimental investigation at L/3, L/2 and 7L/12 distances is 0.02mm, 0.14mm and 0.07mm respectively whereas the deformation obtained from numerical analysis at L/3, L/2 and 7L/12 distance is 0.02mm, 0.13mm and 0.07mm respectively. Similarly, in the case of a 5cm lined tunnel sample, the deformation obtained from the experimental investigation at L/3, L/2 and 7L/12 distance is 0.02mm,0.11mm and 0.05mm respectively whereas the deformation obtained from numerical analysis at L/3, L/2 and 7L/12 distance is 0.02mm,0.11mm and 0.07mm respectively. The Comparison of the deformation profile obtained from experimental and numerical modelling at 3cm and 5cm overburden for a single tunnel of GM-3 material is shown in Fig 6.3.

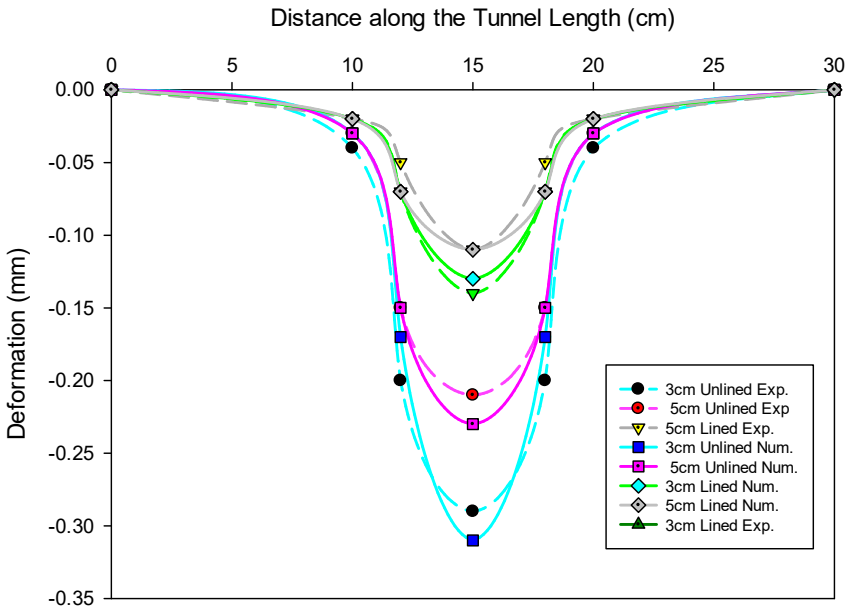

Fig. 6.3 Comparison of deformation profile obtained from experimental and numerical modelling at 3cm and 5cm overburden for a single tunnel of GM-3 material.

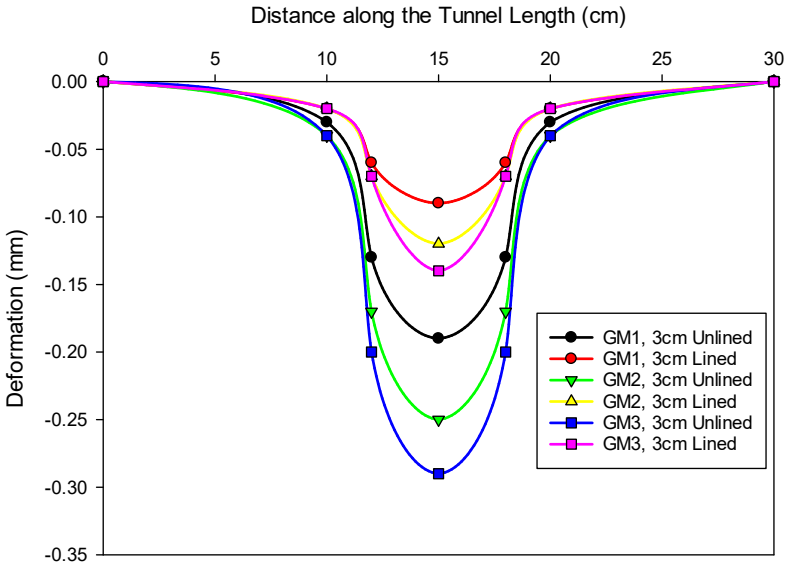

Fig. 6.4: Comparison of deformation profiles of all three model materials at 3cm overburden obtained from experimental results.

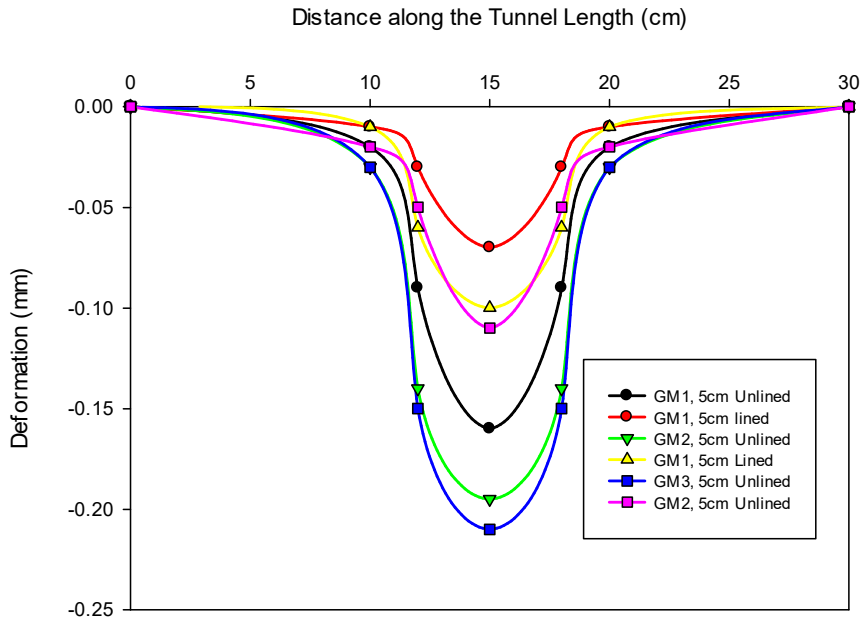

Fig. 6.5: Comparison of deformation profiles of all three model materials at 5cm overburden obtained from experimental results.

6.1.4 Comparison of deformation profiles of 1.5D spacing Twin Tunnel

In the case of Twin tunnel samples having 1.5D centre to centre spacing, the deformation obtained in the case of 3cm unlined tunnel sample from the experimental investigation at L/3, L/2 and 9L/15 distances is 0.03mm, 0.25mm and 0.16mm respectively along the length of the tunnel axis whereas the deformation obtained from numerical analysis in the similar case at L/3, L/2 and 9L/15 distance is 0.05mm, 0.28mm and 0.18mm respectively. Similarly, in the case of a 5cm unlined tunnel sample, the deformation obtained from the experimental investigation at L/3, L/2 and 9L/15 distances is 0.02mm, 0.20mm and 0.12mm respectively whereas the deformation obtained from numerical analysis at L/3, L/2 and 9L/15 distance is 0.03mm, 0.22mm and 0.14mm respectively. For lined tunnels, in the case of a 3cm lined tunnel sample, the deformation obtained from the experimental investigation at L/3, L/2 and 9L/15 distances

are 0.01mm, 0.12mm and 0.07mm respectively whereas the deformation obtained from numerical analysis at L/3, L/2 and 9L/15 distance is 0.02mm, 0.13mm and 0.08mm respectively. Similarly, in the case of a 5cm lined tunnel sample, the deformation obtained from the experimental investigation at L/3, L/2 and 9L/15 distances are 0.01mm,0.10mm and 0.05mm respectively whereas the deformation obtained from numerical analysis at L/3, L/2 and 9L/15 distance is 0.01mm,0.10mm and 0.06mm respectively. The Comparison of deformation profile obtained from experimental and numerical modelling at 3cm and 5cm overburden for 1.5D c/c spaced twin tunnel is shown in Fig 6.6.

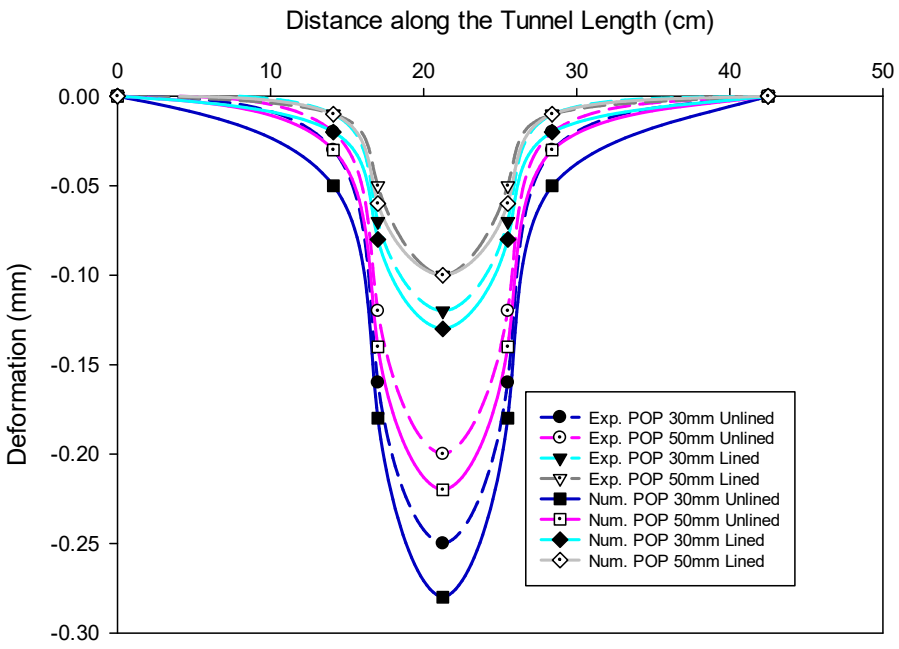

Fig. 6.6 Comparison of deformation profile obtained from experimental and numerical modelling of 1.5D centre to centre spacing tunnels

6.1.5 Comparison of deformation profiles of 2D spacing Twin Tunnel

In the case of Twin tunnel samples having a 2D centre to centre spacing, the deformation obtained in the case of 3cm unlined tunnel sample from the experimental investigation at L/3, L/2 and 9L/15 distances is 0.02mm, 0.22mm and 0.14mm respectively along the length of the tunnel axis whereas the deformation obtained from numerical analysis in a similar case at L/3, L/2 and 9L/15 distance is 0.03mm, 0.23mm and 0.16mm respectively. Similarly, in the case of a 5cm unlined tunnel sample, the deformation obtained from the experimental investigation at L/3, L/2 and 9L/15 distance is 0.02mm, 0.18mm and 0.11mm respectively whereas the deformation obtained from numerical analysis at L/3, L/2 and 9L/15 distance is 0.02mm, 0.20mm and 0.13mm respectively. For lined tunnels, in the case of a 3cm lined tunnel sample, the deformation obtained from the experimental investigation at L/3, L/2 and 9L/15 distances are 0.01mm, 0.10mm and 0.06mm respectively whereas the deformation obtained from numerical analysis at L/3, L/2 and 9L/15 distance is 0.01mm, 0.12mm and 0.07mm respectively. Similarly, in the case of a 5cm lined tunnel sample, the deformation obtained from the experimental investigation at L/3, L/2 and 9L/15 distance is 0.01mm,0.08mm and 0.05mm respectively whereas the deformation obtained from numerical analysis at L/3, L/2 and 9L/15 distance is 0.01mm,0.09mm and 0.06mm respectively. The Comparison of deformation profile obtained from experimental and numerical modelling at 3cm and 5cm overburden for 2D c/c spaced twin tunnel is shown in Fig 6.7.

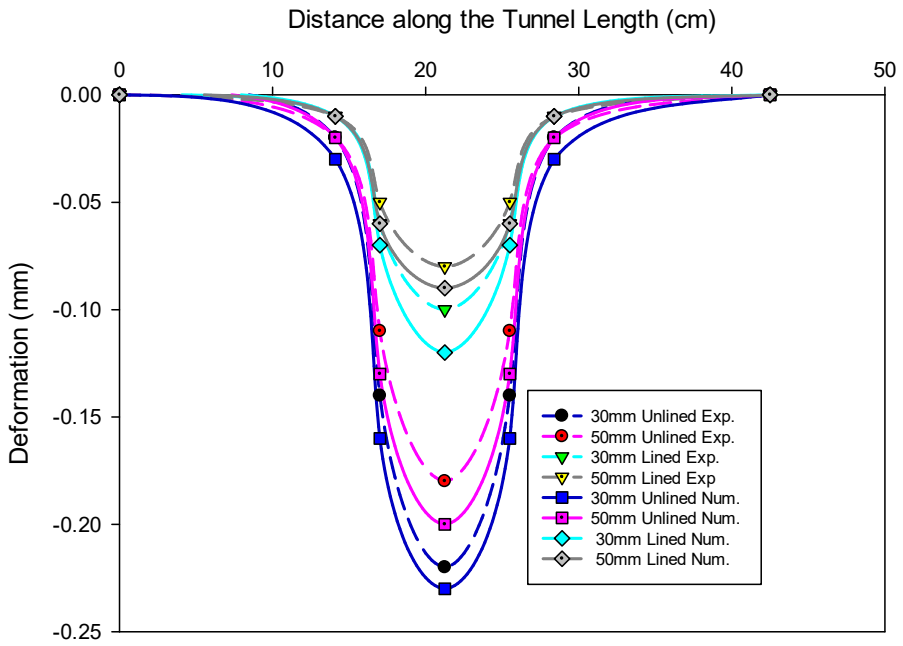

Fig. 6.7 Comparison of deformation profile obtained from experimental and numerical modelling of 2.0D centre to centre spacing tunnels.

6.1.6 Comparison of deformation profiles of 2.5D spacing Twin Tunnel

In the case of Twin tunnel samples having 2.5D centre to centre spacing, the deformation obtained in the case of 3cm unlined tunnel sample from the experimental investigation at L/3, L/2 and 9L/15 distances is 0.02mm, 0.19mm and 0.10mm respectively along the length of the tunnel axis whereas the deformation obtained from numerical analysis in the similar case at L/3, L/2 and 9L/15 distance is 0.02mm, 0.20mm and 0.13mm respectively. Similarly, in the case of a 5cm unlined tunnel sample, the deformation obtained from the experimental investigation at L/3, L/2 and 9L/15 distance is 0.02mm, 0.16mm and 0.09mm respectively whereas the deformation obtained from numerical analysis at L/3, L/2 and 9L/15 distance is 0.02mm, 0.17mm and 0.10mm respectively. For lined tunnels, in the case of a 3cm lined tunnel sample, the deformation obtained from the experimental investigation at L/3, L/2 and 9L/15 distances

are 0.01mm, 0.09mm and 0.04mm respectively whereas the deformation obtained from numerical analysis at L/3, L/2 and 9L/15 distance is 0.01mm, 0.10mm and 0.06mm respectively. Similarly, in the case of a 5cm lined tunnel sample, the deformation obtained from the experimental investigation at L/3, L/2 and 9L/15 distances is 0.01mm,0.08mm and 0.03mm respectively whereas the deformation obtained from numerical analysis at L/3, L/2 and 9L/15 distance is 0.01mm,0.07mm and 0.04mm respectively. The Comparison of deformation profile obtained from experimental and numerical modelling at 3cm and 5cm overburden for 2.5D c/c spaced twin tunnel is shown in Fig 6.8.

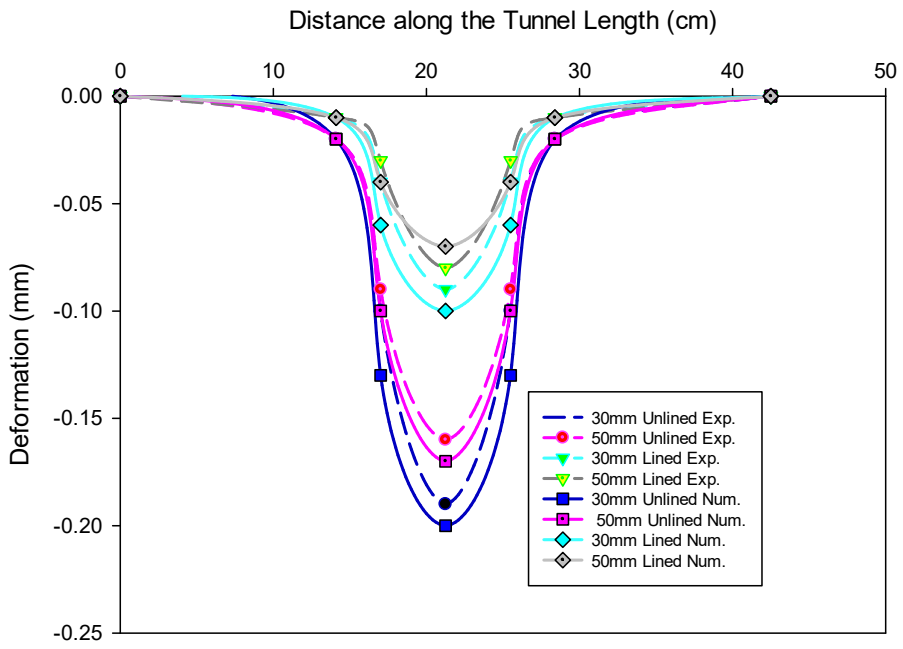

Fig. 6.8 Comparison of deformation profile obtained from experimental and numerical modelling of 2.5D centre to centre spacing tunnels.

6.2 Concluding Remarks

This chapter presents the discussion and validation of the results obtained from experimental and numerical modelling. The results obtained from experimental investigation and numerical analysis are compared. In the present study, the Load vs. deformation behavior of single and twin tunnel is determined under the static loading conditions. The study also shows the effect of different parameters such as strength of rock, cover depth of tunnel, spacing between the tunnel on the deformation behaviour of tunnel. All this is very useful for selecting the design parameters of tunnel which will further help in the safe and economical design of the tunnels. Load settlement behavior is important for finding out the safe cover depth, spacing between the tunnels and support system. The study will be useful for both analytical and numerical analysis and design of tunnel and support system. The conclusions and the future scope of the present work have been presented in the next chapter.

Chapter 7

CONCLUSIONS AND FUTURE SCOPE

7.1 Conclusions

A comparative study is carried out in this study on the deformation behaviour of single and twin tunnels with the help of experimental investigation and numerical analysis. Various unlined and lined single and twin tunnel models are prepared in the laboratory with varying strength properties, cover depth and spacing between the tunnel. These tunnel samples are tested in the laboratory under static loading conditions and the results are analysed. In the present study Chennani-Nashri tunnel is considered as the prototype, from where the properties of rock mass and tunnel lining are chosen for the fixing the dimension of model. The ratio of elastic modulus of lining material to elastic modulus of surrounding rock mass (E_{lining}/E_{rock}) is kept fixed for the laboratory models so that they can represent the actual field conditions. The rock mass present in Chennani-Nashri tunnel consist of sandstone and siltstone. The elastic modulus of sandstone is reported as 15GPa whereas the shotcreting is done using M30 grade concrete whose values of elastic modulus is 28GPa.Therefore it is found that the elastic modulus ratio (E_{lining}/E_{rock}) is 1.9 for field conditions. The deformation in single and twin tunnel is determined for various cases such as variation in the strength characteristics of rock, change in the cover depth of the tunnel, change in the spacing between the tunnel in case of twin tunnel, effect of presence of lining material in the tunnel. The same methodology can be helpful in the field for determining the deformation of tunnel under static loading conditions for deciding the designing parameters of tunnel for its safe and economical design. For the numerical analysis, similar tunnel models are developed with the help of ANSYS software and subjected to similar loading conditions. From the results, it can be concluded that there are various factors which affect the deformation

behaviour of single and twin tunnels. Some of the major factors are the strength properties of rock, cover depth of the tunnel, spacing between the tunnels and presence of liner material. With the increase in the strength properties of rock, the extent of deformation decreases. The deformation along the tunnel axis also decreases with an increase in the cover depth of the tunnel. In the present study, the deformation behaviour of single and twin tunnels is analysed with the help of experimental and numerical modelling. The material used in the present study for modeling rock falls in the group of EM as per the Deere and Miller (1966) classification which stimulates to very low strength and low elasticity.Selection of the material, scale and dimensions has been done in such a way that the results can be utilized in the field.

The following conclusion can be made from the results obtained from experimental and numerical modelling.

- It has been observed that in all the cases, the maximum deformation is noted at the centre of the tunnel, i.e., L/2 distance and the minimum deformation is recorded at distance L/3.From the results, it has been concluded that as the distance from the centre increases, the deformation value will decrease. The deformation value is noted as zero at the face of the tunnel in all cases.
- In the case of the lined and unlined single tunnel of GM-1 model material, the difference in the variation in deformation values obtained from experimental and numerical analysis varies from 5% to 12% whereas in the case of GM-2 model material the variation in deformation obtained from experimental and numerical analysis values varies from 7% to 9%. Similarly, for GM-3 material the variation in deformation values obtained from experimental and numerical analysis varies from 5% to 8%. This shows that experimental and numerical results are in close agreement with each other.

- The extent of deformation in tunnels mainly depends upon the unconfined compressive strength of the model material. The UCS value of GM-2 material is 29.90% less than the UCS value of GM-1. Therefore the deformation in 30mm and 50mm cover depth unlined tunnels of GM-2 material is 18.51% and 14.28% respectively more than that obtained in 30mm and 50mm unlined tunnels of GM-1 material. Similarly, the UCS value of GM-3 model material is 44.85% less than the UCS value of GM-1. Therefore deformation in unlined tunnels of GM-3 material having 30mm and 50mm cover depth is 29.03% and 21.73% respectively more than that obtained in 30mm and 50mm unlined tunnels of GM-1 material. So, it can be concluded that in the case of UCS value of material plays an important role in the deformation behaviour of the tunnel. Therefore, the material having a high compressive strength value should be prefered for the safe and economical design of the tunnel.
- In the case of lined and unlined twin tunnel of GM-1 material, the difference in the variation in deformation values obtained from experimental and numerical analysis in 1.5D centre to centre spacing varies from 7% to 10% whereas, in the case of 2D centre to centre spacing, the deformation values vary from 5% to 16%. From the results, it can be concluded that the critical spacing between the tunnels in the case of twin tunnels is 2D centre to centre spacing. Similarly, for 2.5D centre to centre spacing tunnels, the variation in deformation values obtained from experimental and numerical analysis varies from 5% to 12%. This shows that experimental and numerical results are in close agreement with each other.

7.2 FUTURE SCOPE

The study presents the deformation behaviour of single and twin tunnels under static loading conditions. Various factors are determined which affect the deformation of tunnels. However, the

present study can be further extended in future.In the present study the deformation behavior of tunnels having no joints is determined under static loading conditions. The result obtained from the study can be used for deciding the design parameters of the tunnels. As it is difficult to create the joints in the tunnel model with various changing parameters so the plain rock tunnel models are tested in the present study. But in the future scope of the work the discontinuities or joints can be introduced in the tunnel models for determining their deformation behavior.The future scope of the study is described as follows:

- The study can be extended to determine the deformation behaviour of single and twin tunnels under jointed rock conditions. Joints can be provided at different angles in the tunnel model and further the effect of joints or discontinuities on the deformation behaviour of the tunnel model is determined.
- In the present study, the deformation behaviour of the tunnel is determined under shallow depths. But in the future scope, the deformation behaviour of deep tunnels can be predicted.
- In this study, the deformation behaviour of tunnels is determined under static loading conditions. But in future, the deformation behaviour of tunnels under impact loading conditions can be determined.
- In the case of twin tunnels, the alignment of the tunnel can be varied as vertically and inclined tunnels. The shape of the tunnel can also be varied to a horseshoe or D-shaped tunnel to predict their deformation behaviour.
- In the present thesis the main focus is on the Load-Deformation behavior of single and twin tunnel under static loading conditions and how the deformation behavior of the

tunnel varies when subjected under static loading conditions. Determination of stress distribution around the opening can be done in the future scope of the work.

References

1. Ahmed, M., and Iskander, M. (2012). Evaluation of tunnel face stability by transparent soil models. *Tunnelling and Underground Space Technology*, 27, 101–110.
2. Alagha, A. S. N., and Chapman, D. N. (2019).Numerical modelling of tunnel face stability in homogeneous and layered soft ground. *Tunnelling and Underground Space Technology*, 94,103096,1–14.
3. Atkinson, J.H. and Potts, D.M. (1977).Stability of a shallow circular tunnel in cohesion less soil. *Géotechnique*; 27(2), 203-215.
4. Bayoumi, A., Abdallah, M., and Chehade, F. H. (2016).Non-Linear Numerical Modelling of the Interaction of Twin Tunnels-Structures. *International Journal of Computer and Systems Engineering*, 10(8), 1059–1063.
5. Chakeri, H., Hasanpour, R., and Hindistan, M.A. (2011).Analysis of interaction between tunnels in soft ground by 3D numerical modelling. *Bull Eng Geol Environ*, 70, 439–448.
6. Channabasavaraj, W. and Visvanath, B. (2013).Influence of relative position of the tunnels a numerical study on twin tunnels.*7th International Conference on Case Histories in Geotechnical Engineering,1-8.*
7. Chehade, H. F., and Shahrour, I. (2008).Numerical analysis of the interaction between twin tunnels: Influence of the relative position and construction procedure.*Tunnelling and Underground Space Technology*, 23, 210–214.
8. Chen H. M., Yu H.S. and Smith M.J. (2016).Physical model tests and numerical simulations for assessing the stability of brick-lined tunnels.*Tunnelling and Underground Space Technology,* 53, 109-119.
9. Chen, F., Lin, L., and Li, D. (2019). Analytic solutions for twin tunneling at great depth

considering liner installation and mutual interaction between geomaterial and liners. *Applied Mathematical Modelling*, 73, 412–441.

10. Chen.R.P.,Chen.S.,Wu.H.,Liu.Y.and Meng.F. (2020).Investigation on deformation behaviour and failure mechanism of a segmental ring in shield tunnels based on elaborate numerical simulation. *Engineering Failure Analysis*, 117,104960, 1-15.
11. Chou, W. I., and Bobet, A. (2002).Predictions of ground deformations in shallow tunnels in clay. *Tunnelling and Underground Space Technology*, 17(1), 3–19.
12. Dhamne, R., Mishra, S., Kumar, A., and Rao, K.S. (2018). Numerical study of the cross-sectional shape of shallow tunnels subjected to impact and blast loading. *Journal of Engineering Geology,* 23-37.
13. Do, N. A., Dias, D., Oreste, P., and Djere Maigre, I. (2014).2D numerical Investigation of Twin Tunnel Interaction. *Geomechanics and Engineering*, 6(3).
14. Do, N. A., Dias, D., and Oreste, P. (2016).3D numerical investigation of mechanized twin tunnels in soft ground - Influence of lagging distance between two tunnel faces. *Engineering Structures*, 109, 117–125.
15. Du, D., Dias, D., and Do, N. (2020).Effect of surcharge loading on horseshoe-shaped tunnels excavated in saturated soft rocks. *Journal of Rock Mechanics and Geotechnical Engineering*, 12(6), 1339–1346.
16. Elshamy, E. A., Attia, G., Fawzy, H., and Hafez, K. A. (2013).Behaviour of Different Shapes of Twin Tunnels in Soft Clay Soil. *International Journal of Engineering and Innovative Technology (IJEIT)*, 2(7), 297–302.
17. Elwood, D. E. Y., and Martin, C. D. (2016).Ground response of closely spaced twin tunnels constructed in heavily overconsolidated soils.*Tunnelling and Underground*

Space Technology, 51, 226–237.

18. Fang, Q., Tai, Q., Zhang, D., and Wong, L. N. Y. (2016). Ground surface settlements due to construction of closely-spaced twin tunnels with different geometric arrangements.*Tunnelling and Underground Space Technology*, 51, 144–151.
19. Fu, J. Y., Qing, Z. B., Yu, Y. Z., and Mei, Z. D. (2019). Three-dimensional numerical analysis of the interaction of two crossing tunnels in soft clay. *Underground Space*, 4, 310–327.
20. Gao, S. ming, Chen, J. ping, Zuo, C. qun, and Wang, W. (2017). Monitoring of Three-dimensional Additional Stress and Strain in Shield Segments of Former Tunnels in the Construction of Closely-Spaced Twin Tunnels. *Geotechnical and Geological Engineering*, 35, 69–81.
21. Hashash, Y. M. A., Park, D., and Yao, J. I. C. (2005). Ovaling deformations of circular tunnels under seismic loading, an update on seismic design and analysis of underground structures.*Tunnelling and Underground Space Technology*, 20, 435–441.
22. He, C., Zhou, S., Di, H., and Yang, X. (2019a). Effect of Dynamic Interaction of Two Neighboring Tunnels on Vibrations from Underground Railways in the Saturated Soil.*KSCE Journal of Civil Engineering*, 23(11), 4651–4661.
23. He, C., Zhou, S., Guo, P., Di, H., Zhang, X., and Yu, F. (2019b).Theoretical modelling of the dynamic interaction between twin tunnels in a multi-layered half-space.*Journal of Sound and Vibration*, 456, 65–85.
24. Heidarzadeh.S.,Saeidi.A.and Rouleau.A.(2021).The damage-failure criteria for numerical stability analysis of underground excavations:A review.*Tunnelling and Underground Space Technology*, 107, 103633, 1-17.

25. Hosseini, N., Oraee, K., and Gholinejad, M.(2010).Seismic Analysis of Horseshoe Tunnels Under Dynamic Loads Due To Earthquakes. *Underground Coal Operators' Conference*, 140–145.
26. Huang, Z., Zhang, C., Fu, H., Deng, H., Ma, S., and Fu, J. (2020).Numerical Study on the Disturbance Effect of Short-Distance Parallel Shield Tunnelling Undercrossing Existing Tunnels. *Advances in Civil Engineering*, 2020.
27. Idris, J., Verdel, T., and Al-Heib, M. (2008).Numerical modelling and mechanical behaviour analysis of ancient tunnel masonry structures.*Tunnelling and Underground Space Technology*, 23, 251–263.
28. Idris, J., Al-Heib, M., and Verdel, T. (2009).Numerical modelling of masonry joints degradation in built tunnels.*Tunnelling and Underground Space Technology*, 24, 617–626.
29. Jia, P., and Tang, C. A. (2008).Numerical study on failure mechanism of tunnel in jointed rock mass.*Tunnelling and Underground Space Technology*, 23, 500–507.
30. Jin, D., Yuan, D., Li, X., and Zheng, H. (2018). Analysis of the settlement of an existing tunnel induced by shield tunneling underneath. *Tunnelling and Underground Space Technology*, 81, 209–220.
31. Jose, J., and V, A. (2018).Numerical study of the cross-sectional shape of tunnel under blast effect using ansys.International Research Journal of Engineering and Technology, 5(5), 3582-3586.
32. Khan, I.A., Venkatesh, K. and Srivastava, R.K. (2015).Fractured and Un-fractured analysis of a rock tunnel by finite element method.*Indian Geotechnical Conference*.

33. Kolymbas, D. (2005). Tunnelling and tunnel mechanics: a rational approach to tunneling.

34. Kumar, P. and Shrivastava, A.K. (2017).Various Factors Effecting Stability of Underground Structure:State of Art.*7th Indian Rock Conference,*576-580.

35. Kumar,P. and Shrivastava,A.K. (2019).Deformation Behaviour of Tunnels under Different Loading Conditions: State of Art.*Proceedings of the 4th World Congress on Civil, Structural, and Environmental Engineering (CSEE'19) Rome, Italy-April, 2019, Paper No. ICGRE 130.*

36. Kumar, P., and Shrivastava, A. K. (2019).Stability of single tunnel in rock under static loading condition.*8th Indian Rock Conference*, 424–429.

37. Kumar, P. and Shrivastava, A.K. (2021).Damage Detection in Shallow Tunnels Using 3D Numerical Modelling.*International Conference on Advancements and Innovations in Civil Engineering,* 177-181.

38. Kumar, P., and Shrivastava, A.K.(2021).Physical Investigation of Deformation Behaviour of Single and Twin Tunnel under Static Loading Condition. *Appl. Sci.*,11, 1–18.

39. Kumar, P., and Shrivastava, A.K. (2022).Experimental and Numerical analysis of deformation behaviour of tunnels under static loading conditions.*Sustainable Energy Technologies and Assessments,* 52, 102057, 1-10.

40. Li, Z., Liu, H., Dai, R., and Su, X. (2005).Application of numerical analysis principles and key technology for high fidelity simulation to 3-D physical model tests for underground caverns.*Tunnelling and Underground Space Technology*, 20(4), 390–399.

41. Li, X., Zhou, Z., Zhao, F., Zuo, Y., Ma, C., Ye, Z., and Hong, L. (2009).Mechanical

properties of rock under coupled static-dynamic loads.*Journal of Rock Mechanics and Geotechnical Engineering*, 1(1), 41–47.

42. Li, X., Li, C., Cao, W., and Tao, M. (2018).Dynamic stress concentration and energy evolution of deep-buried tunnels under blasting loads.*International Journal of Rock Mechanics and Mining Sciences*, 104, 131–146.
43. Liang, R., Wu, W., Yu, F., Jiang, G., and Liu, J. (2018).Simplified method for evaluating shield tunnel deformation due to adjacent excavation. *Tunnelling and Underground Space Technology*, 71, 94–105.
44. Liang, R., Xia, T., Hong, Y., and Yu, F. (2016).Effects of above-crossing tunnelling on the existing shield tunnels. *Tunnelling and Underground Space Technology*, 58, 159–176.
45. Liu, X., Fang, Q., Zhang, D., and Wang, Z. (2019).Behaviour of existing tunnel due to new tunnel construction below.*Computers and Geotechnics*, 110, 71–81.
46. Lv, J., Li, X., Li, Z., and Fu, H. (2020).Numerical Simulations of Construction of Shield Tunnel with Small Clearance to Adjacent Tunnel without and with Isolation Pile Reinforcement.*KSCE Journal of Civil Engineering*, 24(1), 295–309.
47. Mahalaxmi, S., Hema, H., Shetty, A.M., Sanjay, B., Srilatha, N. and Kumar, D. (2012).Numerical Analysis of Interaction between Twin-Tunnels with Horizontal Alignment.*Proceedings of International Conference on Advances in Architecture and Civil Engineering,* 1, 247-249.
48. Manouchehrian, A., and Cai, M. (2017).Analysis of rockburst in tunnels subjected to static and dynamic loads.*Journal of rock mechanics and Geotechnical Engineering,* 9, 1031-1040.

49. Meguid, M. A., Rowe, R.K. and Lo, K.Y. (2003).Three dimensional analysis of unlined tunnels in rock subjected to high horizontal stresses.*Can. Geotech. J.*, 40, 1208-1224.

50. Mishra, S., Rao. K.S., Gupta, N.K. and Kumar, A. (2016).Damage to Shallow Tunnels under Static and Dynamic Loading. *Procedia Engineering 173, 1322-1329.*

51. Mishra, S., Challa, A.,Singh, A.,Kumar, A., Rao. K.S. and Gupta, N.K. and Kumar, A. (2017).Parametric study of lined and unlined tunnels at shallow depths under coupled static and cyclic loading conditions. *Tunnelling in Himalayan Geology,* Vol.340.

52. Mishra, S., Rao, K. S., Gupta, N. K., and Kumar, A. (2018).Damage to shallow tunnels in different geomaterials under static and dynamic loading.*Thin-Walled Structures*, 126, 138–149.

53. Mishra, S., Kumar, A., Rao, K.S., and Gupta, N.K. (2021).Experimental and numerical investigation of the dynamic response of tunnel in soft rocks. *Structures*, 29, 2162-2173.

54. Mohammed, J. (2017).Numerical Modelling for circle tunnel under static and dynamic loads for different depth. *Research Journal of Mining*, 1(1), 1-11.

55. Moussaei, N., Sharifzadeh, M., Sahriar, K., and Khosravi, M. H. (2019).A new classification of failure mechanisms at tunnels in stratified rock masses through physical and numerical modeling.*Tunnelling and Underground Space Technology*, 91, 1–12.

56. Naggar, H. El, and Steele, T. (2012).Effect of the Tunnel Lining Stiffness on the Stress Distribution around Shallow Tunnels.*Tunnels and Underground Spaces: Sustainability and Innovations*.

57. Nematollahi, M., and Dias, D. (2020).Interaction between an underground parking and twin tunnels – Case of the Shiraz subway line.*Tunnelling and Underground Space Technology*, 95, 103150,1–16.

58. Niktabar, S.M.M., Rao, K.S. and Shrivastava, A.K., (2018).Automatic Static and Cyclic Shear Testing Machine under Constant Normal Stiffness Boundary Conditions.Geotechnical Testing Journal, 41(3), 508–525.
59. Nguyen, V. M., and Nguyen, Q. P. (2015).Analytical solution for estimating the stand-up time of the rock mass surrounding tunnel.Tunnelling and Underground Space Technology, 47, 10–15.
60. Nunes, M.A. and Meguid, M.A. (2009).A study on the effect of overlying soil strata on the stresses developing in a tunnel lining.*Tunnelling and Underground Space Technology*, 24, 716-722.
61. Oliaei, M., and Manafi, E. (2015).Static analysis of interaction between twin-tunnels using Discrete Element Method (DEM).*Scientia Iranica*, 22(6), 1964–1971.
62. Pakbaz, M. C., and Yareevand, A. (2005).2-D analysis of circular tunnel against earthquake loading.*Tunnelling and Underground Space Technology*, 20, 411–417.
63. Panji, M., Koohsari, H., Adampira, M., Alielahi, H., and Marnani, J. A. (2016).Stability analysis of shallow tunnels subjected to eccentric loads by a boundary element method.*Journal of Rock Mechanics and Geotechnical Engineering,* 8, 480-488.
64. Paternesi, A., Schweiger, H. F., and Scarpelli, G. (2017).Parameter Calibration and Numerical Analysis of Twin Shallow Tunnels.*Rock Mechanics and Rock Engineering*, 50(5), 1243–1262.
65. Qian, H., Zong, Z., Wu, C., Li, J., and Gan, L. (2021).Numerical study on the behavior of utility tunnel subjected to ground surface explosion.*Thin-Walled Structures*, 161, 107422,1–18.
66. Rahaman, O., and Kumar, J. (2020).Stability analysis of twin horse-shoe shaped tunnels

in rock mass.*Tunnelling and Underground Space Technology*,98, 103354,1–18.

67. Ramamurthy, T. (2015) "Engineering in Rocks for Slopes, Foundation and Tunnels".
68. Rao, K.S., Mishra,S. and Gupta,N.K. (2016).The effect of different loading conditions on tunnel lining in soft rocks. *ISRM International Symposium , EUROCK 2016,* Turkey.
69. Rashiddel, A., Kharghani, M., Dias, D., and Hajihassani, M. (2020).Numerical study of the segmental tunnel lining behavior under a surface explosion – Impact of the longitudinal joints shape.*Computers and Geotechnics*, 128, 103822,1–14.
70. Rathod. G.W. ,Varughese, A. , Shrivastava, A.K. and Rao, K.S.. (2012).3Dimensional stability assessment of jointed rock slopes using distinct element modelling. *GeoCongress 2012*, Oakland, California.
71. Sagong, M., Park, D., Yoo, J., and Lee, J.S. (2011).Experimental and numerical analyses of an opening in a jointed rock mass under biaxial compression.*International Journal of Rock Mechanics & Mining Sciences*, 48, 1055-1067.
72. Sahoo.J.P. and Kumar.J. (2012).Seismic stability of a long unsupported circular tunnel. *Computers and Geotechnics*, 44, 109–115.
73. Sakurai, S. (2010).Modeling strategy for jointed rock masses reinforced by rock bolts in tunneling practice.*Acta Geotechnica*, 5(2), 121–126.
74. Scussel, D. and Chandra, S. (2013). A new approach to obtain tunnel support pressure for polyaxial state of stress. *Tunnelling and Underground Space Technology*, 36, 80-88.
75. Scussel, D. and Chandra, S. (2014).New Approach to the Design of Tunnels in Squeezing Ground. *International Journal of Geomechanics, 14(1),* 110-117.
76. Shaalan, O. A., Salem, T. N., Shamy, E. A. El, and Mansour, R. M. (2014).Dynamic

analysis of two adjacent tunnels.*International Journal of Engineering and Innovative Technology*, 4(4), 145–152.

77. Shahin.H.M.,Nakai.T.andOkuno.T. (2019).Numerical study on 3D effect and practical design in shield tunneling.*Underground Space*, 4, 201–209.
78. Shalabi, F. I. (2017).Interaction of Twin Circular Shallow Tunnels in Soils—Parametric Study.*Open Journal of Civil Engineering*, 7, 100–115.
79. Shaofeng, L., Jincai, F., Pinghua, Z., and Xiang, L. (2018).Stability Analysis of Two Parallel Closely Spaced Tunnels Based on Convergence–Confinement Principle.*Journal of Construction Engineering and Management*, 144(6), 1–11.
80. Sharma, H., Mishra, S., Rao, K. S., and Gupta, N. K. (2018).Effect of cover depth on deformation in tunnel lining when subjected to impact load.*ISRM International Symposium - 10th Asian Rock Mechanics Symposium, ARMS*.
81. Shiau.J. and Al-Asadi.F. (2020).Two-dimensional tunnel heading stability factors Fc, Fs and Fγ.*Tunnelling and Underground Space Technology*, 97, 103293,1-10.
82. Shirinabadi, R., and Moosavi, E. (2016).Twin tunnel behavior under static and dynamic loads of Shiraz metro, Iran.*Journal of Mining Science*, 52(3), 461–472.
83. Shrivastava, A. K. (2012).Physical and numerical modelling of shear behaviour of jointed rocks under CNL and CNS boundary conditions. *Ph.D Thesis*, IIT Delhi.
84. Shrivastava, A. K., and Rao, K. S. (2011).Shear behaviour of non planar rock joints.*14th Asian Regional Conference on Soil Mechanics and Geotechnical Engineering*.
85. Shrivastava,A.K. and Rao, K. S. (2013).Development of a Large-Scale Direct Shear Testing Machine for Unfilled and Infilled Rock Joints Under Constant Normal Stiffness

Conditions.Geotechnical Testing Journal, 36(5), 670–679.

86. Shrivastava, A. K., and Rao, K. S. (2015).Shear Behaviour of Rock Joints Under CNL and CNS Boundary Conditions.*Geotechnical and Geological Engineering*, 33, 1205–1220.
87. Shrivastava, A. K., and Rao, K. S. (2018).Physical Modeling of Shear Behavior of Infilled Rock Joints Under CNL and CNS Boundary Conditions.*Rock Mechanics and Rock Engineering*, 51(3), 101–118.
88. Singh,C.S. and Shrivastva,B.K.(2000).Stability analysis of twin tunnels by finite element method.*Indian Journal of Engineering & Materials Science,*7,57-60.
89. Singh, R., Singh, T. N., and Bajpai, R. K. (2018).The Investigation of Twin Tunnel Stability: Effect of Spacing and Diameter.*Journal of the Geological Society of India*, 91, 563–568.
90. Singh, T., Jain, A. and Rao, K.S. (2017).Physico-Mechanical Behaviour of Metamorphic Rocks in Rohtang Tunnel, Himachal Pradesh, India.*Procedia Engineering,*191,419 – 425.
91. Sohaei, H., Hajihassani, M., Namazi, E., and Marto, A. (2020).Experimental study of surface failure induced by tunnel construction in sand.*Engineering Failure Analysis*, 118, 1-11.
92. Sun, Q., Dias,D. and Sousa, L.R. (2020).Soft soil layer-tunnel interaction under seismic loading.*Tunnelling and Underground Space Technology*,98,103329,1-9.
93. Tiwari, R., Chakraborty, T., and Matsagar, V. (2016).Dynamic Analysis of Tunnel in Weathered Rock Subjected to Internal Blast Loading.*Rock Mechanics and Rock Engineering*, 49, 4441–4458.

94. Varma, M., Maji, V. B., and Boominathan, A. (2019).Numerical modelling of a tunnel in jointed rocks subjected to seismic loading.*Underground Space*, 4(2), 133–146.

95. Wang, A., Shi, C., Zhao, C., Deng, E., Yang, W., and He, H. (2020).Response Characteristics of Cross Tunnel Lining under Dynamic Train Load.*Applied Science,* 10, 1-19.

96. Wang, H. N., Gao, X., Wu, L., and Jiang, M. J. (2020b).Analytical study on interaction between existing and new tunnels parallel excavated in semi-infinite viscoelastic ground.*Computers and Geotechnics*, 120, 103385,1–18.

97. Wang, Z., Wong, R. C. K., Li, S., and Qiao, L. (2012).Finite element analysis of long-term surface settlement above a shallow tunnel in soft ground.*Tunnelling and Underground Space Technology*, 30, 85–92.

98. Wu, Z., and Zou, S. (2020).A static risk assessment model for underwater shield tunnel construction.*Sadhana*, 45(215), 1–13.

99. Yang,S.Q., Tao,Y., Xu,P. and Chen,M. (2019).Large-scale model experiment and numerical simulation on convergence deformation of tunnel excavating in composite strata. *Tunnelling and Underground Space Technology*,94,103133.

100. Yang, S.Q., Yin, P.F., Zhang, Y.C., Chen, M., Zhou, X.P., Jing, H. W., and Zhang Q.Y. (2019). Failure behaviour and crack evolution mechanism of a non-persistent jointed rock mass containing a circular hole. International Journal of Rock Mechanics and Mining Sciences, 114, 101-121.

101. Yang, J., Yin, Z. Y., Liu, X. F., and Gao, F. P. (2020).Numerical analysis for the role of soil properties to the load transfer in clay foundation due to the traffic load of the metro tunnel. *Transportation Geotechnics*, 23, 100336.

102. Yang, Y., Xie, X. and Wang, R. (2010).Numerical simulation of dynamic response of operating metro tunnel induced by ground explosion. *Journal of Rock Mechanics and Geotechnical Engineering*,2,4,373–384.

103. Yingjie, L., Dingli, Z., Qian, F., Qingchun, Y., and Lu, X. (2014).A physical numerical investigation of the failure mechanism of weak rocks surrounding tunnels.*Computers and Geotechnics*, 61, 292–307.

104. Yoo, J.K.,Park, J.S., Park,D. and Lee,S.W. (2018). Seismic Response of Circular Tunnels in Jointed Rock. *KSCE Journal of Civil Engineering,* 22,4,1121-1129.

105. Zaid, M., Shah, I. A., and Farooqi, M. A. (2019).Effect of Cover Depth in Unlined Himalayan Tunnel : A Finite Element Approach.*8th Indian Rock Conference*, 448–454.

106. Zaid, M., Sadique, R., Alam, M. M., and Samanta, M. (2020).Effect of shear zone on dynamic behaviour of rock tunnel constructed in highly weathered granite. *Geomechanics and Engineering*, 23(3), 245–259.

107. Zhang, J.F., Chen, J.J., Wang, J.H. and Zhu, Y.F. (2013). Prediction of tunnel displacement induced by adjacent excavation in soft soil. *Tunnelling and Underground Space Technology*, 36, 24–33

108. Zhang, C., Han, K., and Zhang, D. (2015). Face stability analysis of shallow circular tunnels in cohesive-frictional soils. *Tunnelling and Underground Space Technology*, 50, 345–357.

109. Zhang, R., Xiao, Y., Zhao, M., and Zhao, H. (2019). Stability of dual circular tunnels in a rock mass subjected to surcharge loading. *Computers and Geotechnics*, 108, 257–268.

110. Zheng,G., Yang,P., Zhou,H., Zhang,W.,Zhang,T. and Ma,S. (2021).Numerical Modeling of the Seismically Induced Uplift Behavior of Twin Tunnels. *International Journal of Geomechanics*, 21, 1, 04020240.

111. Zhu, Z., Li, Y., Xie, J., and Liu, B. (2015).The effect of principal stress orientation on tunnel stability. *Tunnelling and Underground Space Technology*, 49, 279–286.

List of Publications

1. Kumar, P. and Shrivastava,A.K. (2021).Physical Investigation of Deformation Behaviour of Single and Twin Tunnel under Static Loading Condition.*Applied Science,* Vol-11,11506, pp. 1-18. https://doi.org/10.3390/app112311506. *(SCIE)***.**

2. Kumar,P. and Shrivastava,A.K. (2022).Experimental and numerical analysis of deformation behaviour of tunnels under static loading conditions.*Sustainable Energy Technologies and Assessments,* Vol-52, 102057, pp 1-10 https://doi.org/10.1016/j.seta.2022.102057. (SCIE)

3. Kumar,P. and Shrivastava,A.K. (2021)**.**Development of a testing facility to determine the Stress-Deformation behaviour of tunnel..*Journal of environmental protection and ecology,23(3),946-956.*

4. Kumar,P. and Shrivastava,A.K. (2021).Damage Detection in Shallow Tunnels Using 3D Numerical Modelling.*International Conference on "Advancements and Innovations in Civil Engineering (IC-AICE 2021), pp-177-181.*

5. Kumar,P. and Shrivastava,A.K. (2019).Deformation Behaviour of Tunnels under Different Loading Conditions: State of Art.*Proceedings of the 4th World Congress on Civil, Structural, and Environmental Engineering (CSEE'19) Rome, Italy-April, 2019, Paper No. ICGRE 130 DOI: 10.11159/icgre19.130.*

6. Kumar,P. and Shrivastava,A.K. (2019).Stability of Single Tunnel in Rock under Static Loading Condition.*8th Indian Rock Conference 4-5 November 2019,pp-424-429.*

7. Kumar,P. and Shrivastava,A.K. (2017).Various Factors Effecting Stability of Underground Structure: State of Art.*7th Indian Rock Conference 25-27 October 2017,pp-576-580.*